CANADIAN THESES

THÈSES CANADIENNES

NOTICE

The quality of this microfiche is heavily dependent upon the quality of the original thesis submitted for microfilming. Every effort has been made to ensure the highest quality of reproduction possible.

If pages are missing, contact the university which granted the degree.

Some pages may have indistinct print especially if the original pages were typed with a poor typewriter ribbon or if the university sent us an inferior photocopy.

Previously copyrighted materials (journal articles, published tests, etc.) are not filmed.

Reproduction in full or in part of this film is governed by the Canadian Copyright Act, R.S.C. 1970, c. C-30.

AVIS

La qualité de cette microfiche dépend grandement de la qualité de la thèse soumise au microfilmage. Nous avons tout fait pour assurer une qualité supérieure de reproduction.

S'il manque des pages, veuillez communiquer avec l'université qui a conféré le grade.

La qualité d'impression de certaines pages peut laisser à désirer, surtout si les pages originales ont été dactylographiées à l'aide d'un ruban usé ou si l'université nous a fait parvenir une photocopie de qualité inférieure.

Les documents qui font déjà l'objet d'un droit d'auteur (articles de revue, examens publiés, etc.) ne sont pas microfilmés.

La reproduction, même partielle, de ce microfilm est soumise à la Loi canadienne sur le droit d'auteur, SRC 1970, c. C-30.

THIS DISSERTATION HAS BEEN MICROFILMED EXACTLY AS RECEIVED

LA THÈSE A ÉTÉ MICROFILMÉE TELLE QUE NOUS L'AVONS REÇUE

THE UNIVERSITY OF ALBERTA

Thermal Stability and Application of Emulsion Composed Blocking Agents for Steamflooding

by

Robert M. Decker

A THESIS

SUBMITTED TO THE FACULTY OF GRADUATE STUDIES AND RESEARCH

IN PARTIAL FULFILMENT OF THE REQUIREMENTS FOR THE DEGREE

OF Master of Science

IN

Petroleum Engineering

Department Of Mining, Metallurgical and Petroleum Engineering

EDMONTON, ALBERTA

Fall 1986

ISBN 0-315-32506-2

THE UNIVERSITY OF ALBERTA

RELEASE FORM

NAME OF AUTHOR Robert M. Decker

TITLE OF THESIS Thermal Stability and Application of Emulsion Composed Blocking Agents for Steamflooding

DEGREE FOR WHICH THESIS WAS PRESENTED Master of Science

YEAR THIS DEGREE GRANTED Fall 1986

Permission is hereby granted to THE UNIVERSITY OF ALBERTA LIBRARY to reproduce single copies of this thesis and to lend or sell such copies for private, scholarly or scientific research purposes only.

The author reserves other publication rights, and neither the thesis nor extensive extracts from it may be printed or otherwise reproduced without the author's written permission.

(SIGNED) .....

PERMANENT ADDRESS:

R.M. Decker
723 Queenston Terrace, S.E.
Calgary, Alberta
T2J-6H5 ph.271-7792

DATED June 27 1986

The foundation of every state
is the education of its youth.

Diogenes (412-323 B.C.)

THE UNIVERSITY OF ALBERTA

FACULTY OF GRADUATE STUDIES AND RESEARCH

The undersigned certify that they have read, and recommend to the Faculty of Graduate Studies and Research, for acceptance, a thesis entitled Thermal Stability and Application of Emulsion Composed Blocking Agents For Steamflooding submitted by Robert M. Decker in partial fulfilment of the requirements for the degree of Master of Science in Petroleum Engineering.

.....

Supervisor

.....

.....

Date.....June 21, 1986.....

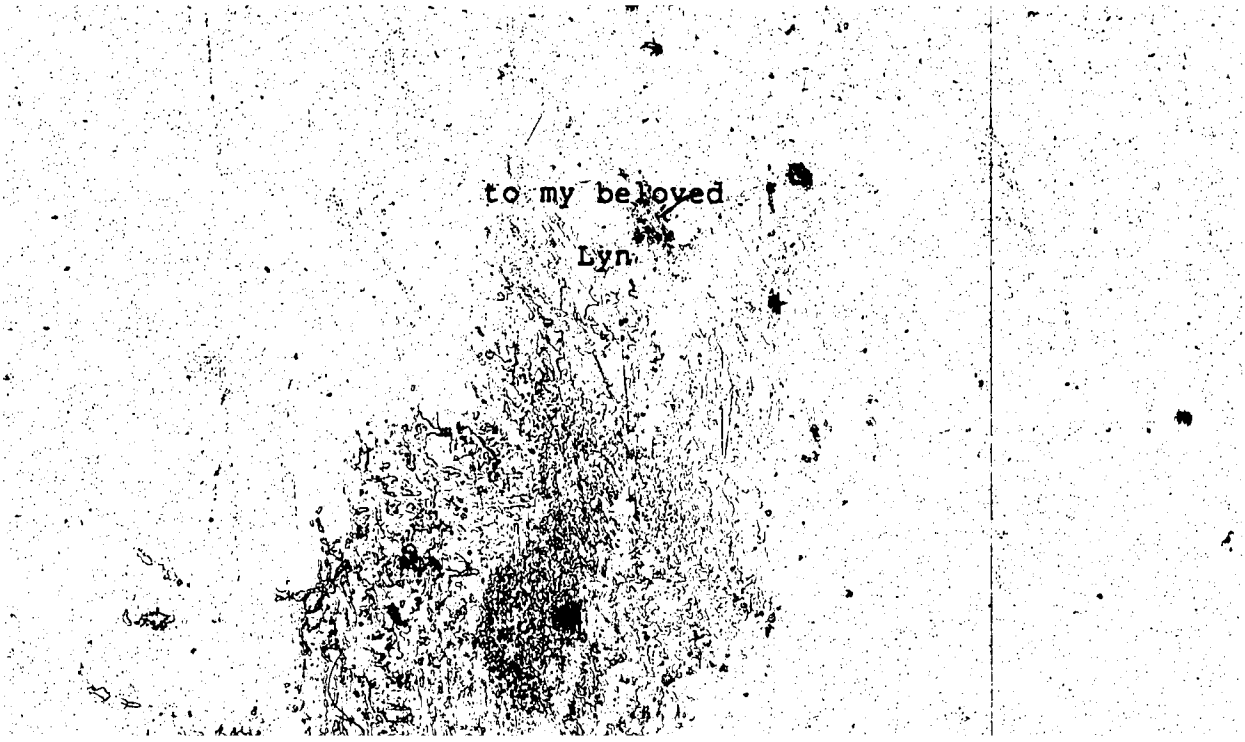
to my beloved
Lyn

ABSTRACT

The investigation into mobility control and blocking agents to improve steamflood conformance has been of ongoing interest. An examination of the use of oil-in-water macroemulsions to block high permeability channels created during steam injection was carried out in this research.

The stability of 5% Primrose and Lloydminster heavy oil emulsions was screened using both an anionic (Vista 250) and a nonionic (Triton X-100) surfactant. Surfactants were used in active concentrations of 25 to 5000 ppm. Visual observations of droplet character and the emulsion pH behavior at different surfactant concentrations over cure temperatures of 2[illegible] to 225 °C were the criteria used to determine stability. Results indicate an optimal surfactant concentration range of 50 to 300 ppm with the Vista 250 maintaining emulsion stability at high temperatures.

Recovery and steamflood behavior were observed in an unscaled linear model containing an oil saturated single sand size. Comparative results using a heterogeneous model containing two parallel oil saturated sand beds of different permeabilities show early breakthrough and reduced recovery due to steam channeling. Externally produced emulsion (5% oil content, 100 ppm Vista 250) was injected to block the more permeable channels. Blockage was tested using the emulsion injected as a slug followed by steam and with the emulsion co-injected with steam. During slug injection the emulsion was injected at a constant pressure with a

permeability reduction on the order of 90% inferred from a change in flow rate data. Emulsion slug injection was more effective through improved blocking and recovery than co-injection of emulsion and steam.

ACKNOWLEDGEMENTS

The author would like to thank Dr. D.L. Flock for his guidance and encouragement in the conduct of this research.

Appreciation is expressed for the diligent assistance of the Petroleum Engineering technical staff, specifically:

Mr. John Czuroski

Mr. Jacques Gibeau

Ms. Birgitte McKinnon

Mr. Bob Smith

Thanks are due to the Vista Chemical Company of Ponca City, Oklahoma who donated surfactant used in this study. Also, to Petro-Canada and Husky for their donations of heavy oil.

Gratitude to the Alberta Oil Sands Technology and Research Authority who granted a scholarship to assist the author financially in carrying out this research.

The author sincerely appreciates the support and encouragement of her wife, Lyn, throughout the course of his research and studies in Petroleum Engineering.

Table of Contents

List of Tables

List of Figures

List of Photographic Plates

Nomenclature

A = area, cm^2

A_H = Hamaker constant

B = number of atoms

G_C = free energy of the continuous phase, N·m

G_D = free energy of the dispersed phase, N·m

G_{DC} = free energy of the interface between phases, N·m

G_S = free energy of the container surface, N·m

G_T = total free energy of the system, N·m

g = gravitational constant, m/sec^2

H = interparticle distance between droplets, m

k = absolute permeability, d or m^2

k_B = Boltzmann's constant

L = distance, m

L_C = core length, cm

L_i = London constant

n = number of ions in bulk solution

p = pressure, psi or Pa

q = volumetric flow rate, cm^3/sec or cm^3/hr

$R_{1,2}$ = radii of curvature, m

r = droplet radius, m

$r_{1,2}$ = pore throat radii, m

T = absolute temperature, K

U = volumetric flow velocity, m/sec

V = creaming rate, m/sec

V_A = potential energy of attraction, N·m

V_R = potential energy of repulsion, N·m

V_T = total potential energy of interaction, N·m

z = charge of bulk solution

Greek Symbols

β = reservoir dip angle

γ = interfacial tension between oil and water, N/m

ϵ = dielectric constant of the medium

η = emulsion viscosity, mPa·s

θ = wetting contact angle

κ = reciprocal thickness of double layer, m

λ = wavelength of electronic oscillations

μ = oil viscosity, mPa·s

ρ = fluid density, kg/m³

ϕ = porosity, fraction

ψ = surface potential

1. INTRODUCTION

In the recovery of fluid from reservoirs containing high viscosity crudes, there are three predominant forces affecting the movement of crude to the producing wells. These forces are related to the flow rate of crude through essentially three independent dimensionless parameters (Prats, 1982).

1. Ratio of Applied Pressure Forces to Viscous Forces

$$\frac{k \cdot \Delta p}{\mu \cdot L \cdot U},$$

where

k = absolute permeability

Δp = pressure drop between measurement points

L = distance between points of pressure measurement

μ = crude viscosity

U = volumetric flow velocity (Darcy velocity).

2. Ratio of Applied Pressure Forces to Capillary Forces

$$\frac{\sqrt{k} \cdot \Delta p}{\gamma \cdot \cos\theta},$$

where

γ = interfacial tension between crude and water

θ = wetting contact angle.

3. Ratio of Applied Pressure Forces to Gravitational Forces

$$\frac{\Delta p}{L \cdot g \cdot \Delta\rho \cdot \cos\beta}$$

where

g = gravitational constant

β = reservoir dip angle

$\Delta\rho$ = difference in crude density between points of pressure measurement.

The above parameters may be manipulated to improve the flow rate and ultimate recovery of crude. Non-thermal techniques (Farouq Ali, 1976) such as emulsion flooding, solvent, and CO_2 assisted displacement processes have been discussed as possible methods of heavy oil recovery. These methods act to alter the effect of viscous and capillary forces on fluids in the reservoir. The above techniques are generally amenable only to crudes of moderate viscosity (50-200 cp).

Thermal methods involving steam injection and in situ combustion have proven to have the highest technical and economic merit; as a result, these methods are currently the most widely employed. Steam injection is currently the most popular thermal method and is used in approximately two-thirds of the enhanced oil recovery field projects in Western Canada. Steam injection with the addition of synergistic agents will likely be necessary in order to make in situ bitumen recovery from tar sand economical

(Doscher, 1984).

Injection of steam (heat) into the reservoir increases the crude temperature and would therefore reduce its viscosity. The increase in temperature causes a reduction in the interfacial tension between the crude and water (Flock, 1984). As well, variation in temperature within the reservoir results in small scale density variations in the crude and increased gravity flow. Thus it may be seen that all three parameters above are affected by steam injection thereby improving the flow rate of the crude.

Chemical alteration of crude properties such as steam distillation (Willman et al., 1961) visbreaking, thermal cracking, and pyrolysis (Hyne et al., 1982) also contribute to improved recovery due to thermal methods.

Recovery efficiency is generally viewed as the product of the flushing efficiency and the volumetric sweep efficiency (conformance). These factors are sometimes referred to respectively as microscopic and macroscopic displacement efficiencies. In most recovery processes, low recovery efficiencies are due to poor conformance much more so than low flushing efficiency (Winestock, 1984).

Conformance due to steam injection is limited by several factors. The displacement of viscous crude, with steam/condensate, is at an unfavourable mobility ratio which results in viscous fingering and consequent bypassing of crude. Conformance is also dependent on the degree of gravity override. Gravity override of steam into the top of

a reservoir occurs due to density differences between the steam and crude. The result is usually a zone of lower oil saturation and higher permeability to steam at the top of a formation through which further injected steam will continue to channel.

Conformance is also limited by variations in lithology causing reservoir heterogeneities or zones of varying permeability and/or porosity. Bottom water or overlying gas (i.e. a strata of lower oil saturation) in an oil reservoir offer zones of higher transmissibility through which the steam may channel. This is not uncommon and often will have a dramatic effect on limiting the conformance of steam injection.

The use of mobility control and blocking/diverting agents to improve conformance has been of long standing importance in the oil industry since 1932 (Harrison, 1972). Navratil et al. (1983) report several products such as those based upon solutions of lignosulfonate reaction products, foams, in-situ polymerized gels, silica gels, polymeric emulsions, and in-situ formation of precipitates as suitable agents for high temperature blocking applications.

The purpose of this study was to examine the use of oil-in-water macroemulsions as a blocking agent to improve conformance for steam injection applications. Macroemulsions are liquid-liquid dispersions with a dispersed droplet size greater than 0.1 μm. The occurrence of emulsions in the petroleum industry has been of long standing importance,

particularly in their breaking during production separation operations. In recent years, researchers have examined the use of micro- and macroemulsions for the purpose of enhanced oil recovery.

The objectives of this preliminary research were to:

1. determine the feasibility of selecting surfactant type and surfactant concentration for heavy oil emulsion stability at high temperatures through examination of droplet character and emulsion pH behavior, and

2. examine from a mechanistic standpoint if a stable emulsion may be applied to block high permeability channels created by steam in a heterogeneous unscaled laboratory model.

2. THEORY AND LITERATURE SURVEY

Emulsion behavior and its flow through porous media have been of ongoing interest. Dispersions such as emulsions (liquid-liquid dispersions) and foams (gas-liquid dispersions) have been investigated for use in mobility control and as blocking agents. In order for a blocking agent to be effective it must withstand the physico-chemical influences of the porous media and the displacing fluid. Accordingly, for blockage in steamflood applications, emulsion stability at high temperatures would be a major consideration. General theoretical considerations as well as the effects of pH and surfactants on emulsion stability are surveyed. In addition, theories and observation of blockage mechanisms attributable to emulsion flow are presented.

2.1 Emulsion Stability

Emulsions, because they are composed of immiscible liquids (e.g. oil and water), are inherently unstable. However, apparent stability may be attained for a certain time duration by manipulation and suppression of the mechanisms causing emulsion breakdown.

2.1.1 Emulsion Formation and Thermodynamic Considerations

Emulsions may be created by applying mechanical energy to two mutually immiscible liquids. The interface between the two phases is deformed to the extent that droplets are formed. This deformation is opposed by the Laplace pressure.

The Laplace pressure at the concave side of a curved interface with interfacial tension, γ, is higher than at the convex side by an amount

$$\Delta p = \gamma(1/R_1 + 1/R_2) \ , \qquad (1)$$

where R_1 and R_2 are the principal radii of curvature for an ellipsoid droplet (e.g. Walstra, 1983). The presence of a surfactant (natural or added) promotes emulsion stability through the reduction of the interfacial tension and, hence, the Laplace pressure.

A thermodynamic approach to emulsion formation assumes the total free energy of the emulsion can be separated into several independent contributors. The total free energy (G_T) of the system just before the emulsification process can be expressed as (Lissant, 1976, 1984)

$$G_T = G_D + G_C + G_{DC} + G_S \ , \qquad (2)$$

where

G_D = free energy of the dispersed phase

G_C = free energy of the continuous phase

G_{DC} = free energy of the interface between dispersed and continuous phases

G_S = free energy of the interface between the liquid phases and surface of the container.

The container/liquid interfacial area is relatively small, in comparison to the other terms above, so the free energy, G_S, is neglected. The free energies, G_D and G_C, will remain approximately the same before and after emulsification. G_{DC}, however, will be at a minimum prior to emulsification. The interfacial free energy, G_{DC}, can be expressed in the form

$$G_{DC} = \gamma_{DC} \cdot A \; , \qquad (3)$$

where γ_{DC} is the interfacial tension and A is the interfacial area. The free energy of emulsion formation, ΔG_E, can be expressed in the form

$$\Delta G_E = \gamma_{DC} \, \Delta A - T \, \Delta S \; , \qquad (4)$$

where ΔS is the change in entropy due to emulsification. The change in the interfacial area of the system, ΔA, may be very great so that $(\gamma_{DC}\Delta A)$ will be larger than the $(T\Delta S)$ term. Therefore, the change in free energy of emulsion formation, ΔG_E will be positive or rather the change in free energy of demulsification is negative. This means, macroemulsions are thermodynamically unstable or metastable with demulsification proceeding spontaneously.

2.1.2 Destablization Mechanisms

Destabilization of macroemulsions is manifested in three basic mechanisms: flocculation, coalescence, and creaming.

Flocculation and coalescence are governed by short range interactions between droplets. Flocculation is the first step of destabilization and involves the congregation of dispersed phase droplets into aggregates. The droplets maintain their individual identity and may be redispersed through shearing action.

Coalescence of small droplets into larger ones is the second step of destabilization. It represents a reduction of free energy of the system and is irreversible. Although 'stability' is a relative term, the degree of stability can be assessed by observing the droplet behavior, i.e. the rate of change of the droplet size or the interfacial area.

Creaming is the relative movement of droplets primarily due to density differences between the two liquid phases leading to phase separation (emulsion breakage). The creaming rate, V, of non-interacting spherical droplets of radius, r, is determined by equating the opposing gravitational and hydrodynamic forces as given by Stokes' Law (Becher, 1965):

$$(4/3)\pi r^3 \Delta\rho g = 6\pi\eta r V \ , \qquad (5)$$

and therefore

$$V = 2\Delta\rho g r^2/(9\eta) \quad . \qquad (6)$$

Therefore, the rate of creaming may be reduced by decreasing the density difference, $\Delta\rho$, between liquid phases , or by increasing the viscosity, η, of the continuous phase, or by reducing the size of dispersed droplets.

Phase inversion is a special mechanism of destabilization where the dispersed phase inverts to become the continuous phase and vice versa. Phase inversion usually occurs suddenly at higher phase volume ratios. However, flocculation, coalescence, and creaming are continuous processes occurring simultaneously.

2.1.3 Short Range Interactions

Macroemulsion stabilty is often discussed in terms of the D.L.V.O theory of colloid stabilty developed independently by Derjaguin and Landau and by Verwey and Overbeek (Sherman, 1968).

The basic premise behind the theory is that dispersed particles are subject to two kinds of forces which can influence the chance of whether or not those particles will come into close contact and remain in contact when under the influence of Brownian motion. These forces are:

1. the London-van der Waals force of attraction,
2. the electrostatic repulsion between electrical double layers of the same charge.

The attractive London-van der Waals forces arise from charge

fluctuation within a molecule due to electronic motion. These forces will therefore operate even between non-polar molecules.

The potential energy of attraction in a vacuum for similar particles of radius, r, can be expressed in the form (Shah, 1985):

$$V_A \cong -(A_H r/\pi)[2.45\lambda/120H^2 - \lambda^2/1045H^2 + \lambda^3/5.65x10^4H^4] \quad , \quad (7)$$

valid for $H > 150$ A°, and

$$V_A \cong -(A_H r/12H)\,[\lambda/(\lambda + 3.5\pi H)] \quad , \quad (8)$$

valid for $H < 150$ A°, where A_H is the Hamaker constant; λ, the wavelength of the intrinsic electronic oscillations of the atoms; H, the interparticle distance between droplets and r is the average radius of the droplets. Note that the potential energy of attraction is negative.

The Hamaker constant, A_H, between two particles in a vacuum is defined by

$$A_H = \pi^2 B_i^2 L_i \quad , \quad (9)$$

where L_i is the London constant; B_i, the number of atoms molecules of the ith kind contained in a cubic centimeter of substance). In a liquid dispersion medium, A_H, is replaced by an effective Hamaker constant

$$A_H = [\sqrt{A_2} - \sqrt{A_1}]^{1/2} , \qquad (10)$$

where A_2 and A_1 are the Hamaker constants for the particles and the dispersion medium, respectively. As A_2 and A_1 become closer in magnitude, A becomes smaller resulting in a smaller attractive potential energy between the particles.

The potential energy of repulsion is given by

$$V_R = (\epsilon r \psi^2/2) \ln(1 + e^{\kappa H}) , \qquad (11)$$

where ϵ is the dielectric constant of the medium; ψ is the surface potential and κ is the reciprocal "thickness" of the electrical double layer, given by

$$\kappa = [8\pi n z^2 e^2/(\epsilon k_B T)]^{1/2} , \qquad (12)$$

where n is the number of ions per cm^2 of bulk solution; z is the charge per cm^3 of bulk solution; ϵ is the dielectric constant of the medium; k_B is Boltzmann's constant and T the absolute temperature.

The total potential energy of interaction is therefore given by

$$V_T = V_A + V_R . \qquad (13)$$

A schematic representation of the summation of repulsive and attractive components is given in Figure 2.1.

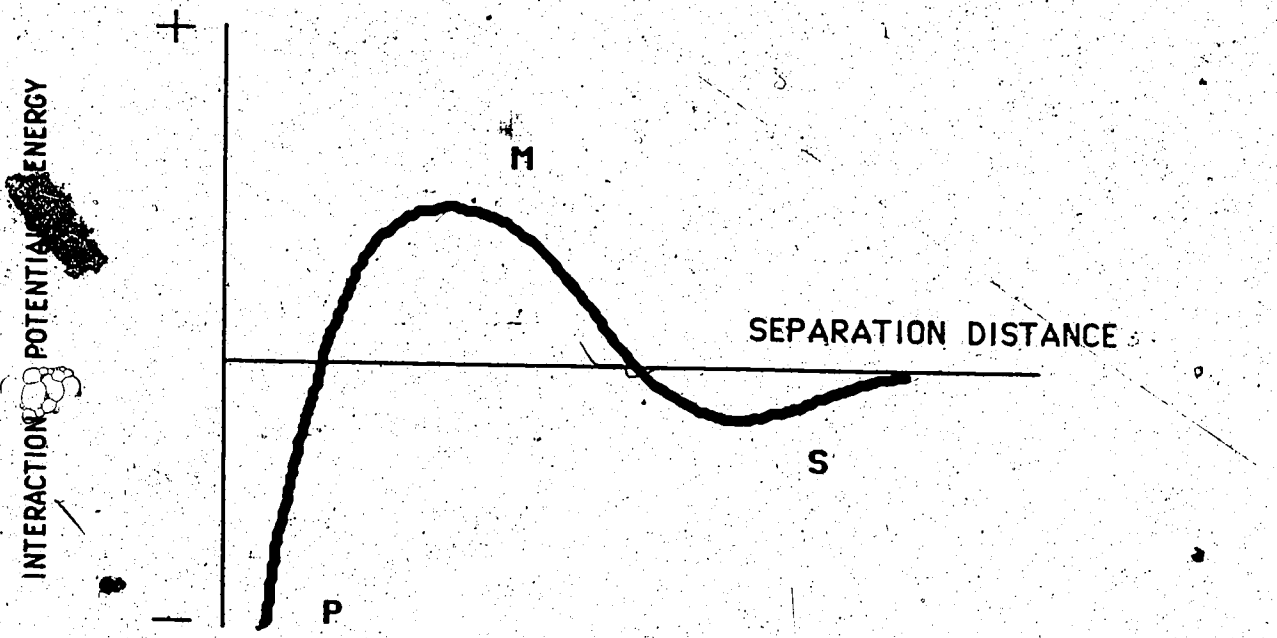

Figure 2.1 Total Potential Energy of Interaction vs. Particle Separation Distance

When droplets interact under the influence of hydrodynamic (e.g. mixing, porous media flow) and/or non-hydrodynamic effects (e.g. Brownian diffusion) the potential for redispersal, flocculation, or coalescence of dispersed phase droplets is determined by the shape of this curve.

The primary minimum represents the potential energy of the two particles (droplets) in close proximity where coalescence will proceed spontaneously. The maximum represents the repulsive energy barrier to coalescence. The secondary minimum denotes the separation distance where droplets will flocculate into aggregates but may be redispersed.

The shape of the potential interaction energy curve is determined by surface potential, thickness of the electrical double layer, and electrolyte concentration. Electrolyte type and concentration have been shown to have a strong influence on surface potential (assumed from zeta potential measurement) and double layer repulsive forces in bitumen emulsions (Takamura and Chow, 1982).

2.1.4 Role of Surfactant

The role of the surfactant or emulsifying agent is to stabilize a basically unstable system (macroemulsion) for a sufficient time so that the emulsion may perform some specific function. The presence of the surfactant (natural or added) through adsorption at the liquid-liquid interface promotes emulsion stability by:

1. reducing the interfacial tension between two liquids and consequently the thermodynamic instability of the system resulting from the increase in the interfacial area between the two phases, and
2. forming steric and/or electrical barriers to droplet coalescence, and
3. creating a sufficiently rigid interfacial film increasing the resistance to mechanical shock and possible film rupture when droplets collide.

Surfactants are characterized by possessing both polar and non-polar regions on the same molecule. The polar or hydrophilic region of the molecule may carry a positive or negative charge for cationic or anionic surfactants, respectively. The non-polar or hydrophobic portion of the molecule is commonly a flexible chain hydrocarbon. Thus, in the same molecule there exists two moieties, one portion which has an affinity for solvent (e.g. water) and one portion which does not (Tadros, 1984).

Through adsorption of an ionic surfactant, the thickness of the electrical double layer is increased. Thus, the potential energy of interaction is rendered increasingly more positive with an increase in the maximum of Figure 2.1, preventing coalescence of droplets in the primary minimum.

A steric barrier is formed by a nonionic surfactant, where the polar group is usually composed of a polyoxyethylene chain. The maximum of Figure 2.1 is increased by the mechanical separation of the dispersed

droplets due to the presence of a nonionic surfactant.

2.1.5 Effect of pH

Strassner (1968) investigated the effect of pH on interfacial films and stability of crude oil-in-water emulsions. It was found that oil field emulsions were stabilized primarily by film-forming, polar asphaltenes and resins containing organic acids and bases. Strassner notes that the addition of inorganic acids and bases, with subsequent alteration in pH, changes the physical properties of these interfacial films and their ability to stabilize emulsions. In tests with 13.2° API gravity Venezuelan crude oil and distilled water, basic pH produced stable oil-in-water emulsions (corresponding to water-wetting mobile soap films).

Further study by Layrisse et al. (1984) with two Venezuelan crudes (Cerro Negre, CN-36, 8.3° API and Zuaty, 9.5° API) found pH to have a strong influence on the natural surfactants present in the crudes and consequently the interfacial behavior of the crude. Emulsion stability is enhanced by minimum interfacial tension. Interfacial tension was found to be minimized at basic pH. The researchers propose at acidic pH's the asphaltenes are probably adsorbed at the interface whereas the lower interfacial tension found at alkaline pH's are due to the more active and lighter resins.

Gillberg et al. (1980) investigated the effect of pH on the solubilization capacity of the mixtures of nonionic and ampholytic surfactants employed in microemulsions. They found microemulsions to be strongly affected by small changes in pH at constant temperature. This was due to the variation in the degree of ionization attributable to the ampholytic surfactant with pH. This would consequently affect the total interaction potential energy by altering the repulsion energy of the surfactant layer.

2.1.6 Effect of Temperature

Levius and Drommond (1982) investigated the effect of elevated temperatures as an artificial breakdown stress to evaluate emulsion stability. They found that increasing the temperature tends to result in a decrease in mean droplet size and droplet concentration due to a more rapid settling rate.

Bennett et al. (1968) reported a test for emulsion stability using "freeze-thaw" cycles. The freezing of the aqueous phase will often cause phase separation. Subsequent thawing may cause the emulsifying film to be damaged resulting in coalescence of the dispersed droplets and phase separation. The solubility balance of the surfactant also changes with the fluctuation in temperature.

Mitsui et al. (1972) found the hydrophilic/hydrophobic nature of certain nonionic surfactants to be temperature dependent consequently affecting the interfacial tension and

emulsion stability. Nonionic surfactants containing ethylene oxide chains as hydrophilic groups suffered dehydration of the ethylene oxide moieties as the temperature increases. Surfactants containing less than ten ethylene oxide units experienced an increase in the interfacial tension with increasing temperature. This would be a destabilizing influence on an emulsion created with such a surfactant.

Saito and Shinoda (1970) investigated the stability of both oil-in-water and water-in-oil type emulsions as a function of temperature. These were cyclohexane-water systems stabilized with the nonionic surfactant polyoxyethylene nonylphenylether. They found the mean droplet diameter of either emulsion type to diminish as the emulsion temperature approaches the PIT (phase inversion temperature) of the system. This was a result of very fast coalescence rates observed for larger droplets near the PIT, and their subsequent creaming out of the solution.

In summary, temperature change affects emulsion stability in various ways (Rosen, 1978):

1. Thermal agitation of droplets increases the interaction/collision rate through Brownian diffusion.
2. The physical properties of the interfacial film are affected by thermal expansion or contraction.
3. The relative solubility of surfactant in either phase is affected.
4. The rheological properties (e.g. viscosity) of the liquid constituents are affected.

2.2 Emulsion Flow in Porous Media and Blockage Mechanisms

The flow of emulsions in porous media has been known to improve recovery efficiencies of oil and bitumen for many years. Emulsification was seen to be an important mechanism in caustic waterflooding. In 1942, Subkow patented the injection of aqueous emulsifying agents such as sodium hydroxide for the recovery of heavy oil or bitumen. Later, in 1962, Doscher and Reisberg patented a process involving the injection of sodium hydroxide into tar sands in a caustic-drive oil recovery process. Both of these processes relied on the in situ emulsification of the crude oil to improve ultimate oil recovery.

Johnson (1976) reviewed the mechanisms through which caustic waterflooding improved oil recovery including:

1. Emulsification and entrainment.
2. Wettability reversal (oil-wet to water-wet).
3. Wettability reversal (water-wet to oil-wet).
4. Emulsification and entrapment.

Emulsification and entrainment was the recovery mechanism in Subkow's patent which involved the in situ emulsification of the crude oil and its consequent entrainment into a continuous flowing alkaline water phase. In order to achieve this the emphasis was on lowering interfacial tension by the caustic which resulted in oil-in-water emulsion formation, and the production of the oil as an emulsion in the produced caustic solution.

Johnson discusses the application of chemicals such as acids, bases, and salts in injection water to reverse rock wettability from oil-wet to water-wet. Oil recovery improvement determined from laboratory tests was postulated to be due to the favorable changes in relative oil and water permeability that accompanied a wettability reversal.

Cooke et al. (1974) reported use of alkaline waters which reacted with naturally occurring organic acids in the crude oil to produce soaps at the oil-water interface. The resulting reduction in interfacial tension would promote wettability reversal of the porous medium from a water-wet to oil-wet under the proper conditions of salinity, pH, and temperature. The low interfacial tension resulted in the in situ formation of water-in-oil emulsions behind the alkaline displacement front. These emulsions had a relatively low oil content and had the appearance of oil films, or lamellae. These lamellae could deform and move through the pore spaces but would also bridge pore throats resisting the deplacement of chase water. This resistance and blockage of pores was evidenced by a large increase in pressure gradient immediately behind the displacement front. The pressure gradients were reported to overcome the capillary forces decreased by low interfacial tension so that the residual oil saturation was decreased further.

The last mechanism described by Johnson was emulsification and entrapment. It was reported that Jennings et al. (1974) performed laboratory experiments involving

caustic injection in preferentially water-wet cores. It was determined that if the interfacial tension was low enough residual oil would be emulsified in situ and move downstream with the flowing alkaline solution to become entrapped later in pore throats too small to allow them to squeeze through. The result was improved volumetric conformance by the displacing medium.

The reason for the entrainment and subsequent entrapment of oil droplets was possibly due to two reasons:

1. The interfacial tension between emulsion droplet and wetting fluid was increased so the droplet could not pass through the pore constriction. In a radial flow model/pattern caustic concentration would decrease with distance from the injector, thus an increase in interfacial tension would result.
2. In a radial flow model/pattern the pressure gradient diminishes with distance from the injector. Therefore, at some distance from the injector the pressure would not be great enough to force the droplet through the pore throat.

McAuliffe (2 refs., 1973) conducted laboratory and field tests to determine if externally produced oil-in-water emulsions would act as a selective plugging agent to improve oil recovery in waterfloods. He describes the flow of macroemulsions in porous media and the blockage of pore throats by emulsion droplets larger than the pore constrictions.

This blockage is known as the "Jamin effect". Figure 2.2 depicts this effect as a single droplet of oil becomes lodged in a pore constriction. As shown in the figure, the radius of curvature of the leading edge has a smaller radius than the radius of the trailing edge of the droplet still in the pore, thus the capillary pressure is greater at the front than at the back. The pressure gradient required to force the droplet through the constriction is given by the Laplace equation of capillary statics (Hallam, 1980):

$$\Delta p = 2\gamma \cos\theta \, (1/r_1 - 1/r_2) \, , \qquad (14)$$

where Δp = pressure differential, (Pa)

γ = interfacial tension between the oil and water, (N/m)

θ = contact angle

r_1 = pore throat radius, (m)

r_2 = upstream oil droplet radius, (m)

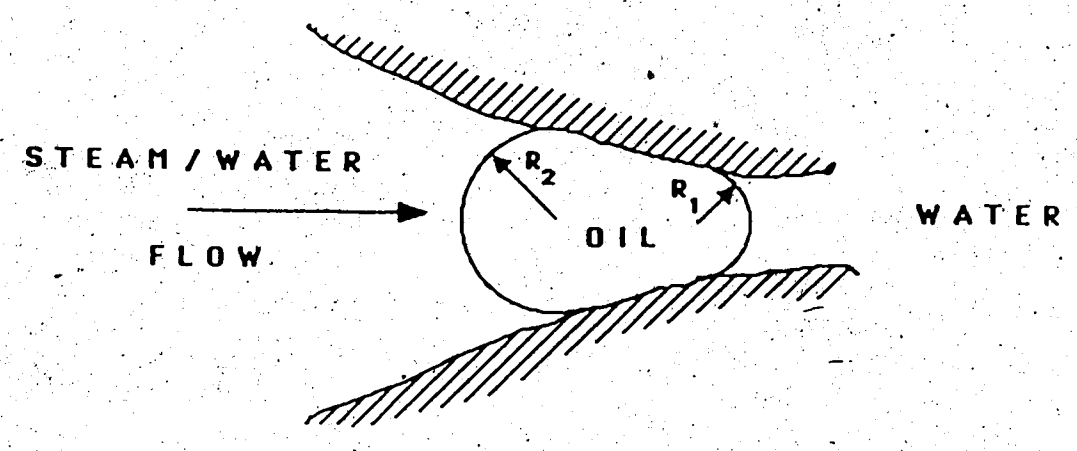

Figure 2.2 - Illustration of an Oil Droplet Lodged in a Pore Constriction

McAuliffe determined from laboratory tests that injection of dilute oil-in-water emulsions resulted in a decrease in effective permeability to water. Rate of change of permeability with pore volume of emulsion injected approximates a logarithmic decay. Therefore, the permeability was reduced to some limiting value dependent on the pressure differential applied across the core. Permeability reductions of up to 35 fold were obtained after 12 pore volumes of 0.5% oil-in-water emulsion were injected into sandstone cores.

In both laboratory and field tests emulsion flooding delayed water breakthrough and increased ultimate oil recovery. Improvement in volumetric conformance was evidenced by lower water-oil ratios and from results of radioactive tracer surveys.

Soo and Radke (2 refs., '1984) examined the flow of emulsions through water-saturated sandpacks of different permeabilities and also in a visual water-saturated micromodel of glassbeads. Permeability reduction in emulsion flow was reported to be primarily due to entrapment. Theoretical and experimental studies of flow mechanisms and velocity effects considered two regimes of capture namely, straining and interception.

Straining capture was the similar effect described by McAuliffe where droplets larger than pore throats become lodged in the pore constriction. At larger velocities (higher pressure gradients) this capture event is followed

by droplet squeezing and re-entrainment. This pseudo-continuous process of straining would account for limiting values of permeability obtained which are characteristic of higher pressure drops. At very high velocities droplet breakup will occur due to snap off mechanisms and hydrodynamic instabilities such as fingering.

Interception capture of droplets smaller than pore throat diameters was seen to occur on the surface of sand grains, in the crevices formed between sand grains, and in dead-space cavern sites or recirculation eddies. Droplets were observed to attach to the surface of [illegible] apparently due to attractive colloidal forces between droplets and sand grains. The droplets were held in the secondary minimum of Fig. 2.1 due to decreased repulsive forces. They would remain there until they were overcome by hydrodynamic forces. Droplets may breakup if high capillary numbers are attained, i.e.,

$$C_a = \frac{\eta \cdot U}{\phi \cdot \gamma}, \qquad (15)$$

where

η = emulsion viscosity, (mPa·s)

U = velocity, (m/s)

ϕ = porosity, (fraction)

γ = interfacial tension between oil and water, (N/m),

where viscous shear forces overcome interfacial attractive

forces.

Cartmill and Dickey (1969) in an effort to determine how oil migrates through porous media studied emulsion flow through a model of crushed glass beads of two separate permeability zones in series. It was observed the droplets would travel easily in the water-wet porous media until the fine permeability interface was encountered. Droplets were seen to attach to glass surfaces and to flocculate into groups which would clog pore throats. This would in turn form a concentrated emulsion at the interface with little tendency for the droplets to coalesce. The flocculation and surface attachment of droplets was thought to be due to electrostatic forces (i.e. attractive van der Waals forces). This supports the observations and contentions of Soo and Radke.

Soo and Radke also observed droplets wedged between the convex surfaces of two sand grains called a crevice site. The drops remain in place by hydrodynamic pressure forces with a velocity increase simply wedging the drops tighter into the crevice. Droplets caught in recirculation eddies and dead spaces called cavern sites were not affected by velocity effects. Neither crevice nor cavern sites were affected unless a significant redistribution of flow, pressure impulses, or vibrations were imposed.

Soo and Radke noted the obvious sensitivity of this study to the surface chemistry of the drops and the porous matrix. In particular, the pH and ionic strength of the

aqueous phase would certainly affect the interception capture of droplets on the rock surface.

A physical interpretation was proposed to describe emulsion flow to steady state with a constant imposed pressure drop. As the emulsion enters the porous medium, drops will be captured in the smaller size pores first. Flow is then diverted to the larger size pores and the drop capture rate increases. Finally, when all drop capture sites are filled, capture ceases and steady state is reached.

It was concluded that two factors affected the overall permeability reduction:

1. the quantity of drops retained in the porous medium, and
2. the effectiveness of those drops in restricting flow.

Studies of the effects of drop size using effluent concentration histories determined that as the drop size of the emulsion increased the drop retention increased. However, for equivalent capture volumes of emulsions, the smaller droplets were more effective at reducing the transient permeability (i.e. restricting the flow) prior to steady state. This was due to their greater number and more thorough dispersal throughout the porous medium for equal volumes of dispersed phase. Eventually, as steady state is approached, the larger droplets caused a larger reduction in absolute permeability than the smaller droplet flow alone due to combined superiority in drop retention and flow restriction.

3. EXPERIMENTAL INVESTIGATION

3.1 Materials

Two heavy crude oils were used in this study namely, Lloydminster and Primrose. Both oils were dewatered by vacuum distillation at 40 °C and any condensed light ends produced were reconstituted with the dried oil. Subsequent distillation of dried oil in toluene showed only a minute trace of water. Lloydminster oil had a viscosity of 10,100 cp (for 1.26 s^{-1}) at 22.5 °C and a density of 0.9738 g/cm^3. Primrose oil had a viscosity of 45,700 cp (for 1.26 s^{-1}) at 22.5 °C and a density of 0.9949 g/cm^3.

Surfactants used as emulsion stabilizers were nonionic Triton X-100 and anionic Vista 250. Triton X-100 is a water soluble compound of iso-octyl phenoxypolyethoxy ethanol with 9 to 10 ethylene oxide units (an ethoxylated phenol). It has a density of 1.065 g/cm^3 and a hydrophilic-lipophilic balance of 13.5. The cloud point of this surfactant was observed to occur in distilled water at 80 °C.

Vista 250 (formerly Conoco CN5) is a sodium alkyl benzene sulfonate with an average molecular weight of 240. This speciality alkylate is 85-90 weight % linear (C_{10}- C_{13}) monoalkylbenzene with the remainder being other alkyl aromatics such as dialkylbenzenes and diphenylalkanes. The sample was received diluted with water for handling resulting in a 28.5% active (company reported) slurry of sodium sulfonate derivative. Apparently this dilution was a

necessary step in the manufacturing process.

Both surfactants were used as received. Triton X-100 is manufactured by Rohm and Haas. Vista 250 is manufactured by Vista Chemical Company.

Distilled, de-ionized water was used as the continuous (external) phase of produced emulsions. Analysis showed this water to be slightly basic at a pH of 7.6 (at 22 °C).

3.2 Emulsification Method

Oil-in-water emulsions with 5% (by volume) oil content were prepared using two oils with two surfactants giving four oil-surfactant combinations. Emulsions were created in each oil-surfactant group with active concentrations of 25, 50, 100, 300, 700, 1200, 2000, and 5000 ppm.

The emulsions were produced using the agent-in-water method whereby the surfactant was dissolved in the distilled water prior to addition of the oil to the aqueous phase. Both aqueous solution and oil were heated to 60 °C prior to mixing. This facilitated proper emulsification of the highly viscous oil in water.

Emulsions were prepared in 1000 mℓ batches with 950 mℓ of aqueous (water and surfactant) solution and 50 mℓ of oil. Emulsification was achieved using a Brinkmann Homogenizer type PT 45/80. This is a rotor-stator device capable of 22,000 rpm. The aqueous solution was mixed at half-speed while the oil was added slowly for the first two minutes. The emulsion was then mixed at high speed for four minutes.

This was then followed by another four minutes at half speed giving a total mixing time per batch of ten minutes. The reduction of mixing speed during the latter stage of emulsification was to allow entrained air to escape as considerable surface foaming did occur depending on the surfactant and concentration used. All emulsions were prepared in identical 2000 mℓ beakers.

3.3 Thermal Stability Test

Two 100 mℓ samples were extracted from each emulsion batch. One was stored in a corked glass flask in a room temperature water bath. The other was contained in a 150 cm^3 stainless steel autoclave pressurized with nitrogen for high temperature curing. Pressurization was necessary in order to suppress vaporization of the emulsions.

Emulsions were cured at temperatures of 25, 75, 125, 175, and 225 °C for a period of one hour. Initial tests determined this time period to be of sufficient duration to evaluate emulsion stability. The autoclaves were subsequently removed from the oven and quenched to room temperature. After depressurization the pH of the cured and uncured samples were compared using a Fisher Combination pH Electrode and Orion Research Model 60/A/Digital Ionalyzer.

Microphotographs of cured emulsions were taken for visual inspection of droplet character. The emulsions in autoclaves were emptied into glass beakers and samples were extracted from mid-beaker volume by pipette. The sample was

deposited on a microscope slide beneath a cover glass and illuminated by white light. Flow fields would sometimes occur due to the pressure of the cover glass and/or the convection currents caused by heating from the light source. Once a stationary field had been located, photographs were taken through a Leitz-Wetzlar microscope with KODAK Tech-Pan 100 film.

3.4 Core Preparation

A cement-lined, stainless steel core chamber of 60 cm length and 6.3 cm I.D. was wet packed with unconsolidated sand and vibrated overnight for 12 to 14 hours. This core was then drained and dried by blowing air through it, again overnight. The core would then be evacuated and saturated with electrolyte water to determine the pore volume. Electrolyte water consisted of 0.18 g/ℓ of KCl and 0.121 g/ℓ of $NaHCO_3$ to simulate reservoir connate water. Permeability was determined using Darcy's Law by flowing this water through the saturated core. The water was in turn displaced by oil using a Ruska pump to a residual water saturation.

Core holders were packed to produce homogeneous linear models of 60-120 mesh (233-130 μm) and 20-40 mesh (833-130 μm) Ottawa silica sand. Heterogeneous linear models were created by simultaneously packing both sand sizes in the same core holder separated by a thin vertical strip. After packing the strip was removed resulting in two parallel sand beds of different permeability. Oil was

displaced through the model vertically downward to take advantage of the density difference between the oil and water during oil saturation of the model. Oil was injected into the model at the slowest rate possible (25 cm^3/hr) to ensure an even displacement through the two layers.

3.5 Steam/Emulsion Flood Apparatus

The core holder was mounted in the steam/emulsion injection apparatus as shown by the schematic diagram in Figure 3.1. The model was in the horizontal position so that the two sand beds were side by side. The core holder and all lines were fully insulated accompanied by thermocouples and pressure transducers. Externally produced emulsions were constantly stirred and preheated to 100 °C prior to injection into the core. Emulsion was injected into the core by two methods: using a pressure regulator with a gas source for a constant pressure displacement and using a Ruska pump for a constant rate displacement of 650 cm^3/hr. Water was displaced by a Ruska pump through the boiler to the inlet core face. The steam temperature attained at the inlet core face was dependent on the flowrate through the boiler. Condensate was bled from the interior of the core face controlled by a back pressure regulator. There were three injection ports located on the inlet flange space. The ports were evenly spaced along the vertical axis through the center of the flange at 1.58, 3.15, and 4.73 cm along the 6.3 cm inner diameter. Emulsion injection was through the

top port. Steam injection and condensate drainage occurred through the center and bottom injection ports, respectively. Maximum system operating conditions were 200 °C and 1380 kpa (200 psi). Production fluids were condensed, collected in graduate cylinders, weighed, and distilled in toluene to determine the respective oil and water contents of produced crude oil and emulsion.

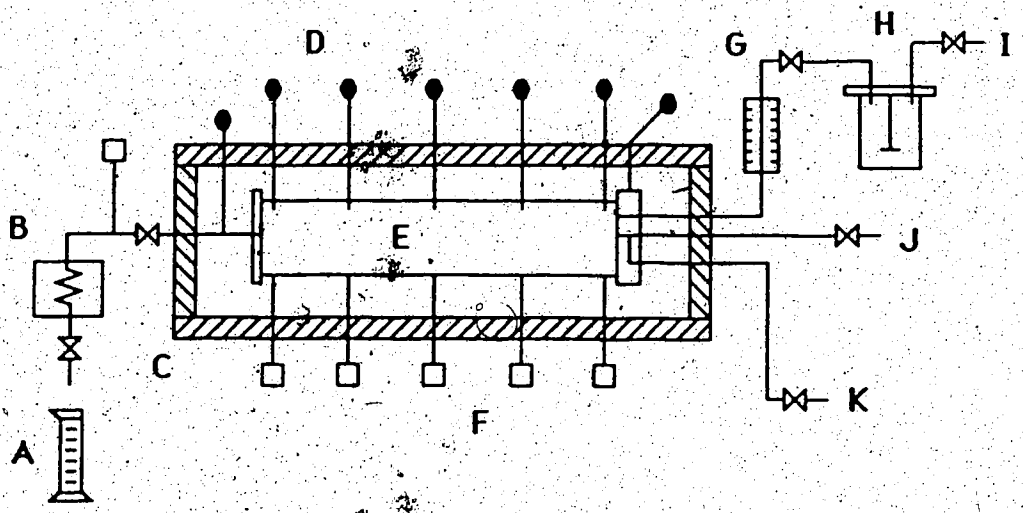

A	COLLECTION GRADUATE	G	HEATED OIL BATH
B	CONDENSER ASSEMBLY	H	EMULSION STIRRER
C	INSULATION	I	DISPLACING PUMP / REGULATOR
D	THERMOCOUPLES	J	STEAM INJECTION
E	CORE HOLDER	K	CONDENSATE BLEED
F	PRESSURE TRANSDUCERS		

Figure 3.1 - Schematic Diagram of Steam / Emulsion Injection Apparatus

4. RESULTS AND DISCUSSION

The following discussion deals with the examination of the thermal stability of heavy oil emulsions and application of optimally stabilized emulsions to block high permeability channels created during steam injection.

4.1 Thermal Stability of Heavy Oil Emulsions

In this section, the thermal stability of a 5% Primrose and Lloydminster heavy oil emulsion was screened using both an anionic (Vista 250) and a nonionic (Triton X-100) surfactant. Visual observations of droplet character and the emulsion pH behavior at different surfactant concentrations of 25, 50, 100, 300, 700, 1200, 2000, and 5000 ppm at cure temperatures of 25, 75, 125, 175, and 225 °C were the criteria used to determine stability.

Microphotographs of the Lloydminster oil/Triton X-100 surfactant group of emulsions are presented in Appendix A. Photographs have been produced at a magnification of 900x. Plate A.1 shows an oil-in-water emulsion cured at 25 °C for one hour with a 25 ppm surfactant concentration. In Plate A.1, droplet size ranged from 1-7 μm with the majority of droplets in the 1-3 μm range. Plate A.2 shows an emulsion with the same surfactant concentration cured at 75 °C. The density of droplet numbers is noticably less with the larger droplets having creamed out of the aqueous phase. Plate A.3 and A.4 are microphotographs of 25 ppm emulsions at cure temperatures of 125 and 175 °C, respectively. The density

and droplet size appears reduced due to coalescence and creaming of the larger drops occurring to a greater extent than at the lower cure temperatures. Finally, in Plate A.5, it can be seen that for a cure temperature of 225 °C with a surfactant concentration of 25 ppm, an almost complete demulsification has occurred.

This trend of increasing demulsification with increasing cure temperature is also evident for emulsions created with higher concentrations of Triton X-100 surfactant. For example, Plates A.11 through A.15 show photos of emulsions with 100 ppm cured at increasing temperatures. Plate A.11 shows an o/w emulsion cured at room temperature with a droplet size ranging from 1.5-4 μm. Oil droplets with internal water droplets (i.e. w/o/w emulsion) occur frequently. In contrast, Plate A.15 shows a 100 ppm emulsion cured at 225 °C where the majority of droplets have coalesced and creamed out of the aqueous phase. There is no evidence of w/o/w emulsion droplets. A possible explanation, for the abscence of dual emulsions, is that the increase in temperature has increased the coalescence rate of internal droplets along with a change in osmotic pressure across the interface thus leading to diffusion outward of the interior water.

Oil-in-water emulsions created with the highest concentration of surfactant used are shown in plates A.36 through A.40. Plate A.36 shows an emulsion (5000 ppm, 25 °C) with a uniform droplet size in the range of 0.5-2 μm. No

occurrence of w/o/w emulsion droplets is visually evident. Plate A.38 shows an emulsion (5000 ppm, 125 °C) with decreasing droplet density and increasing droplet size due to coalescence. The majority of droplets shown are in the 1.5-2.5 μm range with droplets present as large as 4 μm. Plate A.39 and plate A.40 show emulsion breakage at cure temperatures of 175 °C and 225 °C, respectively.

The change in pH for emulsions measured before and after curing are given in Table A.1 of Appendix A. Final pH values of emulsions are presented in Figure 4.1.1. Emulsions cured at 25 °C and 75 °C exhibit a pH only slightly higher than the original distilled water used in their creation. Above 75 °C it can be seen that the o/w emulsions exhibit an increasingly acidic nature corresponding with increasing demulsification. Thus the emulsion instability observed in the photos for increasing cure temperature correlates well with the solution pH measurement just described.

In an effort to explain what causes the decrease in pH of the emulsion above 75 °C certain control tests were performed. The same autoclaves used for the curing of the emulsions were filled with distilled water at 225 °C for one hour; measurements showed only a slight pH decrease from 7.6 to 7.1.

Control tests performed using emulsions of Lloydminster oil in distilled water with no surfactant added (1% oil content in emulsion realized) showed a pH drop from 7.15 to

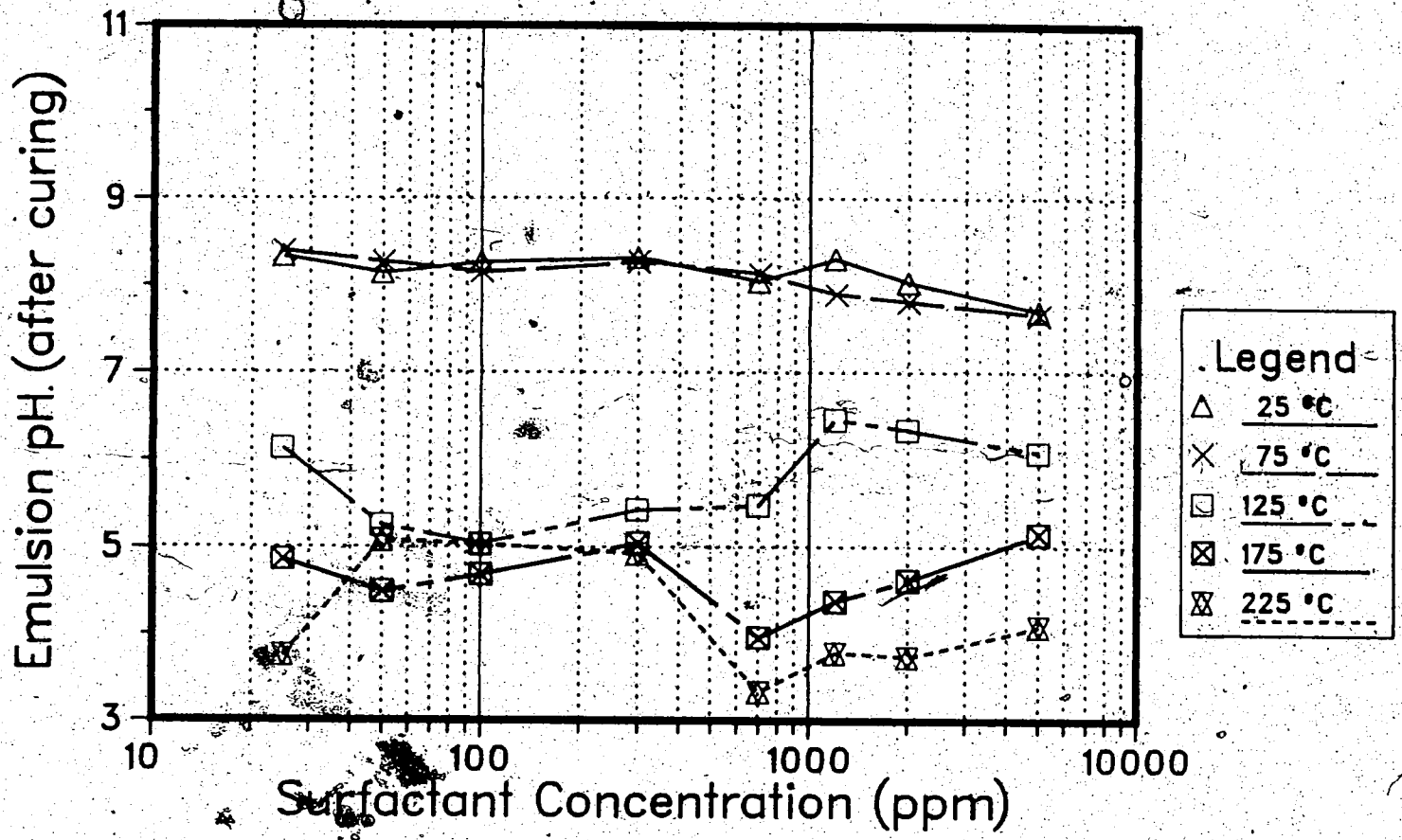

FIGURE 4.1.1 – 5% Lloydminster Oil Emulsion with TX-100 Surfactant
Final Emulsion pH vs. Surfactant Concentration
@ Cure Temperature

6.5 at 225 °C.

Thermal stability of a nonionic surfactant, Igepal CO-850, also an ethoxylated alkyl phenol, has been examined previously (Handy et al., 1982). For heating times on the order of one hour at 180 °C the resulting effective concentration was close to the initial concentration in distilled water. However, control tests performed here on Triton X-100 (all surfactant concentrations, 25-5000 ppm) in distilled water showed a pH change from initial values of 7.5-7.6 to final values of 4.5-5.9. Therefore, it seems likely the nonionic Triton X-100 desolubilized at the cloud point and subsequently dissociated at high temperature resulting in demulsification and an acidic solution.

Microphotographs of Primrose o/w emulsions stabilized with Triton X-100 surfactant are shown in Appendix C. For example, Plate C.11 shows an emulsion with 100 ppm surfactant concentration cured at 25 °C. Measurements indicated droplet sizes to be predominantly in the 1-2 μm range. Plate C.15 shows the corresponding 100 ppm emulsion cured at 225 °C. There is an indication that some coalescence has occurred, but the emulsion was observed to be stable with little creaming.

The influence of higher surfactant concentration is exemplified by Plate C.36 which shows an emulsion produced by 5000 ppm of Triton X-100 and cured at 25 °C. A uniform droplet size of 0.5-1 μm was found for this emulsion. Few instances of w/o/w emulsion droplets were observed at the

higher concentrations of surfactant. Apparently, the smaller diameter droplets and tighter interfacial packing of surfactant molecules would not allow the inclusion of water droplets. Increased coalescence may be observed in Plate C.40 (5000 ppm, 225 °C) with droplet diameters present as large as 6 μm.

Changes in pH data for the Primrose heavy oil emulsions are given in Appendix C. Final pH values of emulsions after curing are presented in Figure 4.1.2. It can be seen from the figure that emulsion pH is maintained to a higher degree than the Lloydminster oil / Triton X-100 emulsions. Final pH for the Primrose emulsions is generally close to a value of 9 until cure temperatures in excess of 175°C were experienced. A drop in pH value is then indicated for all surfactant concentrations.

The maintenance of emulsion pH close to its original value at higher cure temperatures is correlatable with the maintenance of emulsion stability observed in the microphotographs. Although the reason is not clear, apparently certain constituents in the Primrose oil have suppressed the desolubilization and dissociation of surfactant which readily occurred at high temperatures when using the Lloydminster oil. From this different response encountered when using a different oil with the same surfactant, it can be seen that oil composition has an important role in emulsion stability. Based upon the visual observations and pH behavior, the optimal concentration of

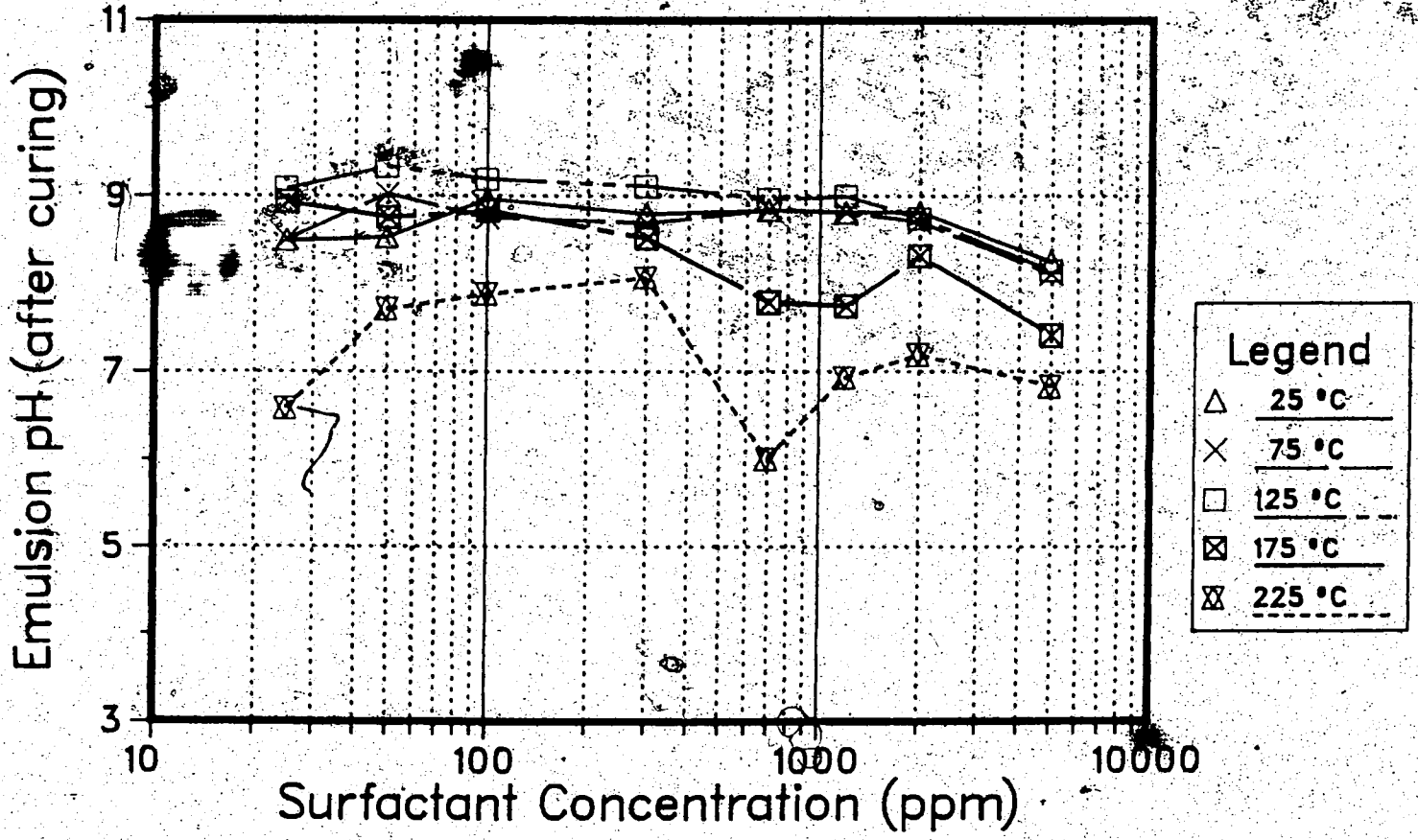

FIGURE 4.1.2 – 5% Primrose Oil Emulsion with TX–100 Surfactant
Final Emulsion pH vs. Surfactant Concentration
◎ Cure Temperature

Triton X-100 for stability of Primrose emulsions is in the 50-300 ppm range.

Microphotographs of Lloydminster oil emulsions created with the anionic surfactant Vista 250 are shown in Appendix B. Plates B.11 through B.15 are indicative of surfactant behavior at lower concentrations. Plate B.11 shows a 100 ppm surfactant cured at 25 °C. Measurements indicate the majority of droplets range from 0.5-2 μm with droplets as large as 10 μm occurring sporadically. Progressing from Plate B.11 through B.15 it can be seen that droplet density is reduced at the higher cure temperatures. Plate B.15 shows a 100 ppm emulsion cured at 225 °C. The majority of droplets are in the 1-3.5 μm range apparently due to coalescence at the higher temperature, but a relatively stable emulsion overall.

Plates B.36 through B.40 show Lloydminster oil emulsions with 5000 ppm Vista 250 surfactant. It can be seen from Plate B.36 that at a cure temperature of 25 °C a high degree of flocculation of oil droplets into aggregates has occurred. Plate B.40 shows that at a higher cure temperature the aggregates of oil droplets are flocculating and coalescing.

Study of the thermal decomposition of Vista 250 surfactant has been conducted previously, (Maini and Ma, 1985) and determined to follow a first order kinetic model:

$$ArSO_3^- + H_2O \rightarrow ArH + SO_4^{-2} + H^+ \quad (16)$$

Consequently, for each sulfonate molecule decom[illegible] one hydrogen ion was generated. Surfactant dissociation would therefore result in emulsion instability and a more acidic emulsion pH due to the above reaction.

Emulsion pH response to curing is shown in Figure 4.1.3 for the Lloydminster oil/Vista 250 surfactant group. It may be seen from the figure that, for all surfactant concentrations, emulsion pH was maintained until cure temperatures of 225 °C were experienced. This suggests the Vista 250 surfactant was stable until at least 175 °C. However, examination of all the plates for emulsions with surfactant concentrations of 700 ppm and greater show that emulsions were not stable regardless of the cure temperature. In other words, the surfactant was stable but the emulsions were not.

A possible reason for this was the presence of inorganic salts and impurities in the commercial sulfonate which have altered the interaction potential energy curve of the system so that flocs may be formed readily in the secondary minimum leading to coalescence and emulsion breakage. Thus, on the basis of emulsion stability observed in the microphotographs and emulsion pH behavior, the optimal surfactant concentration for this emulsion-surfactant group was in the 50 to 300 ppm range.

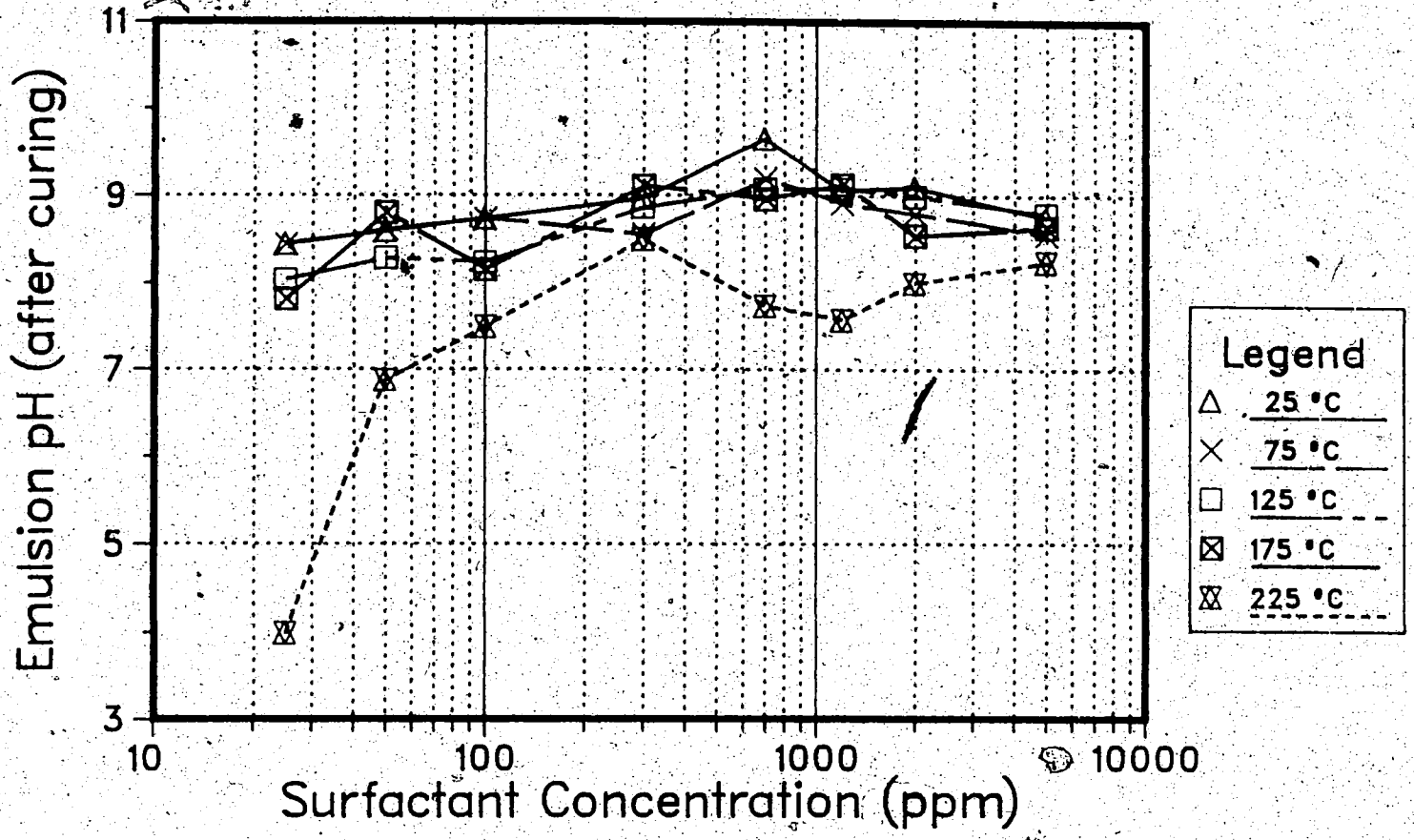

FIGURE 4.1.3 – 5% Lloydminster Oil Emulsion with Vista 250 Surfactant
Final Emulsion pH vs. Surfactant Concentration
@ Cure Temperature

Microphotographs and change in pH data of the Primrose heavy oil emulsions created with Vista 250 surfactant are presented in Appendix D. This series of photographs is one quarter the magnification (i.e. .225x) of previous photographs. Plates D.1 through D.15 are indicative of emulsion behavior at low surfactant concentrations. For example, it can be seen from Plate D.11 (100 ppm) that, there were some very large droplets present in this emulsion. Droplet size typically has a bimodal distribution with droplets mainly in the 2-4 μm and 10-16 μm range. Some droplets as large as 25 μm were present. Progressing from Plates D.11 through D.15 it can be observed that droplet density and size was reduced at higher cure temperatures. Plate D.15 shows that after high temperature curing the larger droplets have creamed out leaving a more uniform droplet size distribution in the range of 2-8 μm.

At higher concentrations of Vista 250 surfactant (e.g. 1200 ppm, Plates D.26-D.30) the oil droplets begin to flocculate into aggregates as the Lloydminster oil did. Plates D.36 through D.40 show the extent of flocculation at 5000 ppm. It may be seen that the aggregates flocculate to form larger aggregates. In general, it appears that droplet density is reduced at the higher cure temperatures as shown by Plate D.40 (225 °C).

Change in emulsion pH data are presented in Appendix D for the Primrose oil/Vista 250 group. Final emulsion pH response after curing is shown in Figure 4.1.4. The pH was

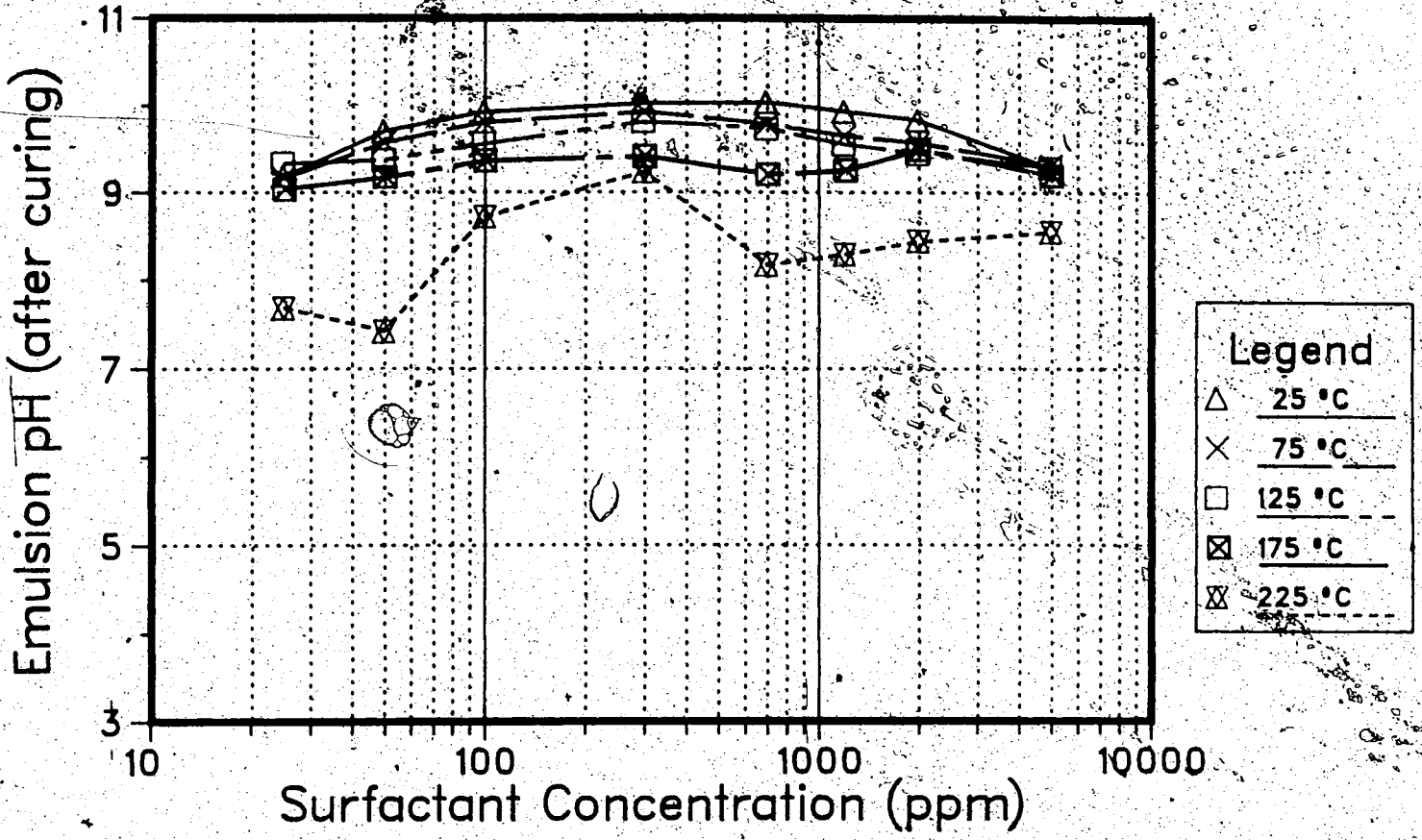

FIGURE 4.1.4 – 5% Primrose Oil Emulsion with Vista 250 Surfactant
Final Emulsion pH vs. Surfactant Concentration
@ Cure Temperature

maintained at a high value (9.5-10.0) with no great drop in pH due to hydrolytic desulfonation until after 175 °C. From emulsion stability observed in the microphotographs and emulsion pH behavior, the optimal surfactant concentration was in the 100-300 ppm range.

On the basis of droplet character and emulsion pH behavior it was determined the anionic Vista 250 should be used in 100 ppm concentrations to create emulsions for the steam blockage experiments.

4.2 Steam/Emulsion Injection into Porous Media

Several horizontal, steam displacement tests were performed using the unscaled linear model depicted in Figure 3.1. The first four tests were base runs with homogeneous sand packs comparing recovery response using two heavy oils in combination with two sand sizes. The permeability was roughly 2 to 3 times greater for the 20/40 mesh than the 60/120 mesh sand. The second series of tests was carried out to examine the recovery from heterogeneous sand packs consisting of two parallel sand beds. In this series of tests externally produced emulsion was injected to block the more permeable channels created by steam in the heterogeneous model. The blocking agent was then followed by steam to improve conformance and ultimate recovery.

Initially, for all tests, steam was injected into highly oil saturated cores at 200°C and 1380 kPa. Condensate was drained at the inlet face to maintain applied steam as

close to the saturated vapour state as possible. Steam front movement was observed through thermocouple readings along the core length. Porosity of all sand packs was in the 35-40% range.

At the beginning of the tests it was typical that clean water and crude were produced until steam breakthrough which would occur at 2.5 to 3 pore volumes of total fluid produced. After steam front breakthrough, production consisted of crude and an oil-in-water emulsion. The system was allowed to blowdown to a pressure of 207 kPa (30 psig) with the production outlet open to atmospheric conditions. Steam injection was continued at the maximum temperature obtainable of 140 °C with a maximum injection rate of 1560 cm^3/hr of equivalent water. Steam injection was continued for 1-2 pore volumes until only a very low oil content emulsion or essentially clean water was produced and further steaming resulted in essentially no further recovery. Three pressure pulse drawdown cycles up to 1380 kPa (200 psig), 200 °C and down to 207 kPa (30 psig), 140 °C were performed totalling one pore volume, to try to scavenge more oil. Experimental data and production results for all runs are presented in Appendix F.

Table F.1 contains the results of a base steamflood run in 60-120 mesh sand containing Lloydminster oil. Absolute permeability was 12.9 darcies. Initial oil saturation was 96.7%. For Run #1 (and typically for all the runs) initial oil recovery was very slow until the hot condensate

preceding the steam front advanced through the model resulting in general oil mobilization. From Table F.1, it can be seen that water content in the crude was relatively low at 23.4% increasing to 71.7% at steam breakthrough. This occurred after five hours of steaming and 2.81 pore volumes of fluid produced. Prior to steam breakthrough water-oil ratios were close to 2 but increased dramatically after breakthrough. The oil production rate peaked at 410 cm^3/hr prior to steam breakthrough as oil mobility was improved considerably through viscosity reduction and distillation effects which would occur with the steam drive process. The cumulative oil recovered at steam breakthrough was 87.1% of the initial oil in place (IOIP). After breakthrough, the fluid production consisted of small amounts of crude with 95.1% water content and a light colored oil-in-water emulsion which was not distilled. Final cumulative oil recovery was 87.4%. Pressure cycling recovered only a small amount of oil in this instance.

Table F.2 contains the sand pack characteristics and production results for a base steamflood run in 20-40 mesh sand containing Lloydminster oil. Absolute permeability was 38.7 darcies. Initial oil saturation was 95.6%. Steam breakthrough was achieved after 3.15 hours of steaming and 2.88 pore volumes of fluid produced. The oil production rate peaked at this time at 600.53 cm^3/hr. Clean water and crude, which separated easily, were produced prior to steam breakthrough. Afterwards small amounts of crude and a light

colored oil-in-water emulsion were produced due to further steaming and pressure cycling. This increased the recovery from 89.2% (IOIP) at breakthrough to 95.2% (IOIP) at the conclusion of the run.

Table F.3 contains the sand pack characteristics and production results for a base steamflood in 60-120 mesh sand containing Primrose oil. Absolute permeability was comparable to Run #1 at 14.3 darcies. Initial oil saturation was 97.6%. This oil had a higher viscosity of 45700 cp and as a result steam breakthrough was achieved after 11 hours and 2.44 pore volumes of produced fluid. Oil recovery at this time was 71.7% (IOIP). The oil production rate was 1258 cm^3/hr just before steam breakthrough. Primrose oil saturated cores would produce at a higher oil rate than the Lloydminster oil just prior to breakthrough. In contrast the Lloydminster oil saturated cores produced at a higher average oil production rate than the Primrose oil from the start of steaming for the same applied pressure and steam temperature. Evidently the hot condensate preceding the steam front through the core was not as effective at mobilizing the Primrose oil as the Lloydminster oil (at this temperature and pressure). It was not until the steam front had advanced along almost the entire core length that general mobilization of the Primrose oil occurred. This resulted in the sudden production of large amounts of higher water content crude. Clean water was produced up until this time followed by an oil-in-water emulsion having a 1.8 wt %

l content. At this point of the base steamflood the Primrose oil would generally yield an emulsion with a higher oil content than the Lloydminster oil. This was indicative of the superior emulsion stabilizing characteristics associated with the Primrose oil. Pressure cycling was started after 4.23 pore volumes of fluid produced to yield 2.2% of the cumulative oil production. Final oil recovery was 82.0% after 6.49 pore volumes of fluid produced.

Table F.4 contains the sand pack characteristics and production results for a base steamflood in 20-40 mesh sand containing Primrose oil. Absolute permeability was 33.9 darcies. Initial oil saturation was 89.2%. Steam breakthrough occurred after 5.25 hours and 2.4 pore volumes of produced fluid. The oil recovery at breakthrough was 75.2% (IOIP). The oil production rate was 944.6 cm^3/hr at this point. Following breakthrough an oil-in-water emulsion with 3.6% oil content was produced. Final recovery was 86.0% (IOIP) after 4.88 pore volumes of throughput.

A summary of sand pack characteristics and saturation results is provided in Table 4.1. Graphs showing cumulative oil recovery versus cumulative fluid produced for the different sand sizes are shown in Figure 4.2.1 and Figure 4.2.2 for the Lloydminster and Primrose oil, respectively. Lower residual oil saturations are shown in Table 4.1 for the higher permeability sand under steam displacement. After the same volume of throughput for all runs (4PV), oil recovery was 5 to 10% higher for the 20-40 mesh sand over

TABLE 4.1 - Summary of Sand Pack and Steam Displacement Results

RUN (#)	OIL (type)	SAND (mesh)	k (d)	Swi (%)	Sor^b (%)	Sor_e^c (%)
1	Lloyd.	60/120	12.9	3.3	12.2	
2	Lloyd.	20/40	38.7	4.4	7.3	
3	Prim.	60/120	14.3	2.4	19.8	
4	Prim.	20/40	33.9	10.8	13.6	
5	L.Slug	2 layer	25.3[a]	16.4	19.0	8.78
6	L.Coin	2 layer	23.0[a]	17.0	17.6	18.8
7	P.Slug	2 layer	17.5[a]	11.1	30.9	37.5
8	P.Coin	2 layer	19.8[a]	12.2	25.3	40.1
9	L.Slug	2 layer	18.9[a]	7.2	13.8	9.1
10	L.Slug	2 layer	17.6[a]	7.3	17.0	14.2
11	L.Slug	2 layer	21.9[a]	6.9	22.2	19.2

NOTES:
(a) Measured average permeability.
(b) Residual oil saturation in model after four (4) pore volumes of fluid produced from initial steaming.
(c) Residual oil saturation after emulsion injection and chase steam.

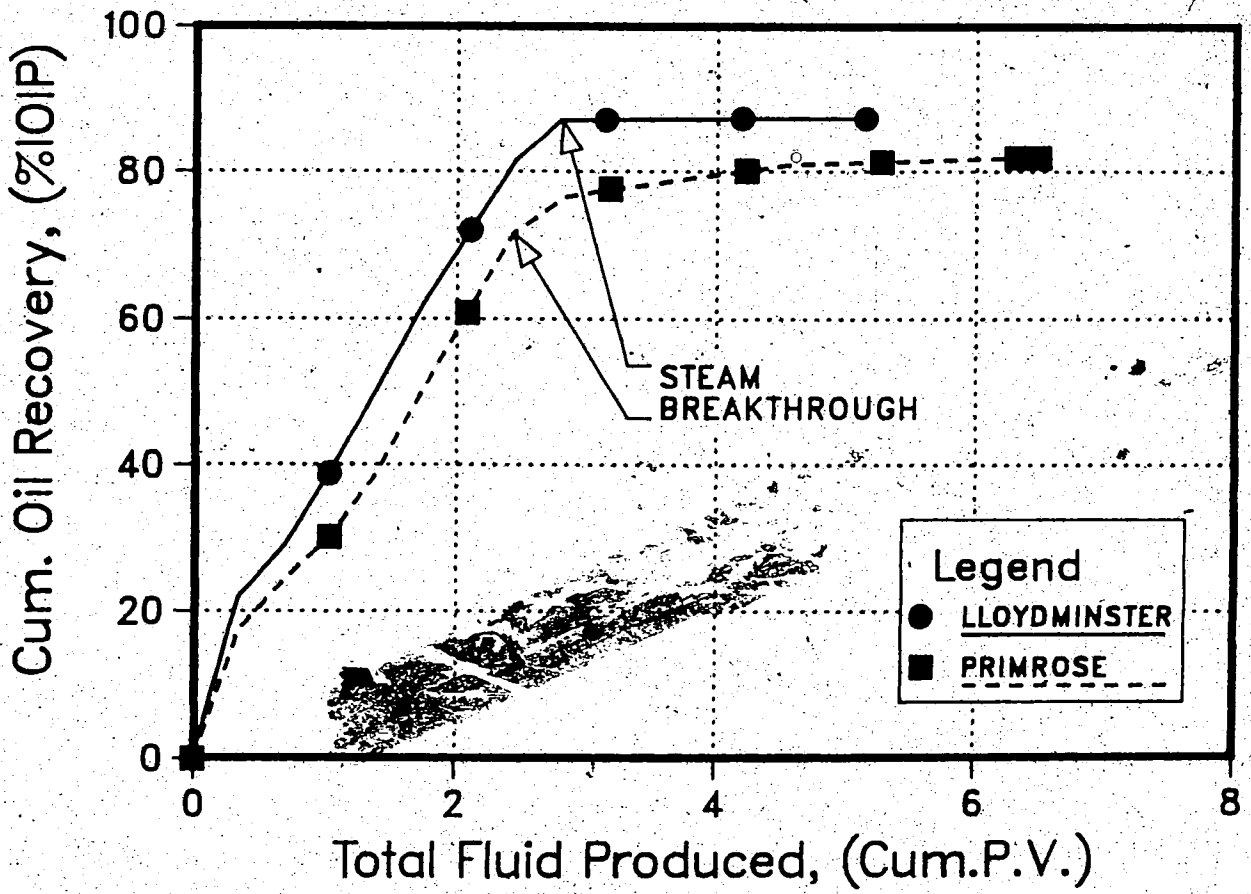

FIGURE 4.2.1 – Base Steamflood : 60–120 Mesh Sand (Runs 1 & 3)
Cumulative Oil Recovery vs. Total Fluid Produced

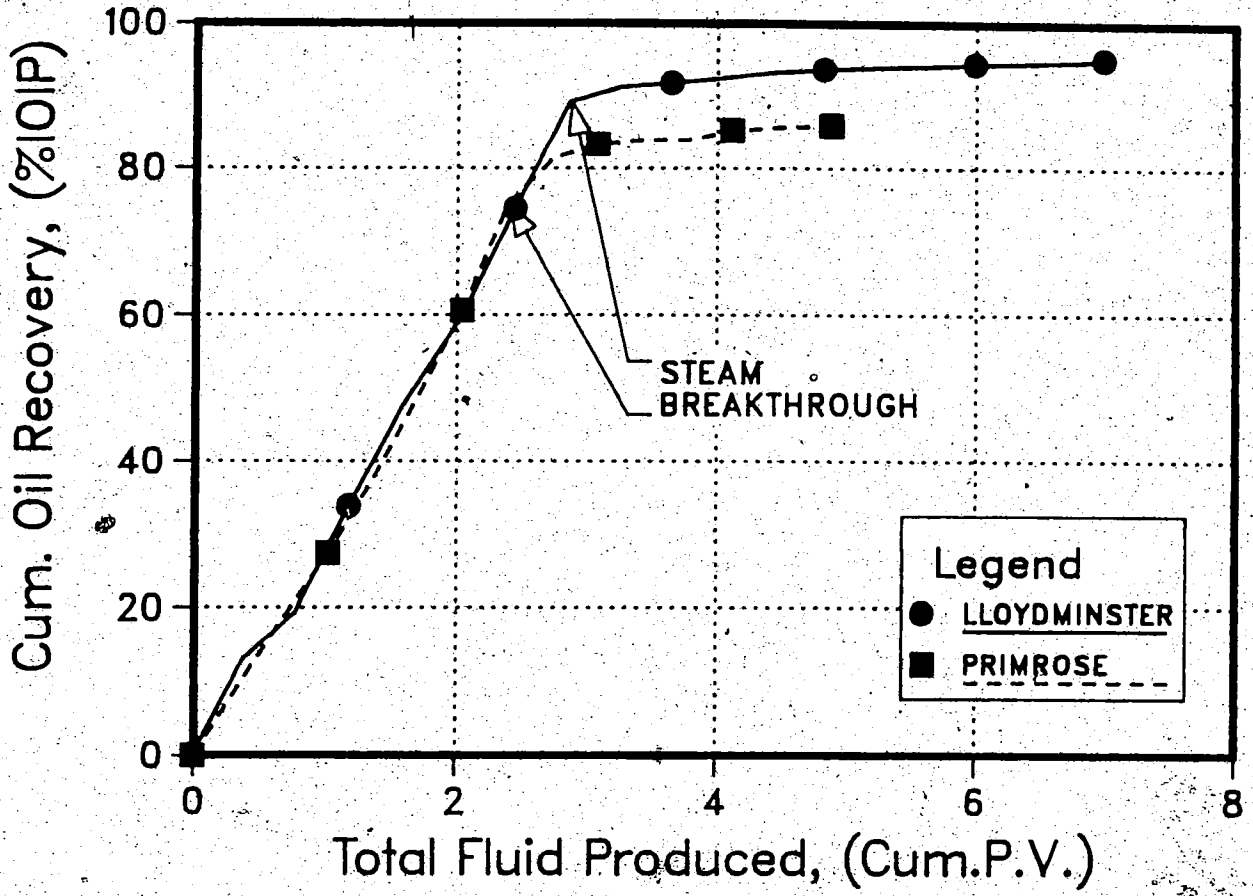

FIGURE 4.2.2 – Base Steamflood : 20–40 Mesh Sand (Runs 2 & 4)
Cumulative Oil Recovery vs. Total Fluid Produced

the less permeable 60-120 mesh. Residual oil saturations at 4 pore volumes of throughput were found to vary from 12.2 to 19.8% and 7.3 to 13.6% for the same two sands. As well, for the more viscous Primrose crude, the residual oil saturation was approximately 8-10% higher than the Lloydminster oil runs in all instances. These results compared favourably with those previously reported by Closmann et.al. (1983).

On post-run core inspection, (Runs 1,2,3, and 4) a relatively clean sand with little oil staining was generally found along the top 1/2 to 3/4 of the cross-sectional area of the core. Apparently, gravity override of steam in the model was present to a certain extent.

Steam displacement tests were performed on heterogeneous models in Runs 5 through 8 (see Table 4.1) prior to emulsion injection. Detailed experimental data and production results are presented in Table F.5 through Table F.8 in Appendix F. Initial water saturations were 10 to 15% higher than for homogeneous sand packs. This was due to the flooding procedure and is always a difficulty encountered when trying to saturate a stratified model. All runs were steamed to residual oil saturations which were 50 to 150% greater than their homogeneous sand pack counterparts. It was evident from the lower oil recoveries, earlier steam breakthrough times, and post-core inspection of the heterogeneous model, that steam/condensate had preferentially channeled through the higher permeability sand bed leaving a finite amount of oil unrecovered. These

heterogeneous sand packs underwent steam displacement and pressure cycling in a similar procedure as was used with the homogeneous sand packs.

At this point, the emulsion heated to 100°C was injected into the core. In Runs 5 and 7, slugs of the emulsions made up of 5% Lloydminster and Primrose oil were injected into the cores containing the same residual oil. Table F.5 and F.7 show detailed production results for these respective runs. Figure 4.2.3 shows the net cumulative oil recovery versus total fluid produced for these two runs. The net cumulative oil recovery was based on initial and post-injected oil-in-place. Cumulative oil recovery (see Table values, Appendix F also) increased in a normal fashion until the emulsion was injected. The net cumulative oil recovery was seen to decline at this point, as injection of emulsion amounts to the addition of oil back into the system which was not totally offset by the oil production. It may be inferred from the slope of the decline in Figure 4.2.3 that a high degree of oil droplet filtration and blockage was occurring. This conclusion was supported by microphotographs of fluid produced during emulsion injection, showing only small numbers of oil droplets.

For slug injection, the emulsion was injected at a constant pressure of 138 kPa (20 psig) with the production end open to atmospheric conditions. The change in flow rate was observed with constant pressure drop across the core so that a pseudo-total fluid mobility was calculated as an

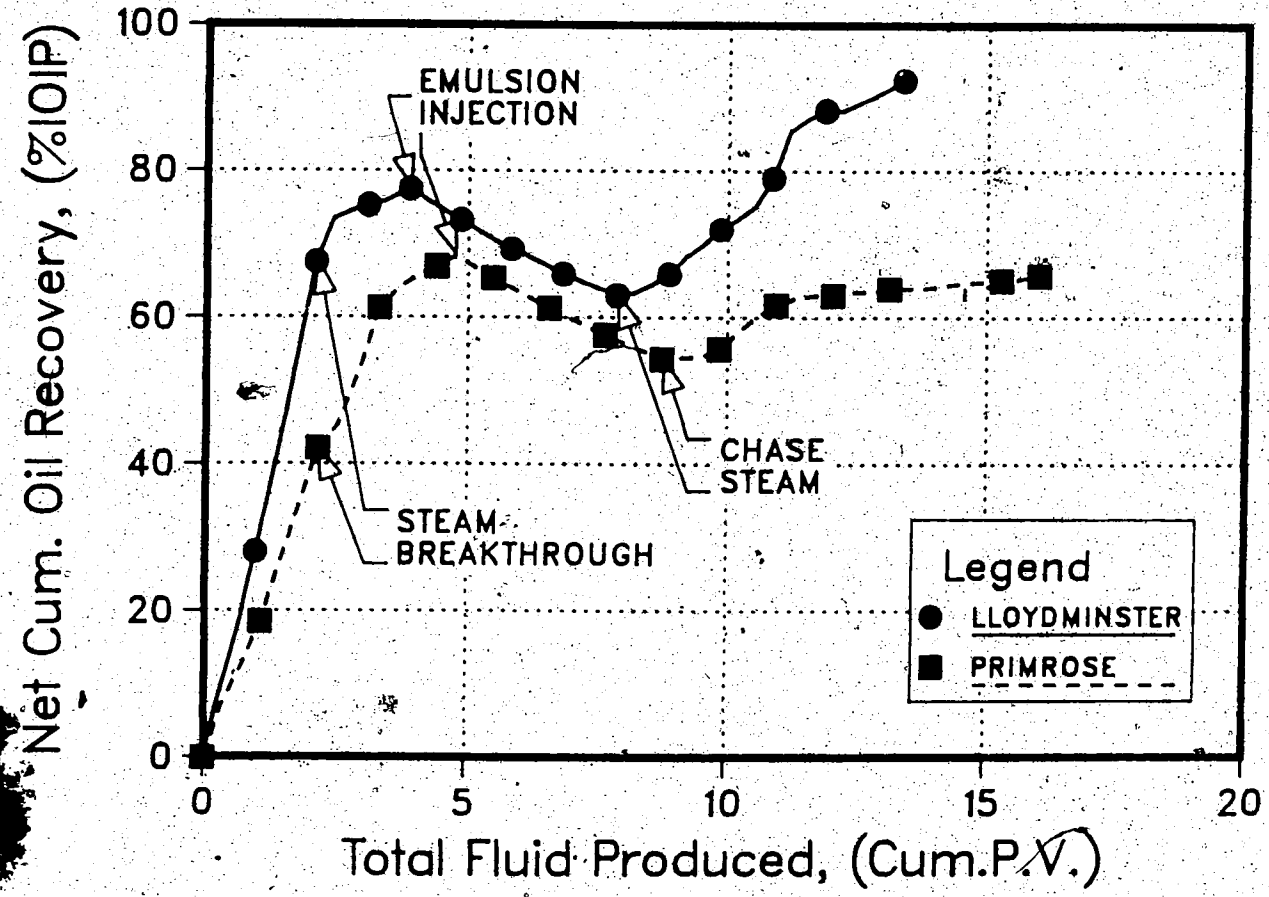

FIGURE 4.2.3 – Steamflood / Emulsion Block : Slug Injection (Runs 5 & 7)
Net Cumulative Oil Recovery vs. Total Fluid Produced

indication of blockage from Darcy's Law, i.e.,

$$(k/\mu)_p = \frac{q \cdot L}{\Delta p \cdot A} , \qquad (17)$$

The reduction in pseudo-mobility from the start of the emulsion injection is shown in Figure 4.2.4. After one pore volume, the pseudo-mobility of fluid produced through the Primrose oil core in Run #7 was 2.5 times less than the Lloydminster value. This was possibly due to the more viscous Primrose oil droplets not being dislodged as easily from the pore throats as the Lloydminster oil under the same applied pressure. After 2 pore volumes of slug injection, a limiting value in pseudo-mobility was attained which was characteristic for this applied pressure drop. This limiting value represents a 90% reduction in pseudo-total fluid mobility from the start of the emulsion injection.

Viscosity measurements of the oils and their emulsions used in this study are presented in Appendix E. Figure E.2 depicts the variation of absolute viscosity of 5% Primrose and Lloydminster oil emulsions with temperature at atmospheric pressure. Measurements indicated the viscosity of these relatively low oil content emulsions was very close to that of water at elevated temperature with only a slight non-Newtonian behavior. Therefore, one would expect permeability to be reduced to the same relative degree as was observed for the pseudo-total fluid mobility.

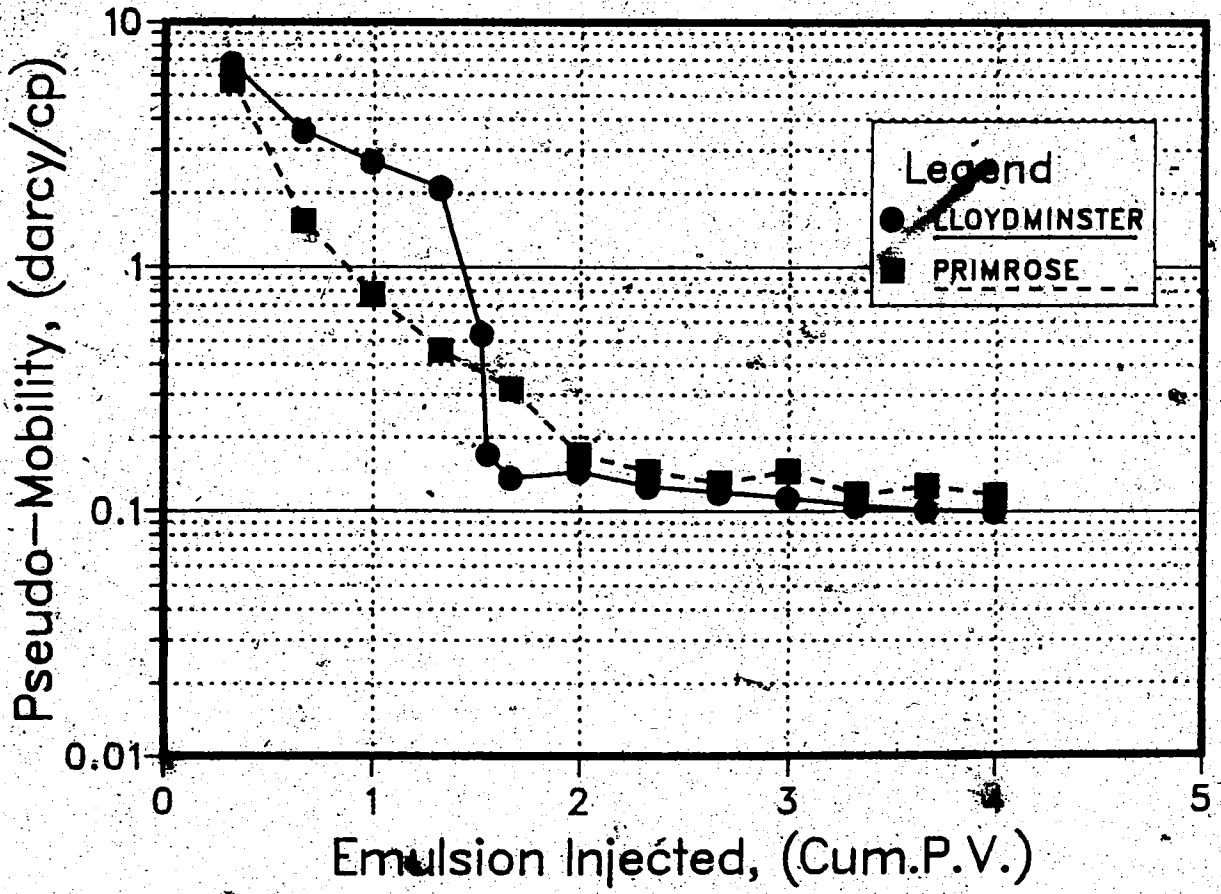

FIGURE 4.2.4 – Mobility Reduction / Emulsion Slug Injection (Runs 5 & 7)
Pseudo–Fluid Mobility vs. Emulsion Injected

From Figure 4.2.3 it can be seen after four pore volumes of emulsion injection, steam injection was reapplied. Blockage was observed to hold and a steamfront was attained in the core. In Table F.5, it can be seen that chase steam was started with an oil-in-water emulsion being produced for 1-1.5 pore volumes followed by significant amounts of high water content crude and oil-in-water emulsion. Table F.7 shows the results of the Primrose oil run and after roughly 2/3 pore volume of chase steam injected, crude was produced in significant amounts. In both of the above runs the majority of crude to be produced was recovered after 2-3 pore volumes of fluid produced from the start of chase steam. Pressure cycling for one pore volume recovered some crude at the end of the experiment.

For the Lloydminster oil case (Run 5), as can be seen from Figure 4.2.3, all the oil that was injected in the emulsion slug was recovered, and an additional 14.3% more oil above the 77.3% recovery on initial steaming. This amounts to a recovery of 65% of the remaining oil in the model after primary steaming, resulting in a final residual oil saturation (Sor_e) of 8.78% as shown in Table 4.1. From Figure 4.2.3 and Table F.7 it can be seen for the Primrose oil emulsion (Run 7) followed by chase steam the final recovery obtained reached only 66.4%, which was very close to that obtained during the primary steaming stage (i.e. 68.2%). It is understood the recovery of the more viscous Primrose oil would be lower than for the Lloydminster oil at

the same input of thermal energy (steam at 200°C, 1380 kPa).

Results of recovery due to the emulsion co-injected with the steam are shown in Figure 4.2.5 (see also Table F.6 and F.8). Recoveries due to primary steaming were 79.5% and 72.4% (IOIP) for the Lloydminster (Run 6) and Primrose oil (Run 8), respectively. Four pore volumes of 5% oil-in-water emulsion were co-injected with four pore volumes of steam both at a constant injection rate of 650 cm^3/hr. Blockage was observed to occur for short times by pressure drop increases in the core indicated by transducer readings. From Figure 4.2.5 it can be seen the slope of the line after starting co-injection was not as great as with the slug injection case. To explain the different response it was noted that during co-injection of emulsion and steam, crude was being produced during the emulsion injection period (see Table F.6). This production of crude then offset the amount of crude being injected back into the model in the form of emulsion. In comparison, for the slug injection case significant amounts of crude were not produced until after chase steam was applied. This gave a lower net cumulative recovery and accounts for the greater slope of the curve.

The Lloydminster oil case (Run 6), produced small amounts of crude and oil-in-water emulsion during co-injection. This amounted to 41% of the emulsion oil injected during co-injection. Following with chase steam and pressure cycling resulted in a final recovery of 82.8% or 3.3% more oil than after primary steaming. The Primrose oil

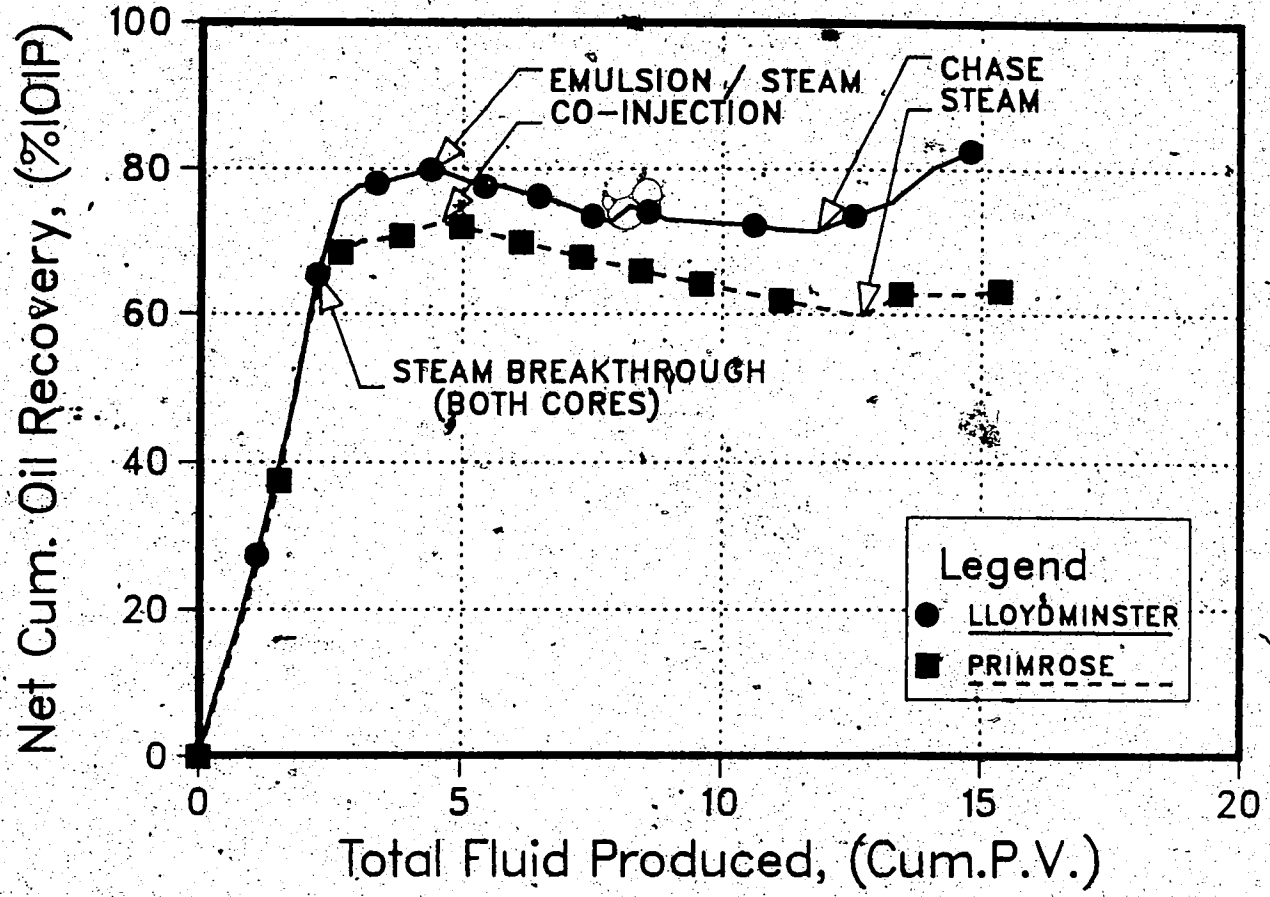

FIGURE 4.2.5 – Steamflood / Emulsion Block : Co-Injection (Runs 6 & 8)
Net Cumulative Oil Recovery vs. Total Fluid Produced

case (Run 8) produced a light colored oil-in-water emulsion and no measurable amounts of crude during co-injection (see Table F.8). Following with chase steam produced no measurable amounts of oil. The pressure cycling action produced some crude giving a final oil recovery of 63.5%.

Final oil recoveries for the emulsion slug followed by steam were higher than the co-injection of emulsion and steam for both oils. This was likely due to the high mobility of the steam preferentially displacing the emulsion from the more permeable paths during co-injection so that emulsion blockage was not fully effective. Following then with chase steam did not result in a displacement as efficient as compared to the slug injection case.

Runs 9 through 11 were performed to evaluate the blocking effectiveness and improved recovery when using a smaller emulsion slug size. This was evaluated using Lloydminster oil only and graphs of net cumulative oil recovery versus total fluid produced are shown in Figures 4.2.6 through 4.2.8. Detailed experimental data and production results are presented in Tables F.9 through F.11.

In Figure 4.2.6 (Run 9) it may be seen that after four pore volumes from initial steaming, an emulsion slug of one half pore volume was injected at a constant rate of 650 cm³/hr. This was then followed by chase steam. After steam injection and pressure cycling the residual oil saturation was reduced from 13.8 % after primary steaming to 9.1% (see Table 4.1).

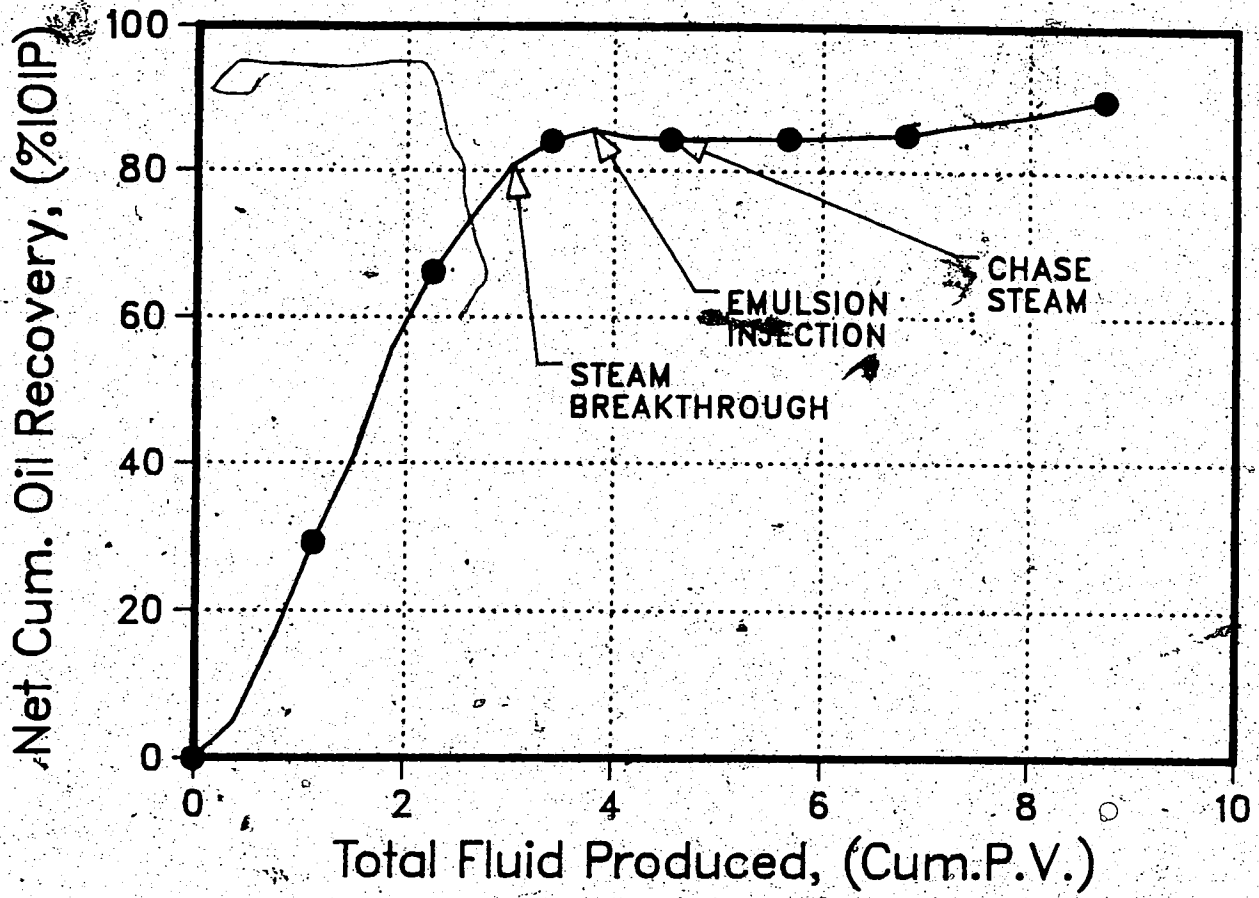

FIGURE 4.2.6 – Steamflood / Emulsion Block : Run 9
Lloydminster Oil: Slug=0.5 PV @Const.Rate
Net Cumulative Oil Recovery vs. Total Fluid Produced

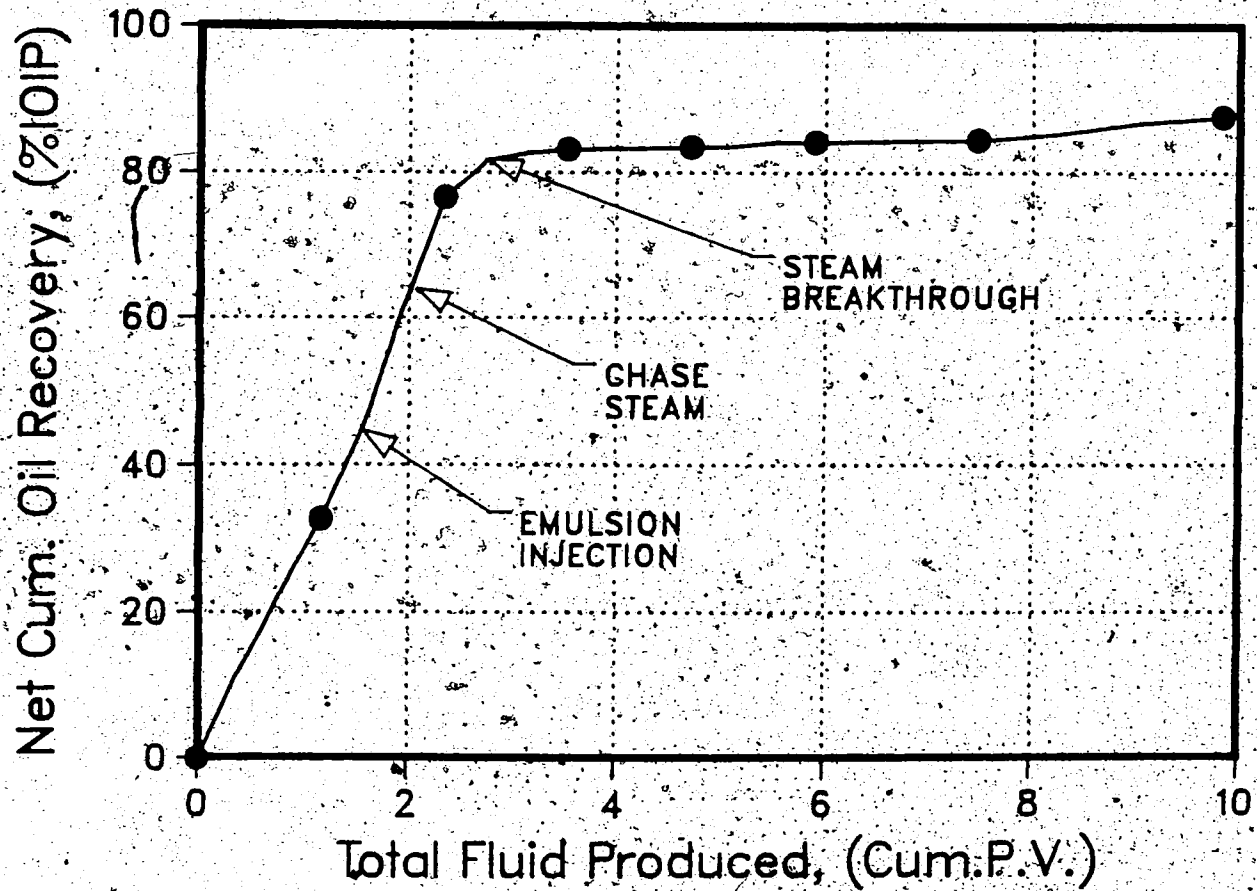

FIGURE 4.2.7 – Steamflood / Emulsion Block : Run 10
Lloydminster Oil: Slug=0.5 PV @Const.Rate
Net Cumulative Oil Recovery vs. Total Fluid Produced

In Figure 4.2.7 (Run 10) it may be seen that the emulsion injection was started well before steam breakthrough. After one half pore volume of emulsion injection, chase steam was started. In this instance, (because it is prior to steam breakthrough), the emulsion slug was subjected to the maximum system operating temperature and pressure of 200 °C and 1380 kPa.

In Figure 4.2.8 (Run 11) it may be seen that one half pore volume of emulsion was injected after four pore volumes of fluid were produced. This time the emulsion was injected with a constant pressure drop across the core of 207 kPa (30 psig). After steam injection and pressure cycling the residual oil saturation was reduced from 22.2% after primary steaming to 19.2%. The injection pressure was perhaps too high in this case causing the smaller slug to travel too quickly through the core model. A lower injection pressure of 69 kPa (10 psig) may allow the smaller emulsion slug to filter in a more thorough manner through the model leading to improved blocking effectiveness.

In the application of the emulsion created for use as a blocking agent, the emphasis of the research was to investigate the effectiveness of the blocking agent and system response. Since the experiments were conducted using an unscaled model, significance should not be placed on the magnitude of the recovery parameters. For example, in Table 4.1 it can be seen that the residual oil saturation after emulsion injection and chase steam was greater than after

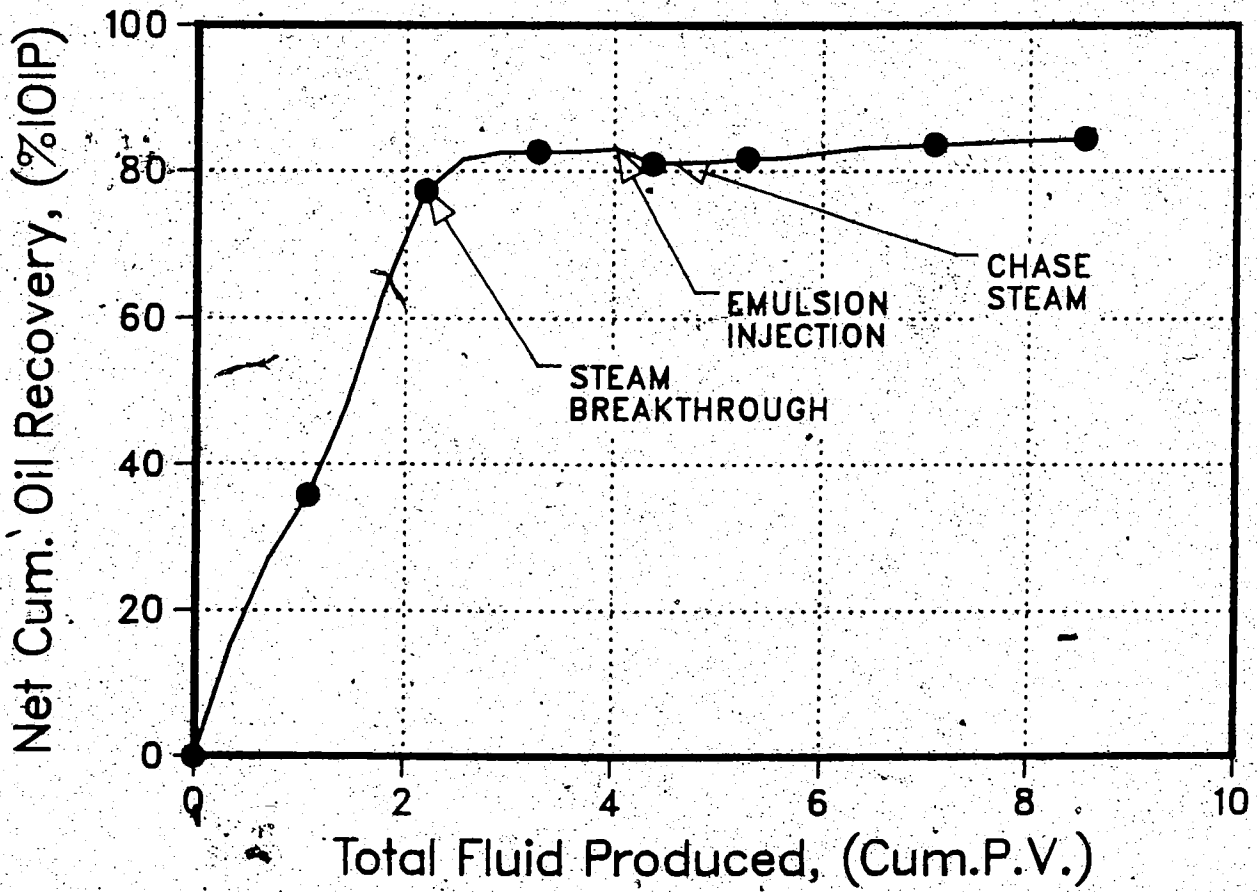

FIGURE 4.2.8 – Steamflood / Emulsion Block : Run 11
Lloydminster Oil: Slug=0.5 PV @Const.Pressure
Net Cumulative Oil Recovery vs. Total Fluid Produced

primary steaming for Runs 7 and 8. However, from Figure 4.2.4, it can be seen that the Primrose oil emulsion was just as effective at reducing the pseudo-total fluid mobility as the Lloydminster oil emulsion. Therefore, the lower oil recoveries (higher residual oil saturations) for the Primrose oil runs do not reflect on the blocking effectiveness of emulsion created with the Primrose oil. This response was due to a system limitation which confined the steam temperature and pressure to be the same as that applied in the Lloydminster oil runs. Under these constraints the Lloydminster oil would be mobilized to a higher degree than the more viscous Primrose oil.

The results of this thesis suggest improved oil recovery might be obtained from a stratified or a heterogeneous reservoir by the injection of a macroemulsion slug followed by steam, resulting in a diversion of the steam into previously unswept regions of the porous media. No attempt was made to examine the economic viability of the process. This study was directed towards investigating the mechanism of possible oil recovery. It is believed this process may have a potential application to a heavy oil reservoir with a bottom water zone as well as stratified or heterogeneous reservoirs.

CONCLUSIONS

Based upon the results obtained from this research work the following conclusions have been formed:

1. Observance of droplet character and solution pH proved to be an effective screening criteria in selecting the proper surfactant type and surfactant concentration for heavy oil emulsion stability at high temperatures.
2. The Primrose oil emulsions created with Triton X-100 responded differently to high temperature curing than the Lloydminster oil emulsions created with the same surfactant. As a result of this response, it is concluded the oil composition will influence emulsion stability due to the interaction between active constituents present in the oil and the surfactant.
3. Optimal emulsion stability was obtained for both Lloydminster and Primrose heavy oils with the anionic Vista 250 surfactant employed in concentrations of 50-300 ppm for temperatures up to 175 °C.
4. Application of a 5% oil-in-water emulsion slug (stabilized by 100 ppm Vista 250 surfactant) was effective in blocking the high permeability channels created in a heterogeneous unscaled laboratory model previously steamed to apparent residual oil saturation.
5. The emulsion, when it is injected as a slug, was a more effective blocking agent than the emulsion when it is co-injected along with the steam. Final oil recovery was higher for both oils when using the slug injection

scenario.

RECOMMENDATIONS

1. Analyse the effect of droplet size on permeability reduction in both water saturated cores and cores containing residual oil.
2. Develop a mathematical model for linear flow of emulsions in water saturated cores and cores containing residual oil accounting for the change in saturation profile and emulsion properties within the core.
3. Categorize the response of oil constituents (e.g. alkane, asphaltene, and resin content) with surfactant type in order to more fully understand the effect of oil composition on emulsion stability.

BIBLIOGRAPHY

Becher, P.: "Emulsions: Theory and Practice", 2nd. Ed., Reinhold Publishing Corp., New York, (1965).

Bennett, H., [redacted] Jr., J.L., and Wulfinghoff, M.E.: "Practical [redacted]sions", Chemical Publishing Company, Inc., New Yo[redacted] (1968).

Cartmill, J.C., and Dickey, P.A.: "Flow of a Disperse Emulsion of Crude Oil in Water in Porous Media", SPE 2481, (1969).

Closmann, P.J., and Seba, R.D.: "Laboratory Tests on Heavy Oil Recovery by Steam Injection", Soc. Pet. Eng. J., (June, 1983), p. 417-426.

Cooke, Jr., C.E., Williams, R.E., and Kolodzie, P.A.: "Oil Recovery by Alkaline Waterflooding", J. Pet. Tech., (Dec., 1974), p. 1365-1374.

Doscher, T.M., and Reisberg, J.: "Oil Recovery From Tar Sands", Canadian Patent No. 639050 (March 27, 1982).

Doscher, T.M., and Ghassemi,F.: "Limitations on the Oil/Steam Ratio for Truly Viscous Crudes", J. Pet. Tech., (July, 1984), p. 1123-1126.

Farouq Ali, S.M.: "Non-Thermal Heavy Oil Recovery Methods", SPE 5893, (1976).

Flock, D.L., Lee, T.H., and Gibeau, J.P.: "The Effect of Temperatures on the Interfacial Tension of Heavy Crude Oils Using the Pendant Drop Apparatus", Petroleum Society of CIM Paper 84-35-33, (1984).

Gillberg, G., and Eriksson, L.: "ph-Sensitive Microemulsions", Ind. Eng. Chem. Prod. Res. Dev., (1980), 19, p. 304- 309.

Hallam, R.J.:"The Flow of Oil-in-Water Emulsions in a Porous

Medium", M.Sc. Thesis, University of Alberta, (1980).

Handy, L.L., Amaefule, J.O., Ziegler V.M., and Ershagi, I.: "Thermal Stability of Surfactants for Reservoir Application", Soc. Pet. Eng. J., (October, 1982), p. 722-730.

Harrison, N.W.: "Diverting Agents - History and Application", J. Pet. Tech., (May 1972), p. 593-98.

Hyne, J.B., Clark, P.D., Clarke, R.A., and Koo, J.: "Aquathermolysis of Heavy Oils", Rec. Tec. Interep, (July, 1982), 2(2):87-94.

Jennings, Jr., H.Y., Johnson, Jr. C.E., and McAuliffe, C.D.: "A Caustic Waterflooding Process for Heavy Oils", J. Pet. Tech. (Dec. 1974), p. 1344-1352.

Johnson, C.E.: "Status of Caustic and Emulsion Methods", J. Pet. Tech., (Jan., 1976), p. 85-92.

King R.: "Heavy Oil Emulsion Rheology", M.Sc. Thesis, University of Alberta, (1985).

Layrisee, I., and Rivas, H.: "Isolation and Characterization of Natural Surfactants Present in Extra Heavy Crude Oils", J. Disp. Sci. Tech., (1984), 5(1), p. 1-18.

Levius, H.P., and Drommond, F.G.: "Elevated Temperature as an Artificial Breakdown Stress in the Evaluation of Emulsion Stability", J. of Pharmaceutical Pharmacology, (1953), v. 5, p. 743-756. as quoted by R. Steinborn, M.Sc. Thesis, University of Alberta, (1982).

Lissant, P.: "Emulsion Science" Academic Press, London and New York, (1968).

Maini, B.B., and Ma V.: "Thermal Stability of Surfactants for Reservoir Application", SPE Paper - 13572, (1985).

McAuliffe, C.D.: "Oil-in-Water Emulsions and their Flow Properties in Porous Media", J. Pet. Tech., (June 1973), p. 727-728

McAuliffe, C.D.: "Crude Oil-in-Water Emulsions To Improve Fluid Flow in an Oil Reservoir", J. Pet. Tech., (June 1973), p. 721-726.

Mitsui, T., Nakamura, S., Harusawa, F., and Machida, Y.: "Changes in the Interfacial Tension with Temperature and Their Effects on Particle Sizes and Stability of Emulsions", Kolloid-Z.U.Z. Polymere, 250:P. 227-230.

Navratil, M., Sovak, M., and Mitchell, M.S.: "Formation Blocking Agents: Applicability in Water- and Steamflooding", SPE 12006, (1983).

Prats, M.: "Thermal Recovery", Henry L. Doherty Series, Society of Petroleum Engineers, Monograph Volume 7, (1982)).

Rosen, M.J.:"Surfactants and Interfacial Phenomena", Wiley: Toronto, (1978).

Rosen, M.R.: "A Rheogram Template for Power Low Fluids: A Technique for Characterizing the Rheological Properties of Emulsions and Polymer Solutions", J. Coll. Int. Sci., (July, 1971), V. 36, No. 3, p. 350-358.

Rosen, M.R.: "A Rheogram Template for Power Low Fluids: II. Rapid Rheological Characterization in a Coaxial Cylinder", J. Coll. Int. Sci., (May, 1972), V. 39, No. 2, p. 413-417.

Saito, H., and Shinoda, K.: "The Stability of W/O Type Emulsions as a Functton of Temperature and of the Hydrophilic Chain Length of the Emulsifier", J. Coll. Int. Sci., 32(4), (April, 1970), p. 647-651.

Shah, D.O., ed.: "Macro- and Microemulsions: Theory and Application", ACS Symposium Series 272, (1985).

Sherman, P. ed.: "Emulsion Science", Academic Press, (1968).

Soo, H., and Radke, C.J.: "Velocity Effects in Emulsion Flow through Porous Media", J. Coll. Int. Sci., (Dec. 1984), p. 462-476.

Soo, H., and Radke, C.J.: "The Flow Mechanism of Dilute, Stable Emulsions in Porous Media", Ind. Eng. Chem. Fundam., (1984), v. 23, p. 342-347.

Strassner, J.E.: "Effect of pH on Interfacial Films and Stability of Crude Oil-Water Emulsions", J. Pet. Tech., (March, 1968), p. 303-312.

Subkow, P.: "Process for the Removal of Bitumen From Bituminous Deposits", U.S. Patent No. 2, 288, 857, (July 7, 1942).

Tadros, Th.F.: "Surfactants", Academic Press, Inc., Toronto, (1984).

Takamura, K., and Chow, R.: "The Stability of Bitumen Emulsion", Energy Processing/Canada, (September-October 1982), V74, N7, p. 29-31.

Van Wazer, J.R., Lyons, J.W., Kim, K.Y., and Colwell R.E.: "Viscosity and Flow Measurement, A Laboratory Handbook of Rheology," Interscience Publishers, New York, (1963).

Walstra, P.: "Encyclopedia of Emulsion Technology", P. Becher, Ed., Dekker: New York, (1983).

Wellmann, V.E., and Tartar, H.V.: "A Study of Factors Controlling Type of Water-Soap-Oil Emulsions", J. Physical Chemistry, (1930), v. 34, p. 379-409.

Willman, B.T., Valleroy, V.V., Runberg, G.W., Cornelius, A.J. and Powers, L.W.: "Laboratory Studies of Oil Recovery by Steam Injection", J.P.T., V. 13, (1981) p. 681-690.

Winestock, A.G.: "Conformance and Recovery Improvements - Some Basic Considerations", Presented at the Fifth Annual "Advances in Petroleum Recovery and Upgrading Technology" Conference, (June 14-15 1984), Calgary, Alberta.

APPENDIX A

Microphotographs and pH Data for 5% Lloydminster Oil Emulsions Stabilized with Triton X-100 Surfactant

LLOYDMINSTER OIL/TRITON X-100

Surfactant Concentration = 25 ppm. @ Cure Temperature

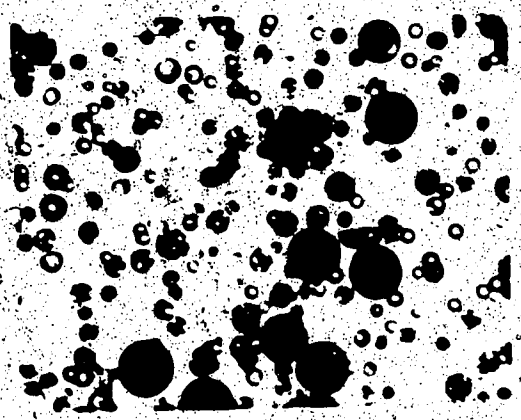

Plate A.1, 25°C

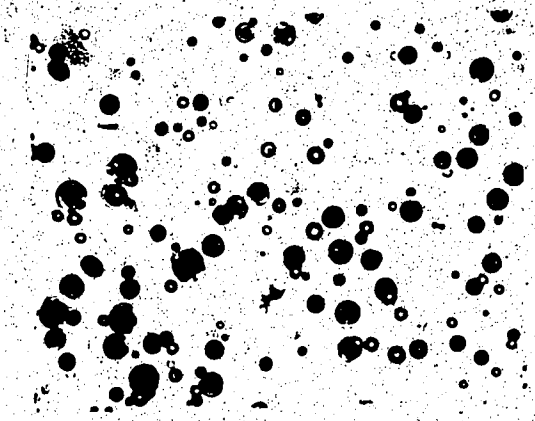

Plate A.2, 75°C

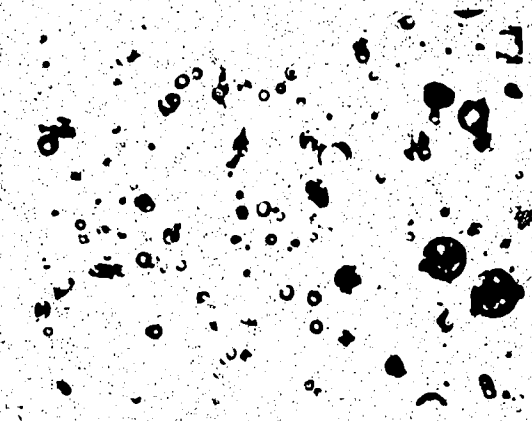

Plate A.3, 125°C

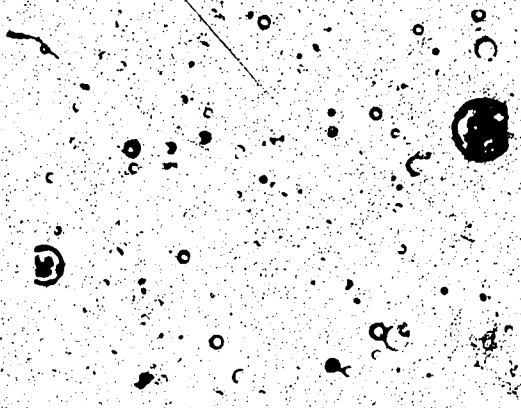

Plate A.4, 175°C

Plate A.5, 225°C

LLOYDMINSTER OIL/TRITON X-100

Surfacatnt Concentration = 50 ppm @ Cure Temperature

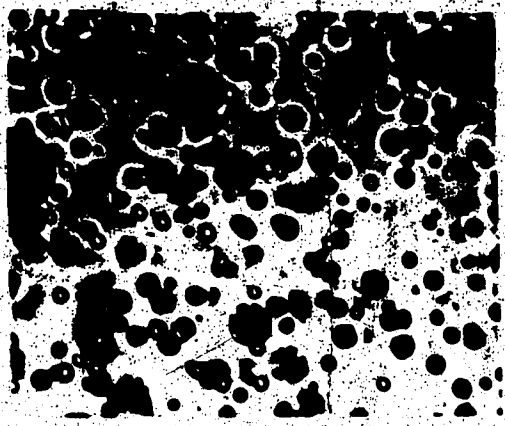

Plate A.6, 25°C

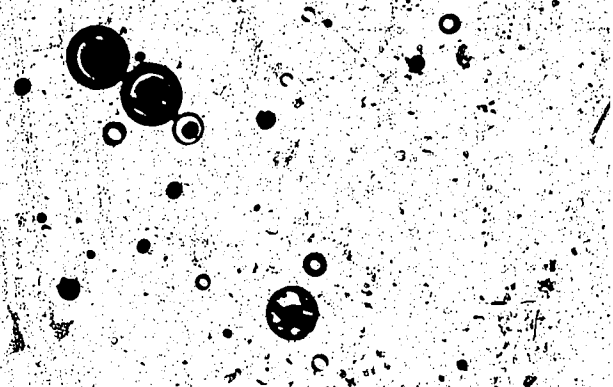

Plate A.9, 175°C

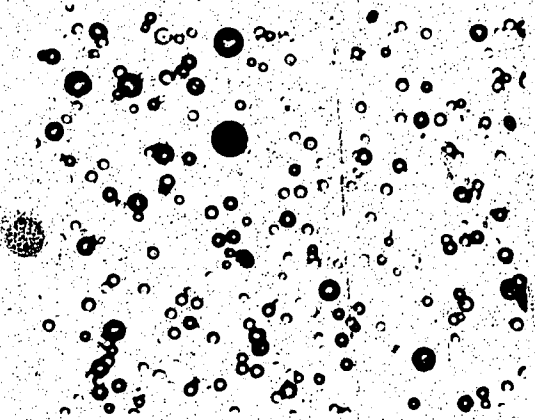

Plate A.7, 75°C

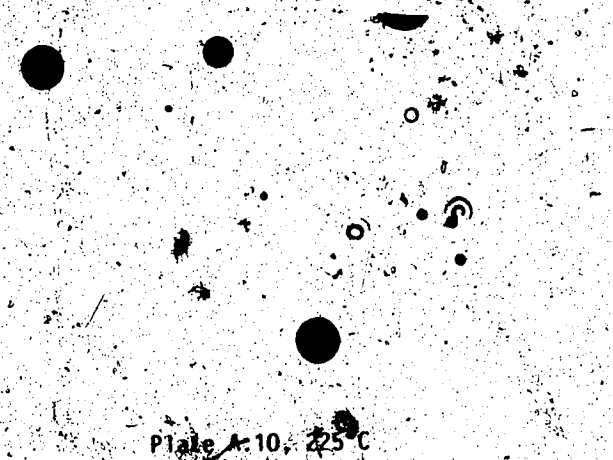

Plate A.10, 225°C

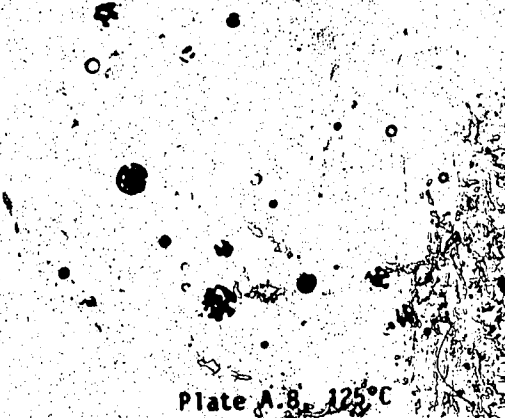

Plate A.8, 125°C

LLOYDMINSTER OIL/TRITON X-100

Surfactant Concentration = 100 ppm @ Cure Temperature

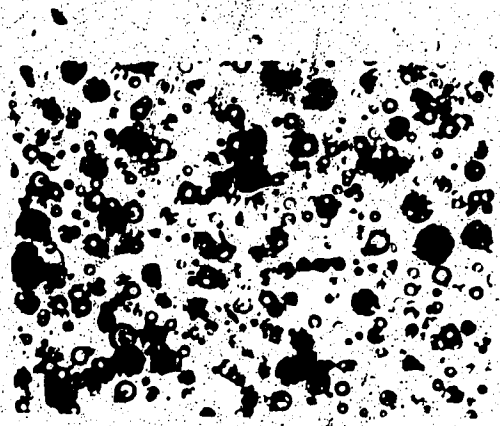

Plate A.11, 25°C

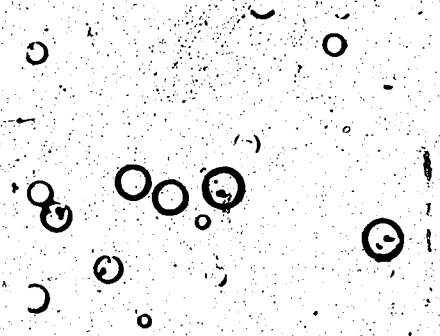

Plate A.14, 175°C

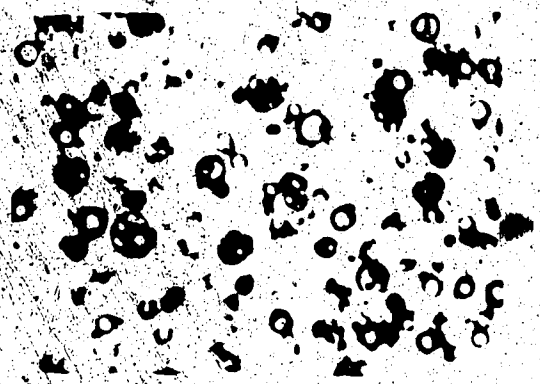

Plate A.12, 75°C

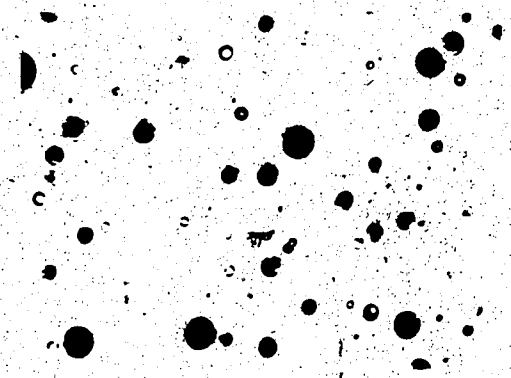

Plate A.15, 225°C

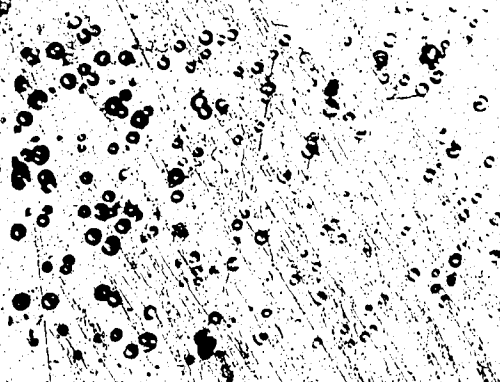

Plate A.13, 125°C

LLOYDMINSTER OIL/TRITON X-100

Surfactant Concentration = 300 ppm @ Cure Temperature

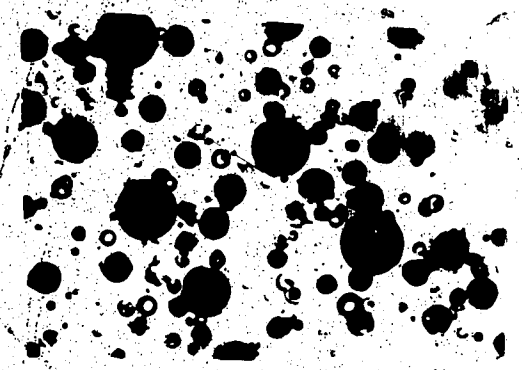

Plate A.16, 25°C

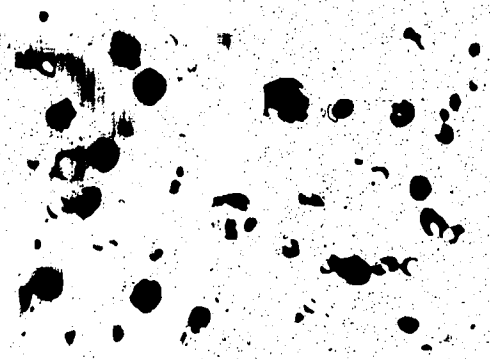

Plate A.19, 175°C

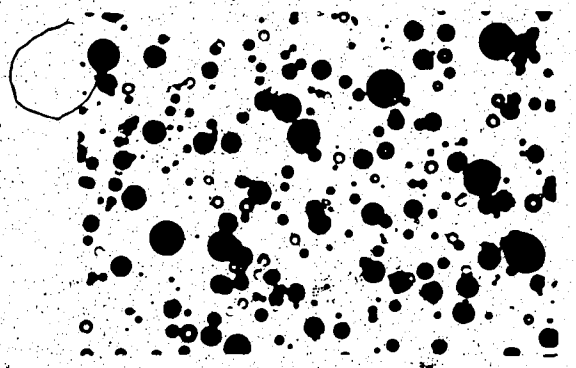

Plate A.17, 75°C

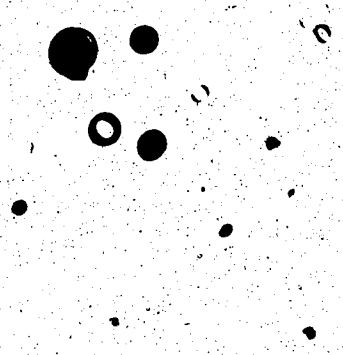

Plate A.20, 225°C

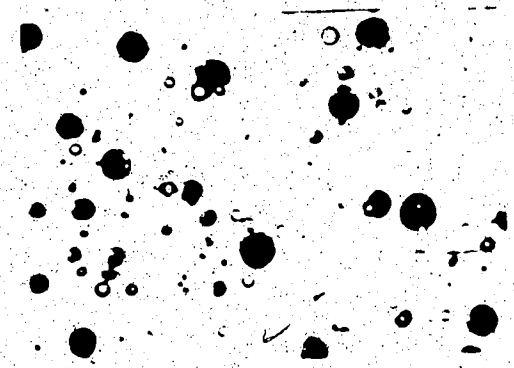

Plate A.18, 125°C

LLOYDMINSTER OIL/TRITON X-100

Surfactant Concentration = 700 ppm @ Cure Temperature

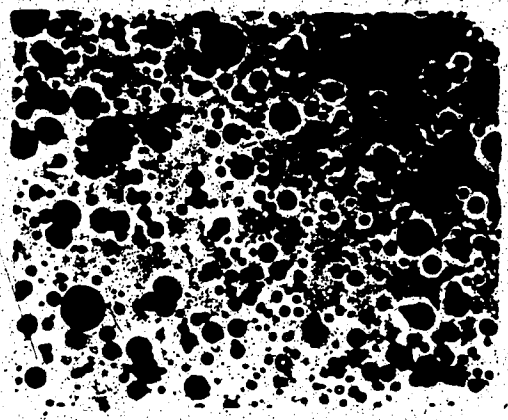

Plate A.21, 25°C

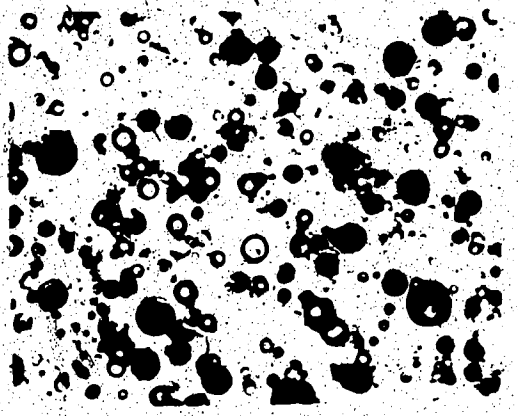

Plate A.22, 75°C

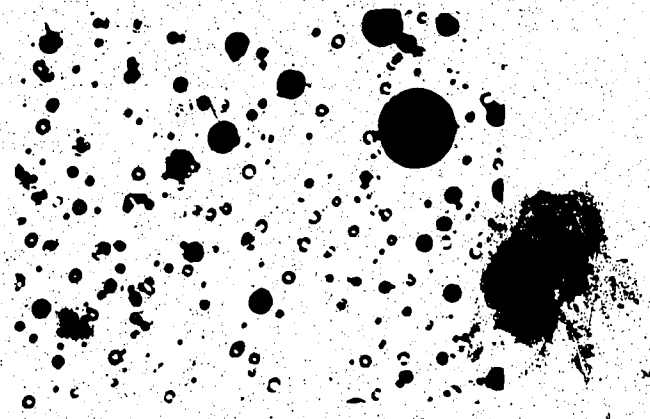

Plate A.23, 125°C

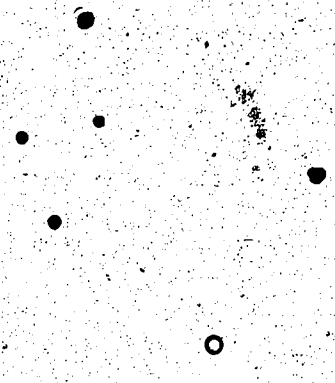

Plate A.24, 175°C

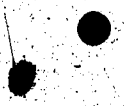

Plate A.25, 225°C

LLOYDMINSTER OIL/TRITON X-100

Surfactant Concentration = 1200 ppm @ Cure Temperature

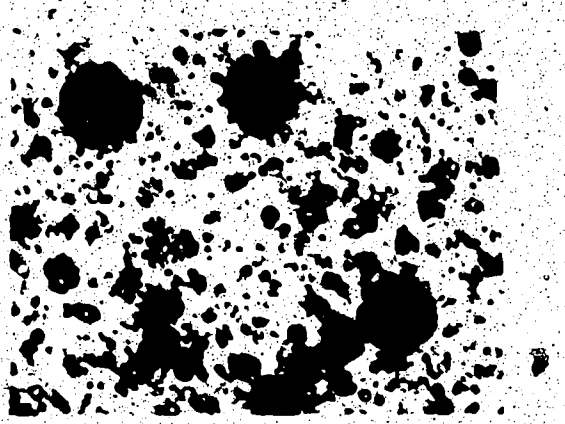

Plate A.26, 25°C

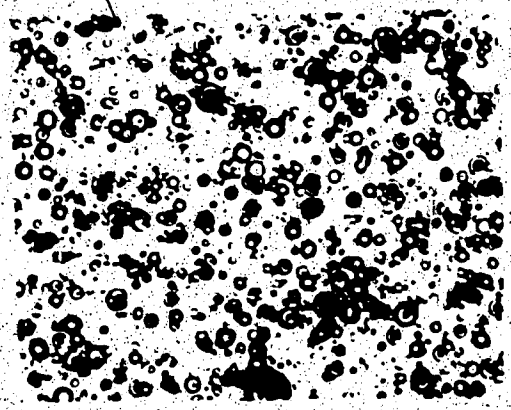

Plate A.27, 75°C

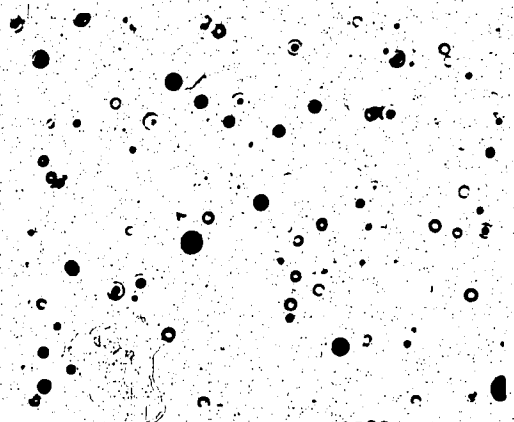

Plate A.28, 125°C

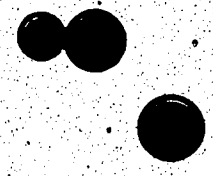

Plate A.29, 175°C

Plate A.30, 225°C

LLOYDMINSTER OIL/TRITON X-100

Surfactant Concentration = 2000 ppm @ Cure Temperature

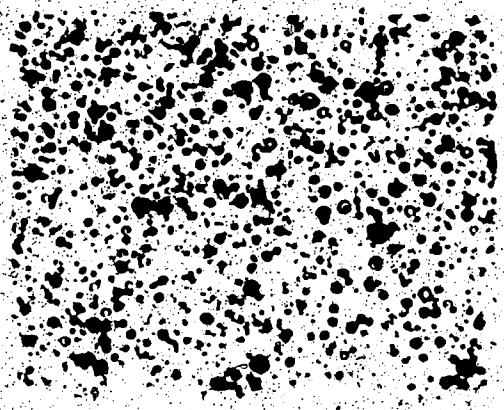

Plate A.31, 25°C

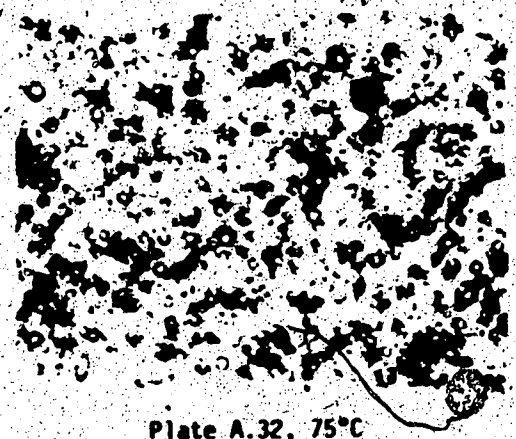

Plate A.32, 75°C

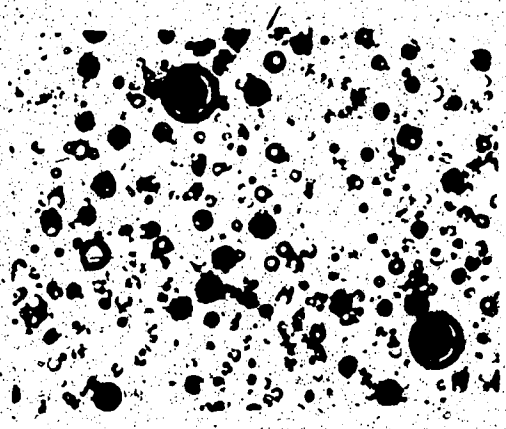

Plate A.33, 125°C

Plate A.34, 175°C

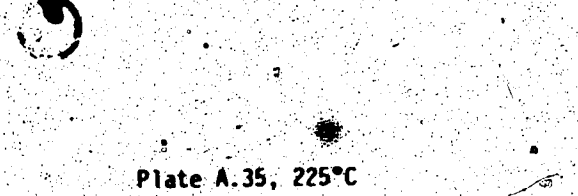

Plate A.35, 225°C

KLOYDMINSTER OIL/TRITON X-100

Surfactant Concentration = 5000 ppm @ Cure Temperature

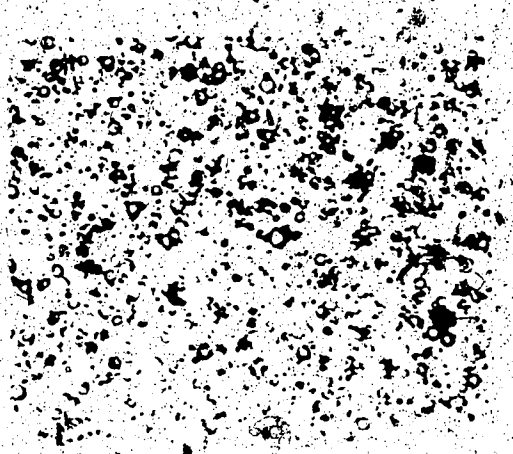

Plate A.36, 25°C

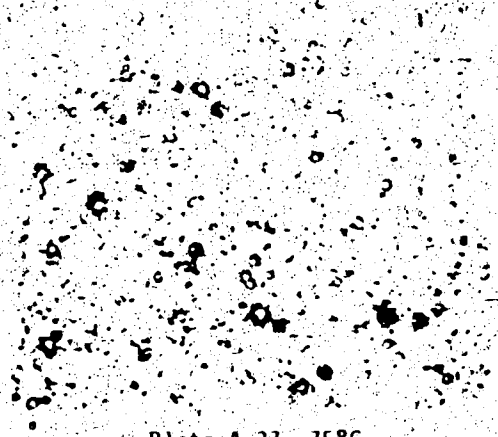

Plate A.37, 75°C

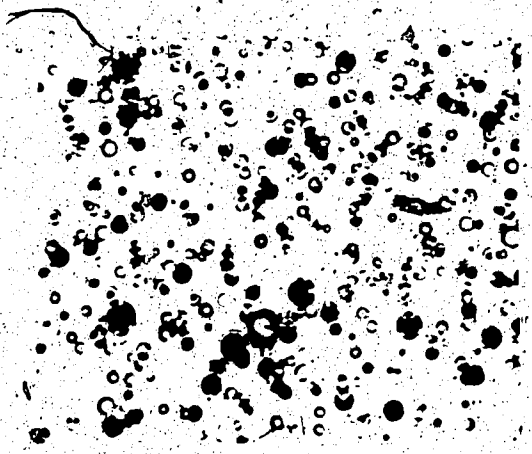

Plate A.38, 125°C

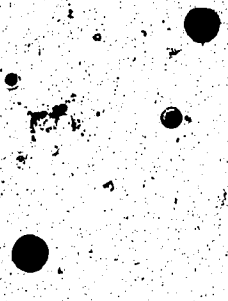

Plate A.40, 225°C

TABLE A.1 - Change in pH for 5% Lloydminster Oil Emulsions with Triton X-100 Surfactant @ Cure Temperature

SURFACTANT CONCENTRATION (ppm)	CURE TEMPERATURE °C				
	25	75	125	175	225
25	8.46/8.35*	8.65/8.41	8.52/6.15	8.11/4.86	8.33/3.77
50	8.07/8.15	8.21/8.28	8.29/5.27	7.98/4.49	8.33/5.10
100	8.22/8.28	8.32/8.16	7.92/5.06	8.07/4.64	8.18/5.05
300	8.41/8.33	8.37/8.28	8.25/5.45	8.53/5.05	8.13/4.95
700	8.16/8.05	8.10/8.14	8.37/5.50	8.23/3.96	8.46/3.34
1200	8.44/8.32	8.25/7.90	8.62/6.48	8.51/4.38	8.52/3.80
2000	8.07/8.04	8.02/7.81	8.29/6.36	8.17/4.62	8.37/3.75
5000	7.79/7.70	7.78/7.66	7.50/6.10	8.02/5.15	7.87/4.11

* - Data Values : (pH in/pH out)

@ Cure Time = 1 hour

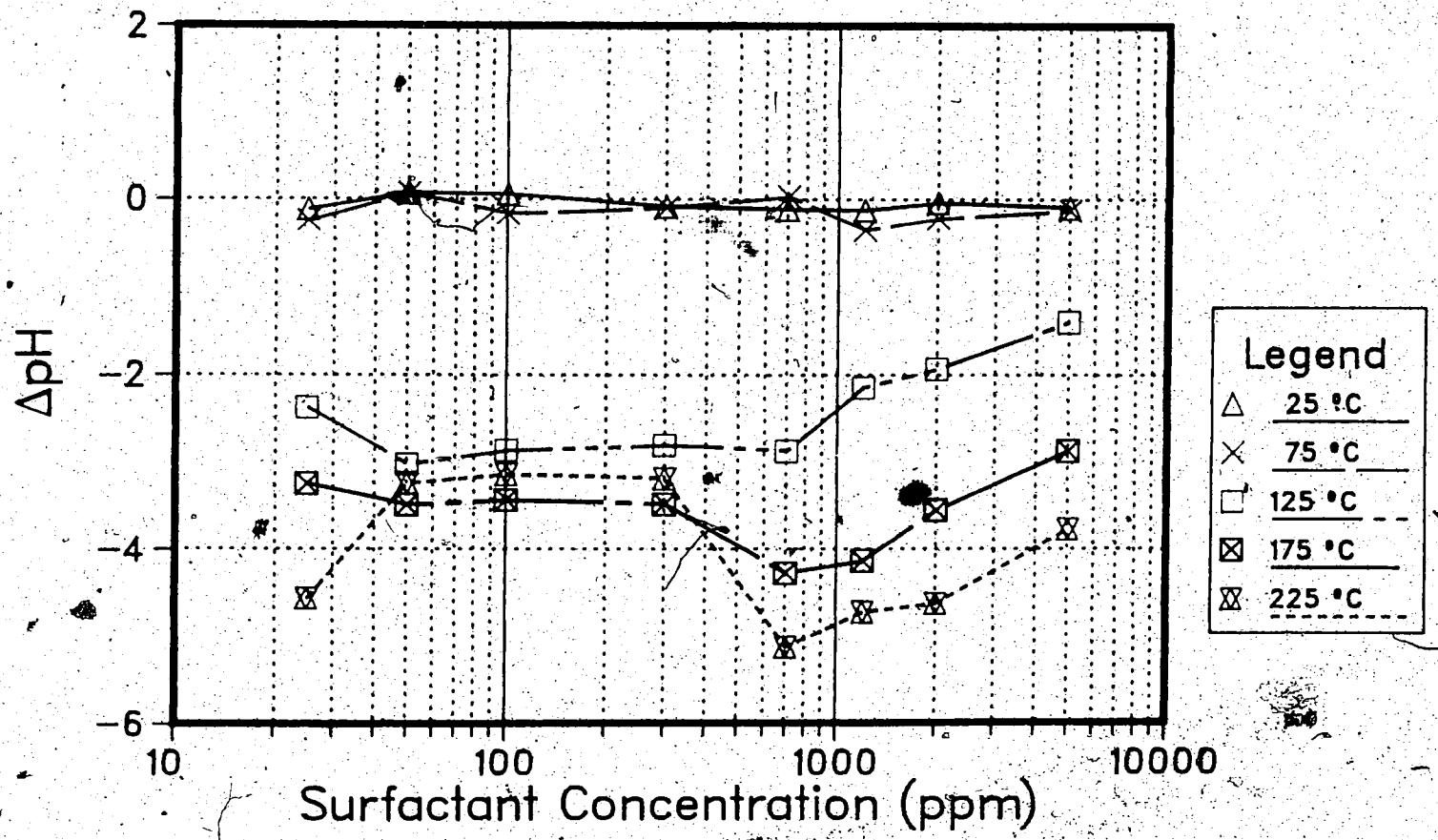

FIGURE A.1 – Lloydminster Oil / TX–100 Surfactant
ΔpH vs. Surfactant Concentration @ Cure Temperature

APPENDIX B

Microphotographs and pH Data for 5% Lloydminster Oil Emulsions Stabilized with Vista 250 Surfactant

LLOYDMINSTER OIL/VICSIA 250

Surfactant Concentration 25 ppm @ Cure Temperature

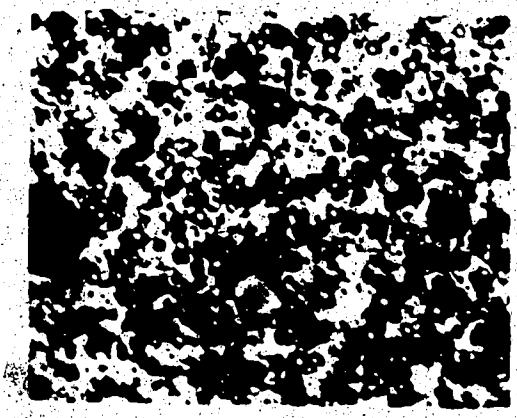

Plate B.1, 25°C

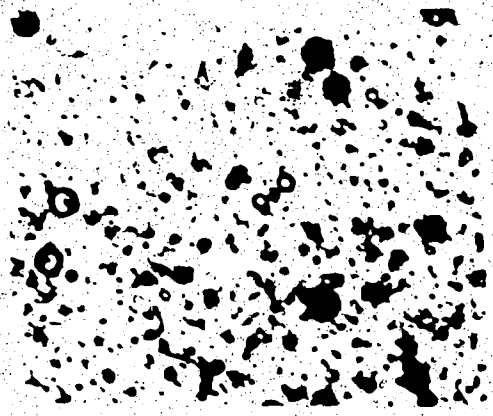

Plate B.4, 175°C

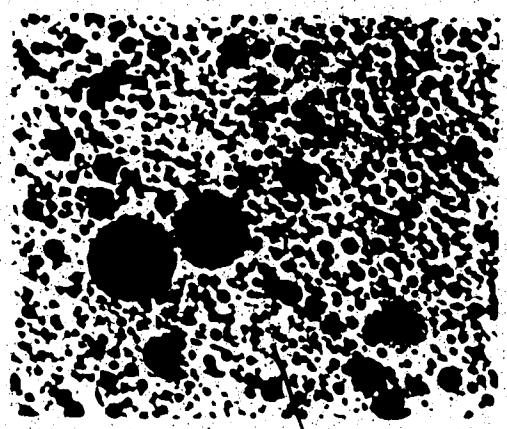

Plate B.2, 75°C

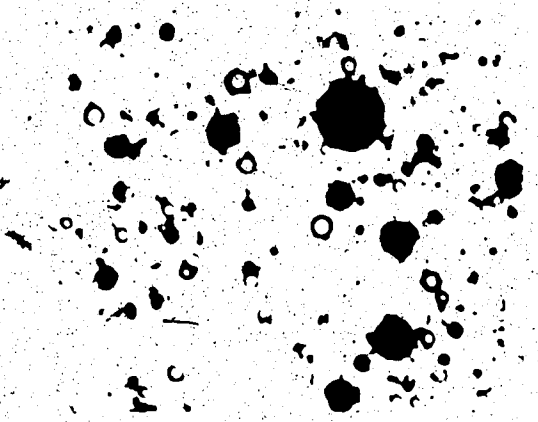

Plate B.5, 225°C

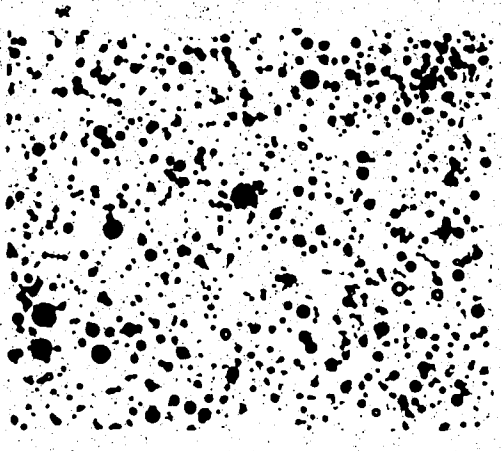

Plate B.3, 125°C

LLOYDMINSTER OIL/VISTA 250

Surfactant Concentration = 50 ppm @ Cure Temperature

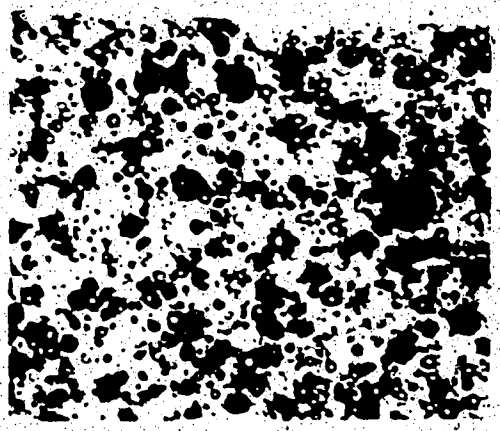

Plate B.6, 25°C

Plate B.9, 175°C

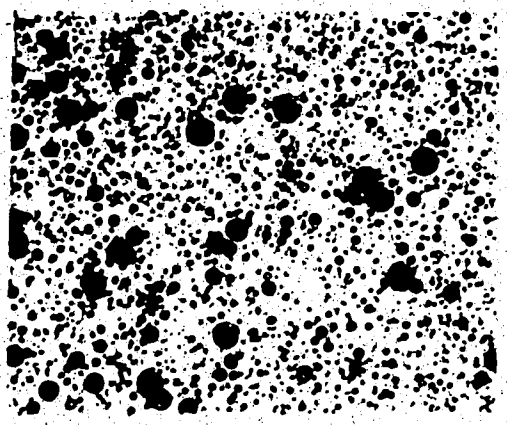

Plate B.7, 75°C

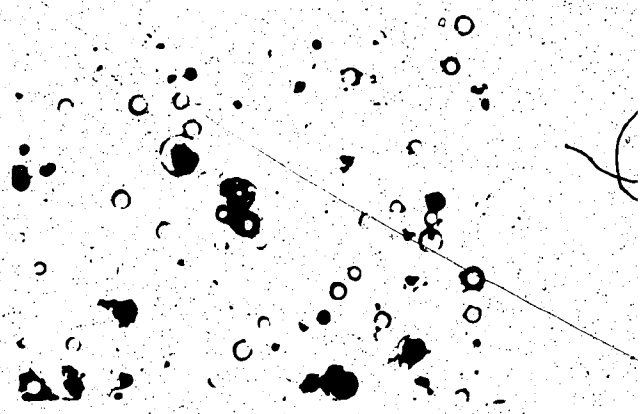

Plate B.10, 225°C

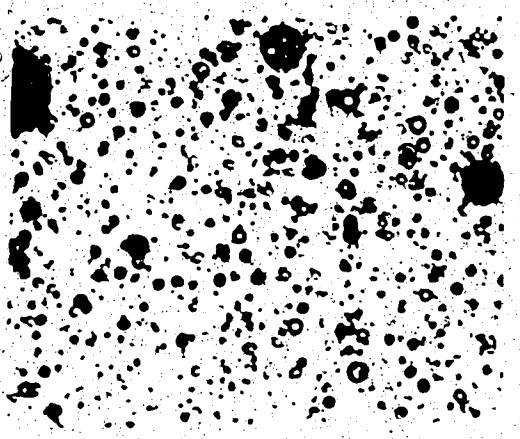

Plate B.8, 125°C

LI[illegible]STER OIL/VISTA 250

Surfactant Concentration - 100 ppm @ Cure Temperature

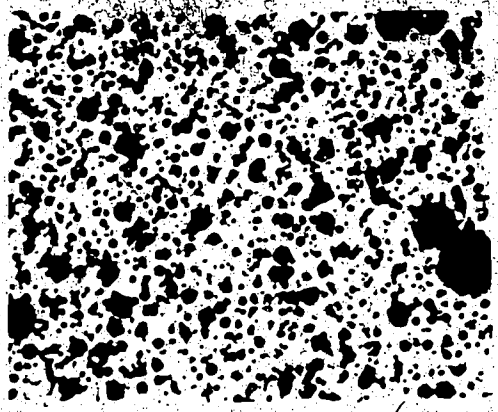

Plate B.11, 25°C

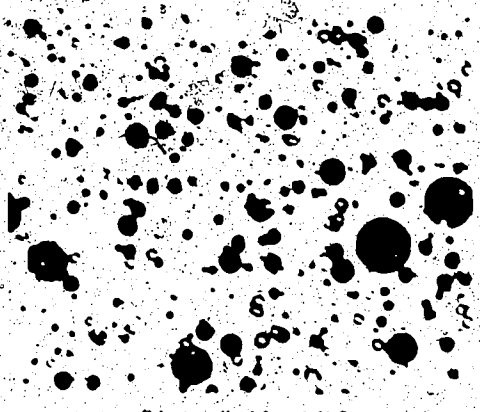

Plate B.14, 175°C

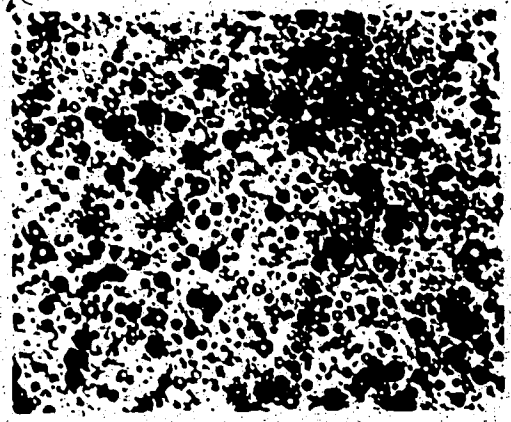

Plate B.12, 75°C

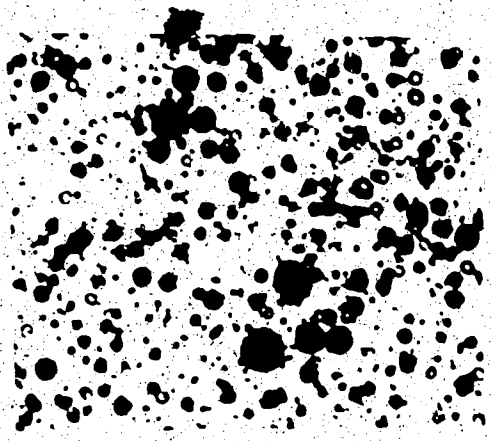

Plate B.15, 225°C

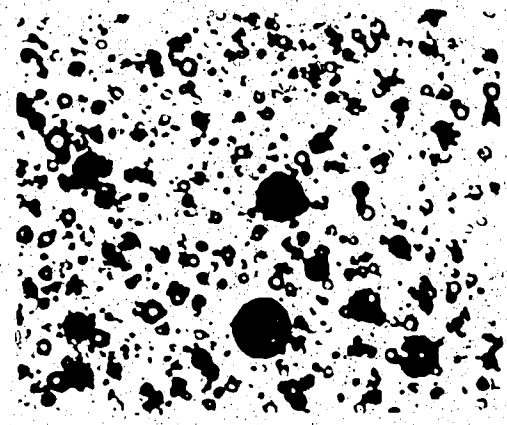

Plate B.13, 125°C

LLOYDMINSTER OIL/VISTA 250

Surfactant Concentration 300 ppm @ Cure Temperature

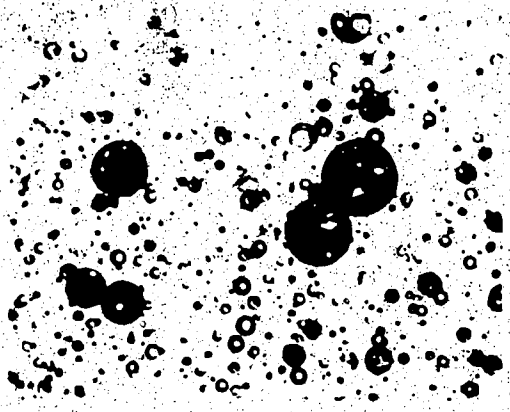

Plate B.16, 25°C

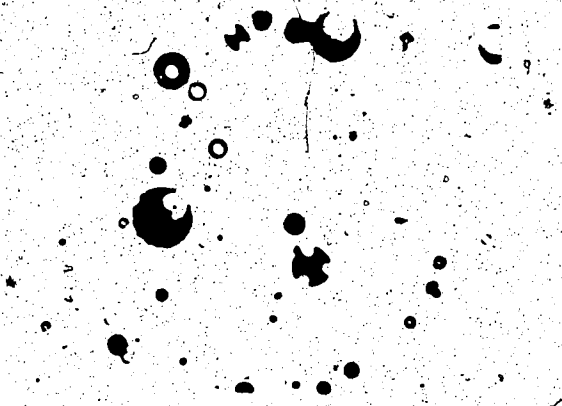

Plate B.19, 175°C

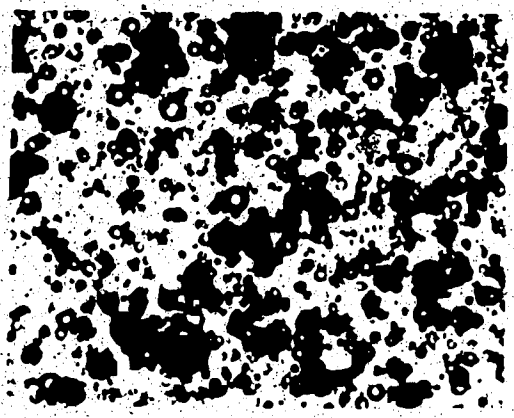

Plate B.17, 75°C

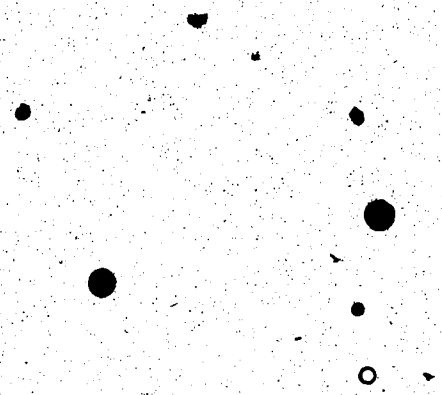

Plate B.20, 225°C

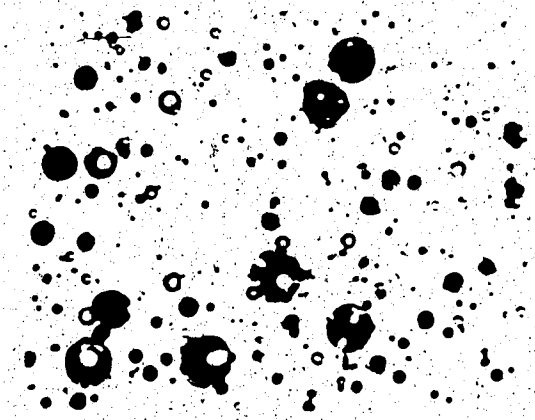

Plate B.18, 125°C

LLOYDMERE ITR-011 /VISTA 250

Surfactant Concentration /00 ppm @ Cure Temperature

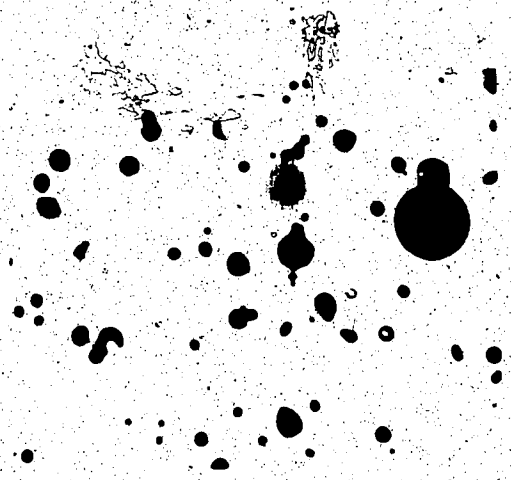

Plate B.21. 25°C

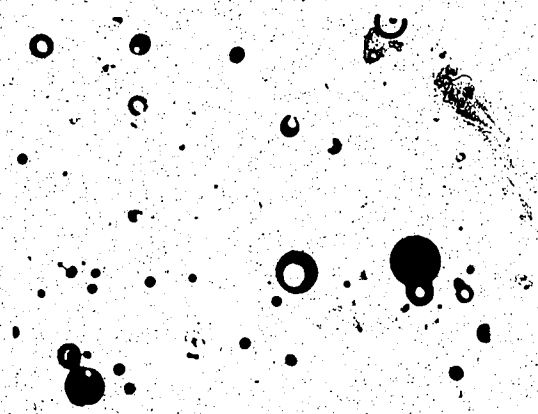

Plate B.24. 175°C

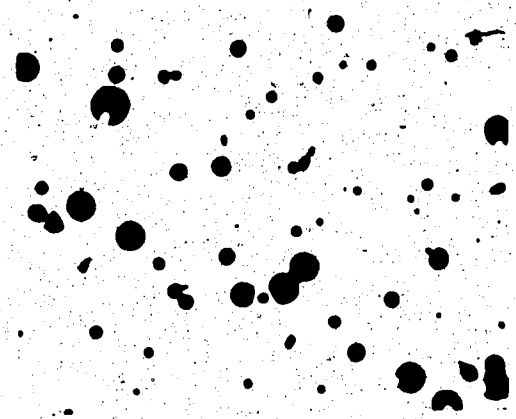

Plate B.22. 75°C

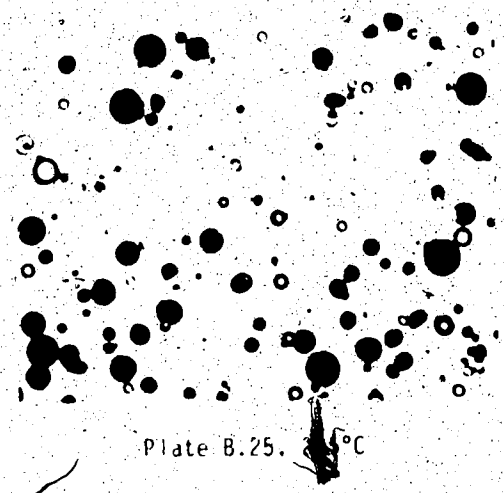

Plate B.25. [illegible]°C

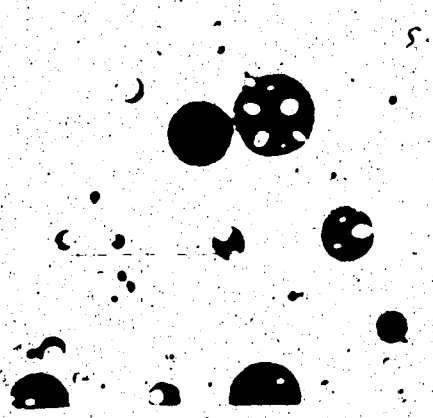

Plate B.23. 125°C

LLOYDMINSTER OIL /VISTA 250

Surfactant Concentration 1200 ppm P Cure Temperature

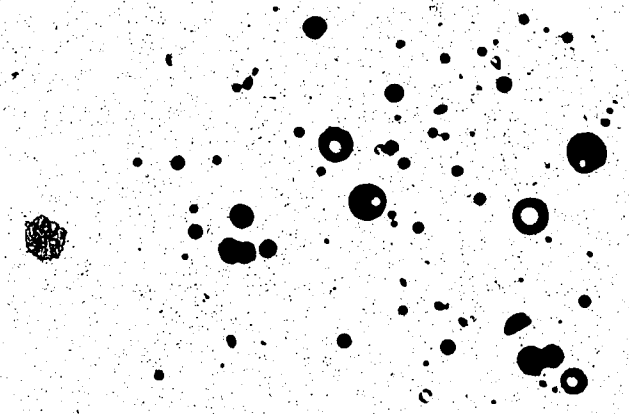

Plate B.26. 25°C

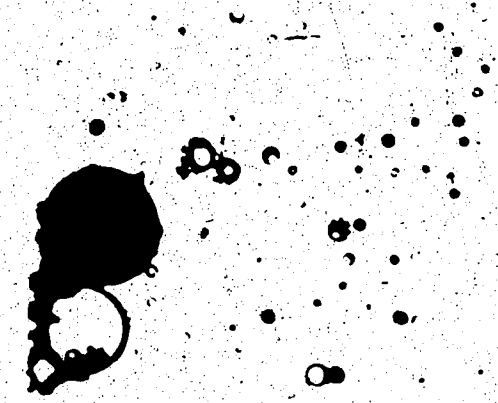

Plate B.29. 175°C

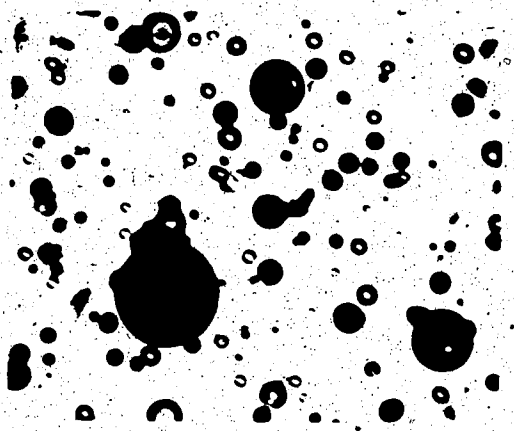

Plate B.27. 75°C

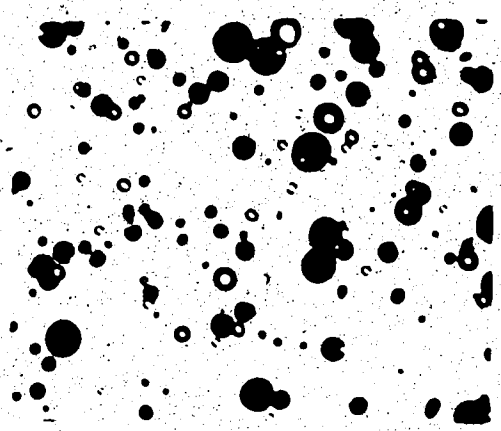

Plate B.30. 225°C

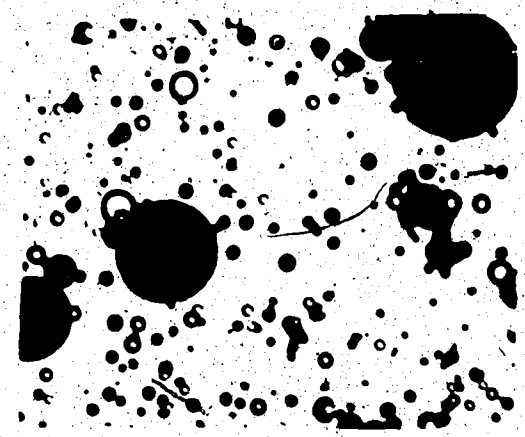

Plate B.28. 125°C

LLOYDMINSTER OIL/VISTA 250

Surfactant Concentration 2000 ppm @ Cure Temperature

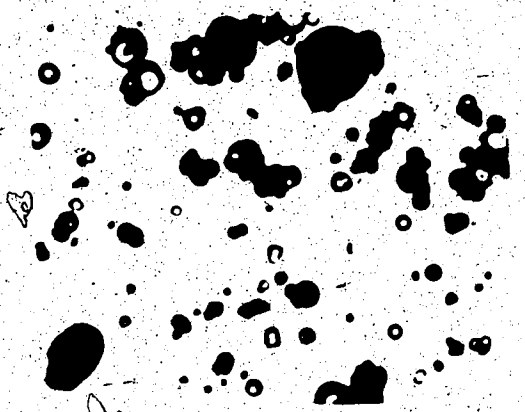

Plate B.31, 25°C

Plate B.34, 175°C

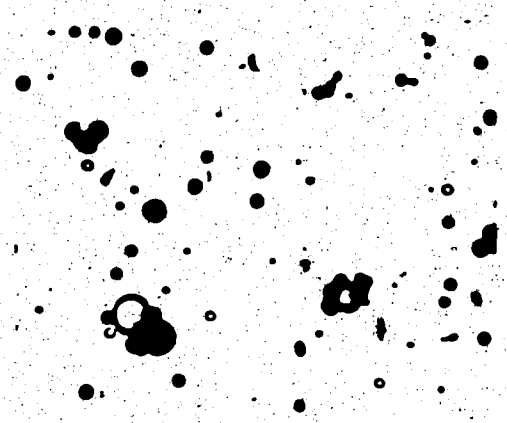

Plate B.32, 75°C

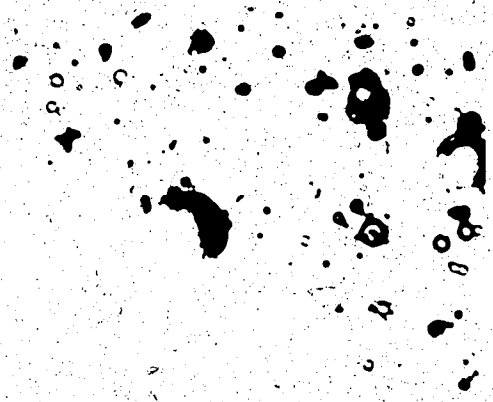

Plate B.35, 225°C

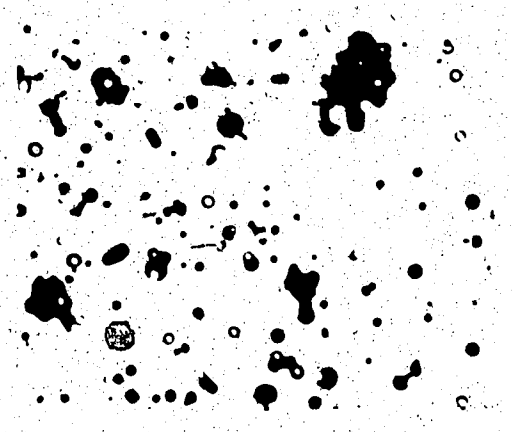

Plate B.33, 125°C

LLOYDMINSTER OIL/VISTA 250

Surfactant Concentration 5000 ppm @ Cure Temperature

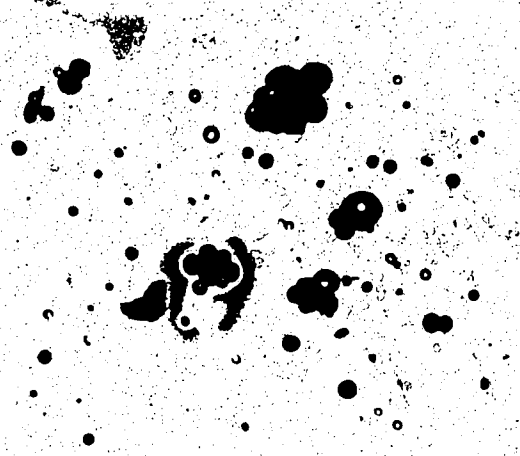

Plate B.36, 25°C

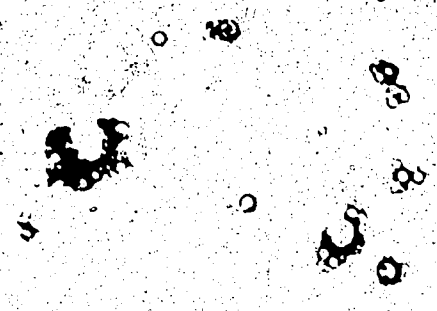

Plate B.39, 175°C

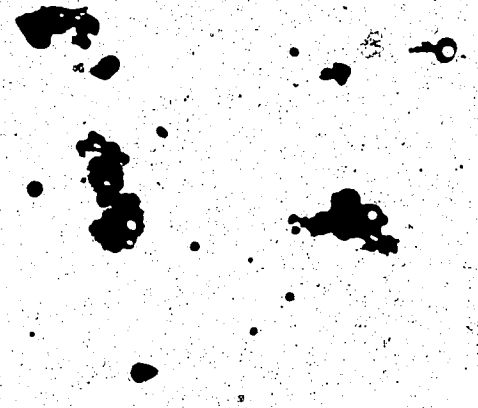

Plate B.37, 75°C

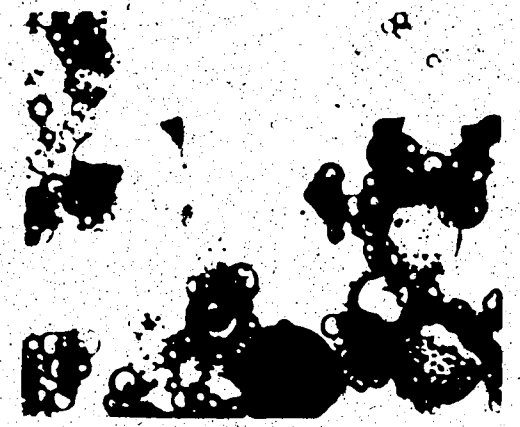

Plate B.40, 225°C

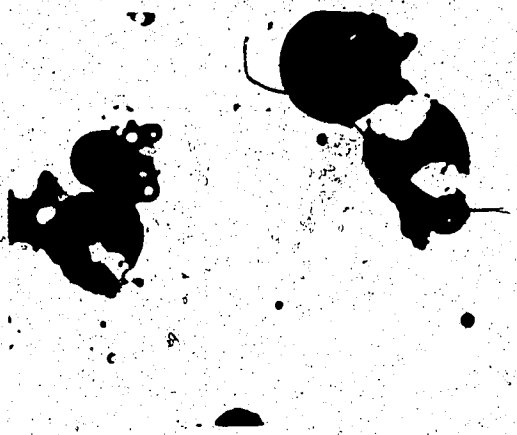

Plate B.38, 125°C

TABLE B.1 - Change in pH for 5% Lloydminster Oil Emulsions with Vista 250 Surfactant @ Cure Temperature

SURFACTANT CONCENTRATION (ppm)	CURE TEMPERATURE °C				
	25	75	125	175	225
25	8.48/8.45*	8.50/8.45	8.51/8.04	8.74/7.81	8.86/3.99
50	8.53/8.60	8.70/8.62	8.74/8.29	8.92/8.80	9.03/6.87
100	8.76/8.74	8.70/8.74	8.98/8.24	9.10/8.15	9.05/7.49
300	9.02/8.97	8.96/8.56	9.16/8.87	9.47/9.11	9.52/8.50
700	9.62/9.65	9.58/9.20	9.48/9.08	9.[illegible]96	9.49/7.73
1200	9.15/9.06	9.17/8.92	9.45/9.09	9.48/9.13	9.40/7.57
2000	9.17/9.10	9.08/8.80	9.22/9.00	9.21/8.55	9.29/8.00
5000	8.82/8.75	8.76/8.57	9.18/8.80	9.09/8.65	9.24/8.25

* - Data Values : (pH in/pH out)

Cure Time = 1 hour

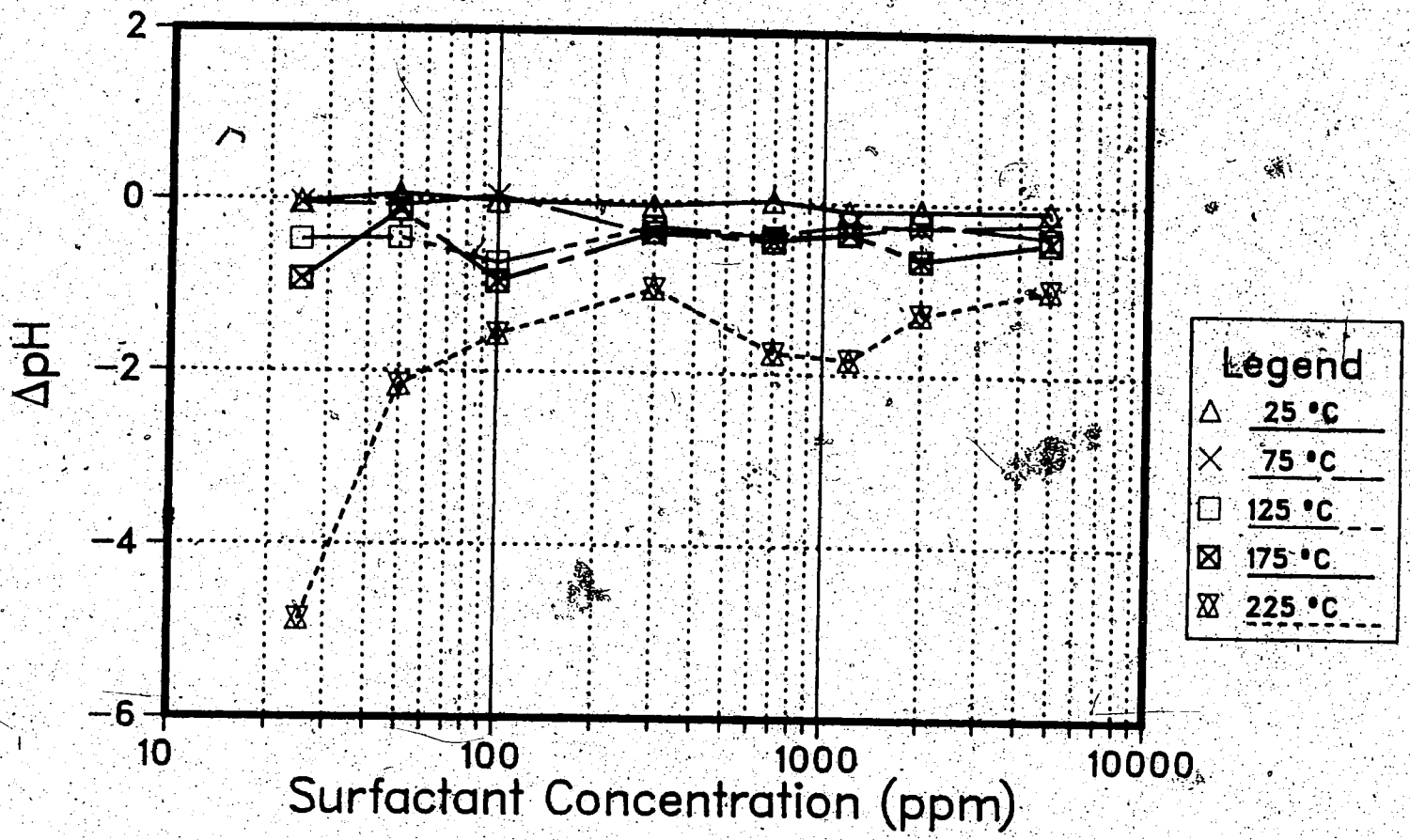

FIGURE B.1 – Lloydminster Oil / Vista 250 Surfactant
ΔpH vs. Surfactant Concentration @ Cure Temperature

APPENDIX C

Microphotographs and pH Data for 5% Primrose Oil Emulsions Stabilized with Triton X-100 Surfactant

PRIMROSE OIL/TRITON X-100

Surfactant Concentration = 25 ppm @ Cure Temperature

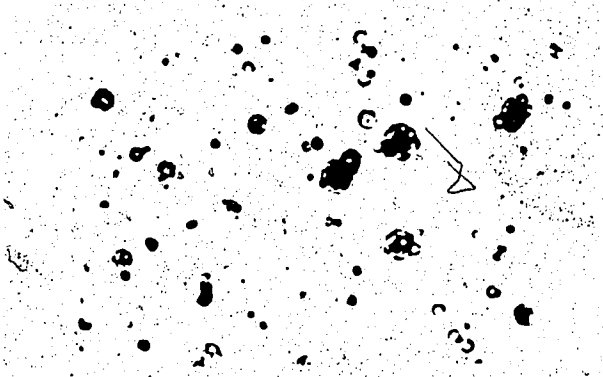

Plate C.1, 25°C

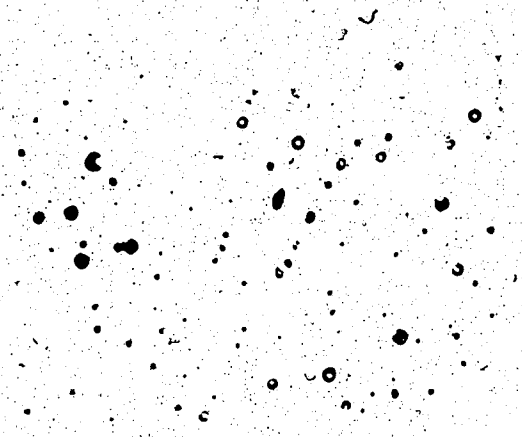

Plate C.4, 175°C

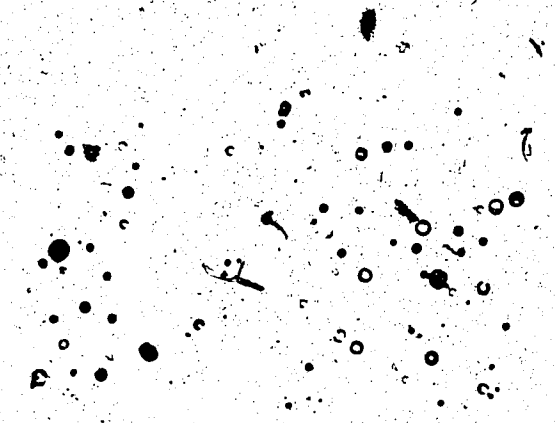

Plate C.2, 75°C

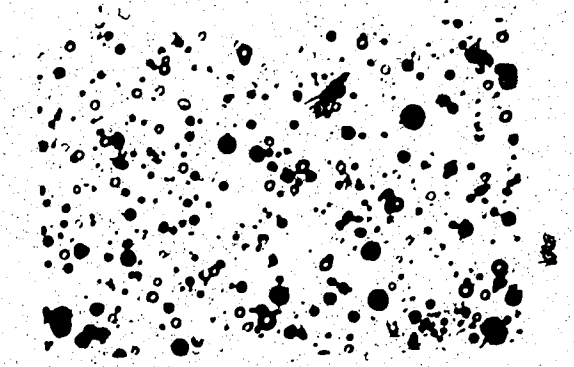

Plate C.5, 225°C

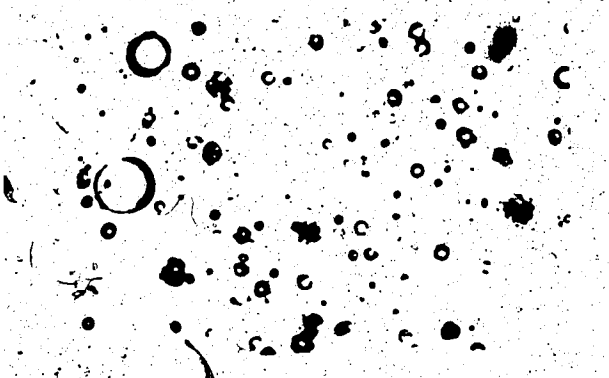

Plate C.3, 125°C

PRIMROSE OIL/TRITON X-100

Surfactant Concentration = 50 ppm @ Cure Temperature

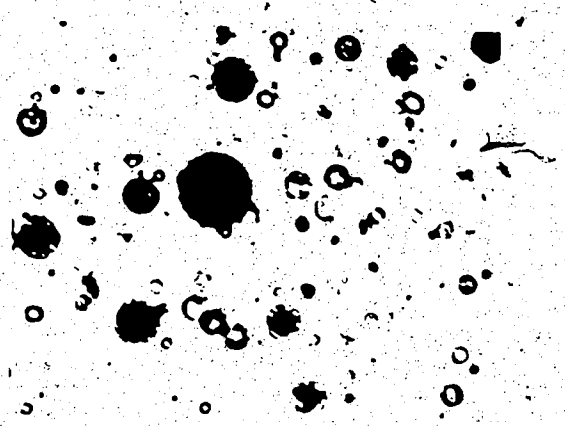

Plate C.6, 25°C

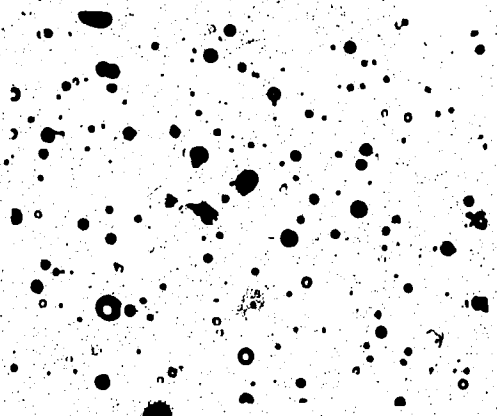

Plate C.9, 175°C

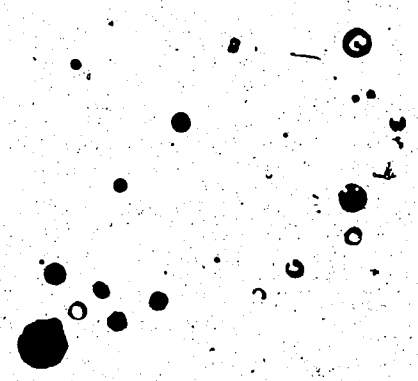

Plate C.7, 75°C

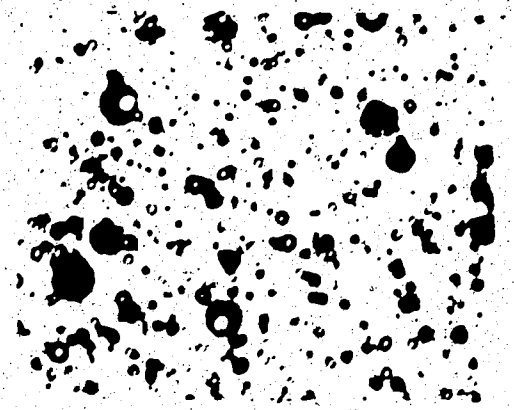

Plate C.10, 225°C

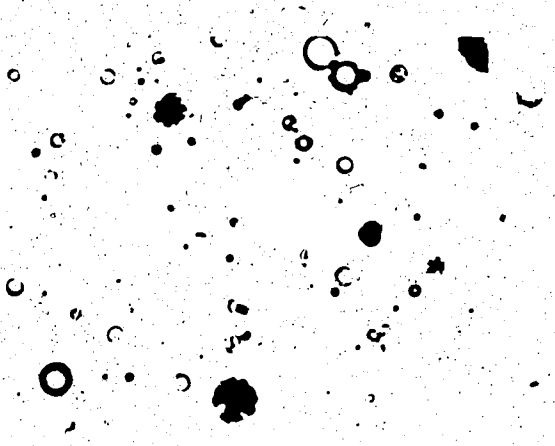

Plate C.8, 125°C

PRIMROSE OIL/TRITON X-100

Surfactant Concentration = 100 ppm @ Cure Temperature

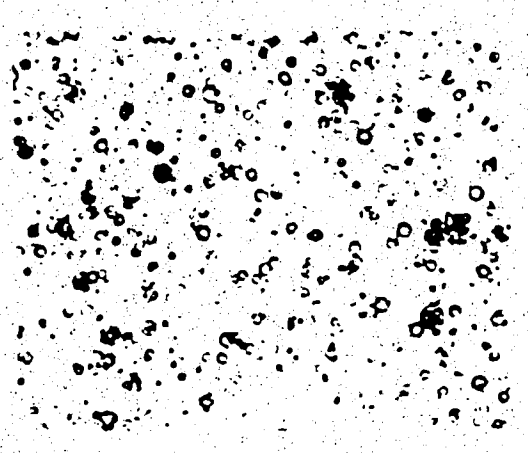

Plate C.11, 25°C

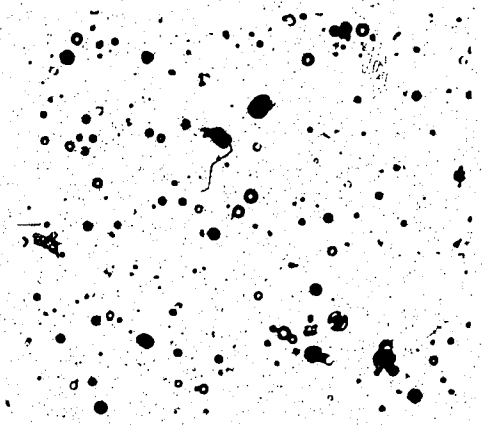

Plate C.14, 175°C

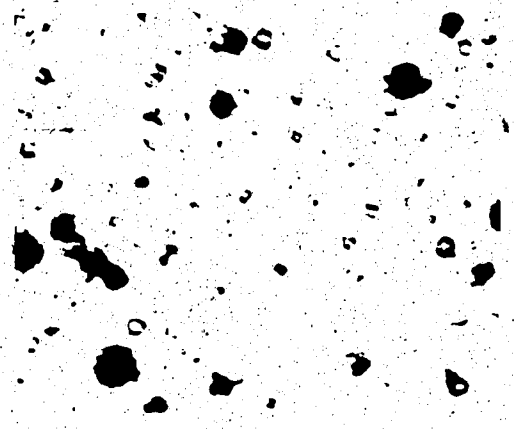

Plate C.12, 75°C

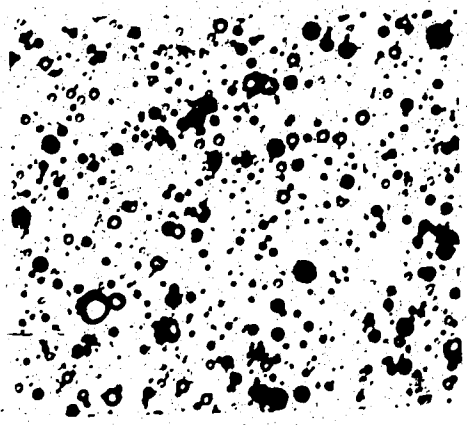

Plate C.15, 225°C

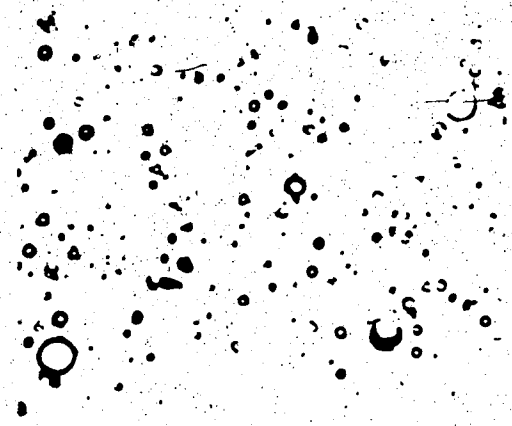

Plate C.13, 125°C

PRIMROSE OIL/TRITON X-100

Surfactant Concentration = 300 ppm @ Cure Temperature

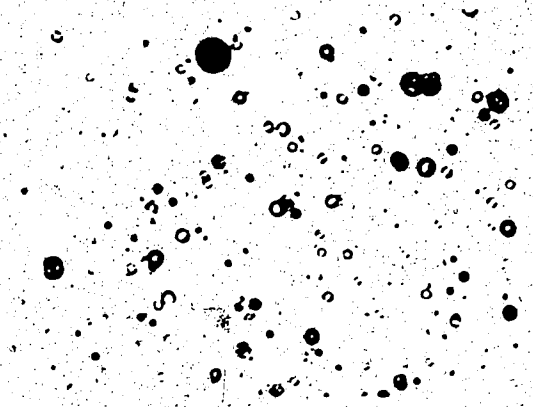

Plate C.16, 25°C

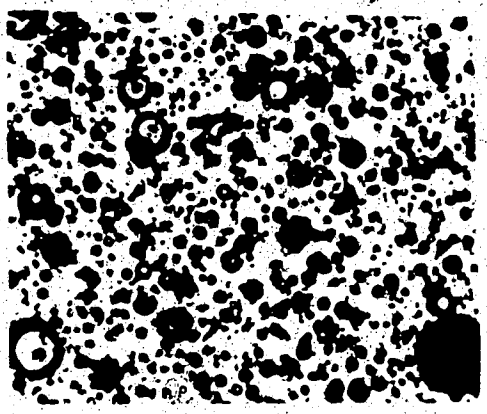

Plate C.19, 175°C

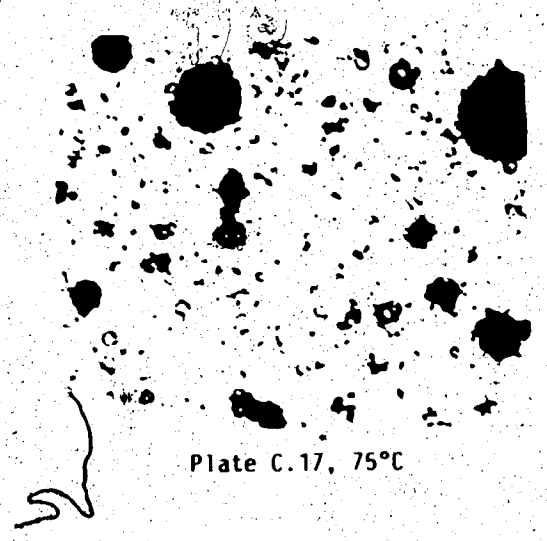

Plate C.17, 75°C

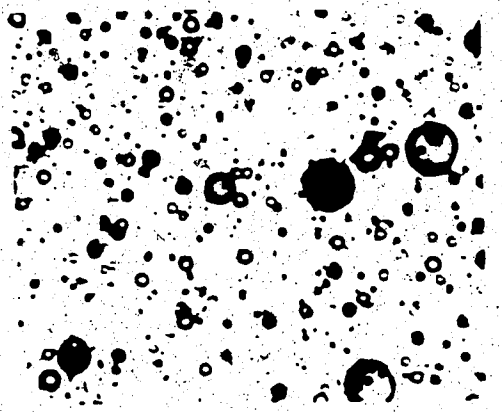

Plate C.20, 225°C

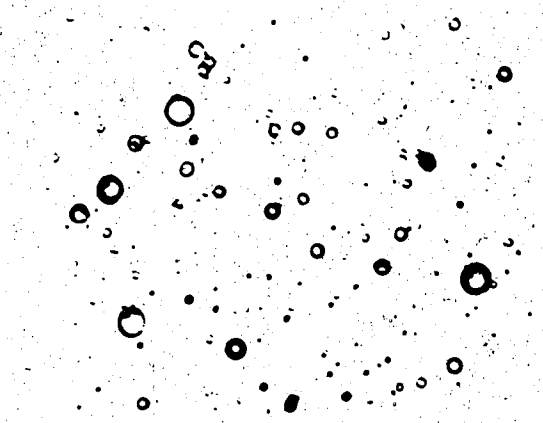

Plate C.18, 125°C

PRIMROSE OIL/TRITON X-100

Surfactant Concentration = 700 ppm @ Cure Temperature

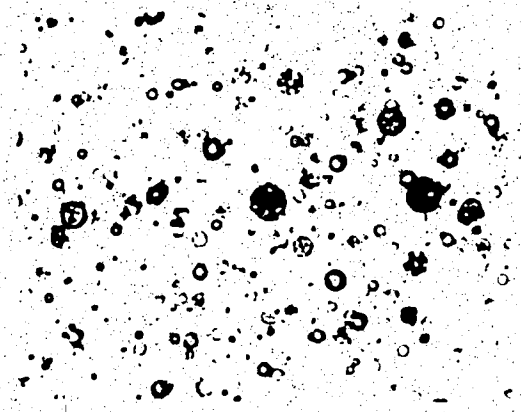

Plate C.21, 25°C

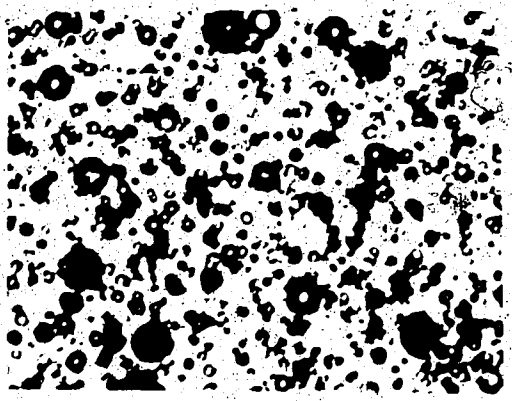

Plate C.24, 175°C

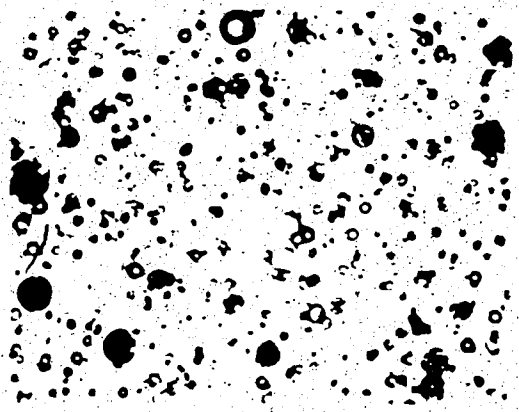

Plate C.22, 75°C

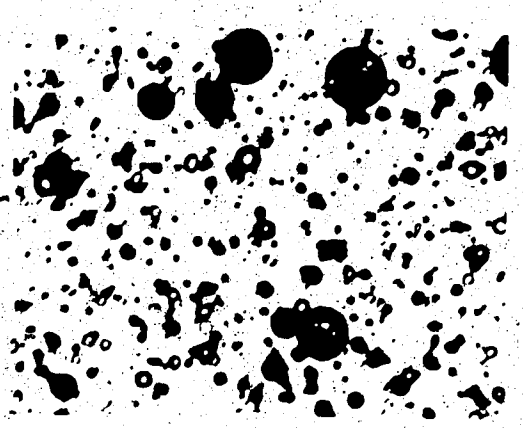

Plate C.25, 225°C

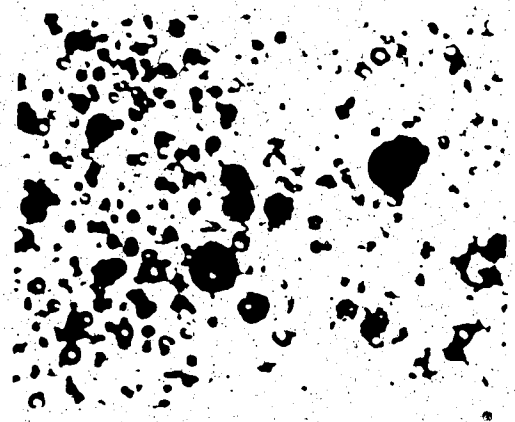

Plate C.23, 125°C

PRIMROSE OIL/TRITON X-100

Surfactant Concentration = 1200 ppm @ Cure Temperature

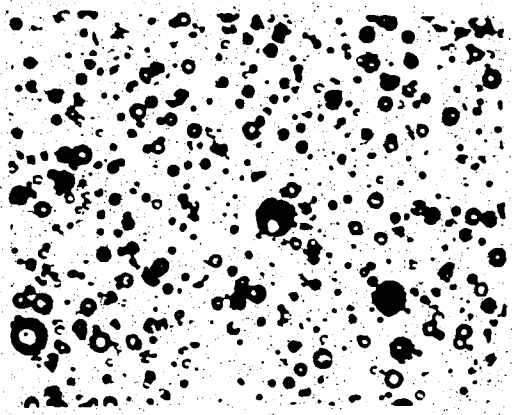

Plate C.26, 25°C

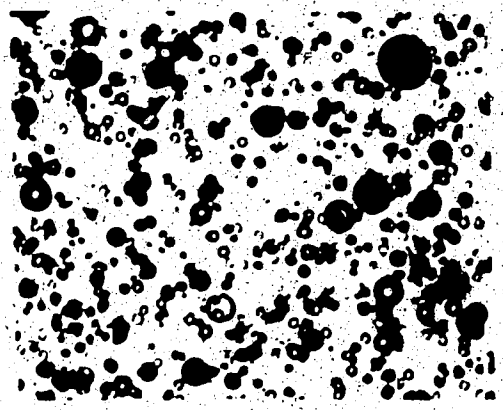

Plate C.29, 175°C

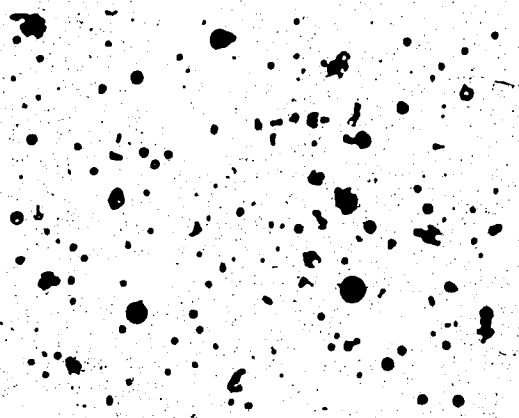

Plate C.27, 75°C

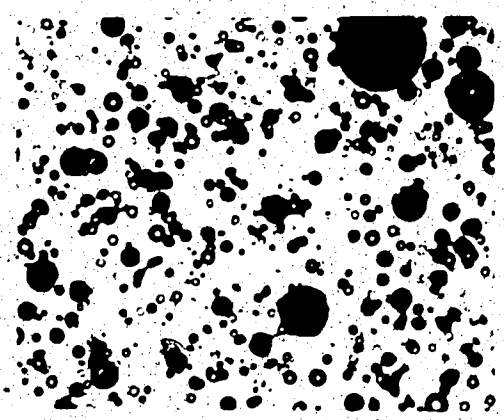

Plate C.30, 225°C

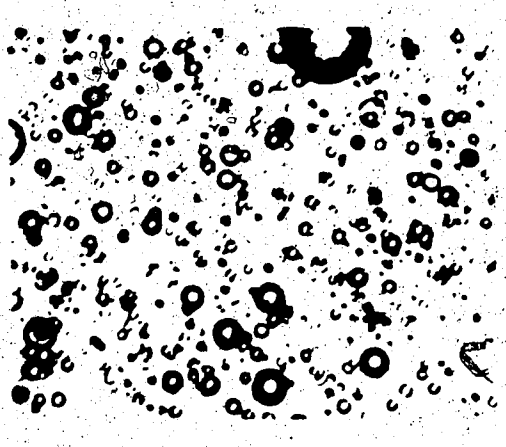

Plate C.28, 125°C

PRIMROSE OIL/TRITON X-100

Surfactant Concentration = 2000 ppm @ Cure Temperature

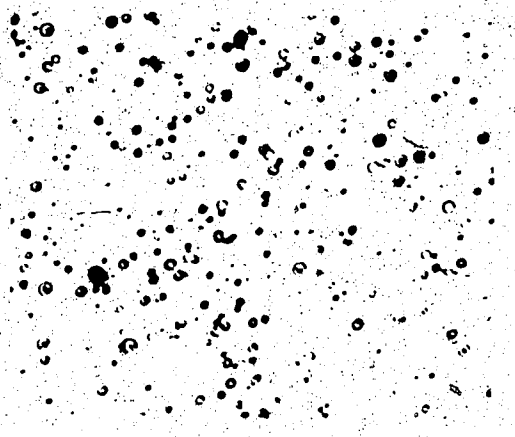

Plate C.31, 25°C

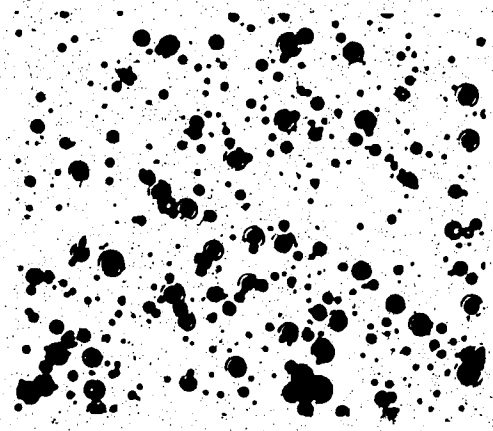

Plate C.34, 175°C

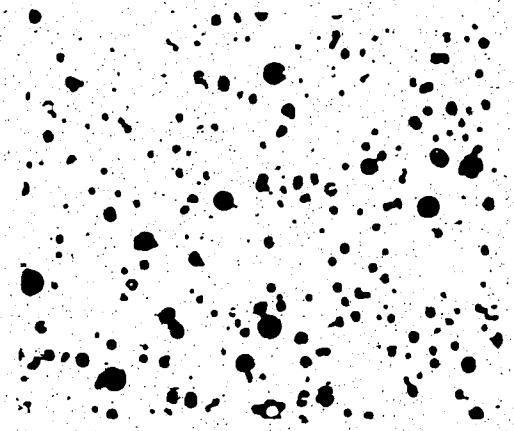

Plate C.32, 75°C

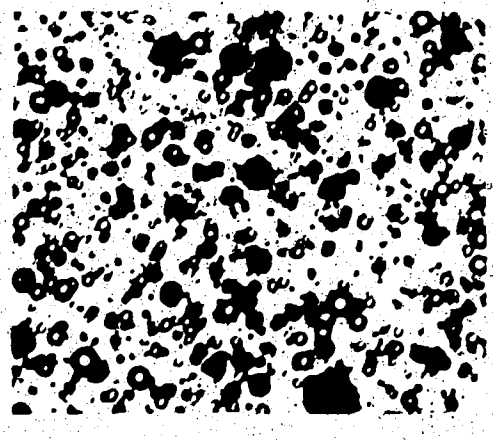

Plate C.35, 225°C

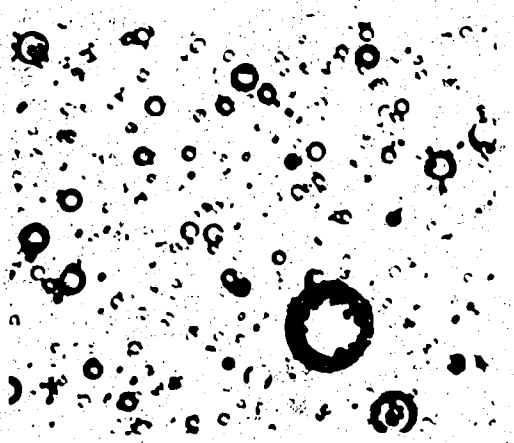

Plate C.33, 125°C

PRIMROSE OIL/TRITON X-100

Surfactant Concentration = 5000 ppm @ Cure Temperature

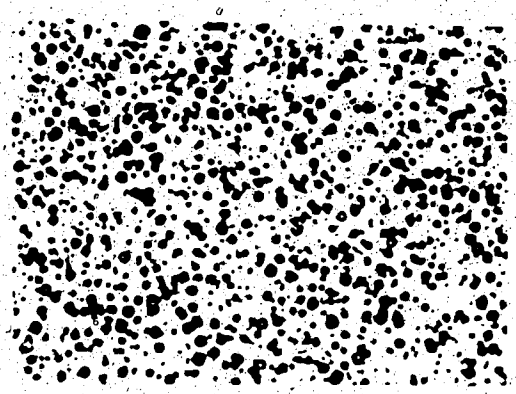

Plate C.36, 25°C

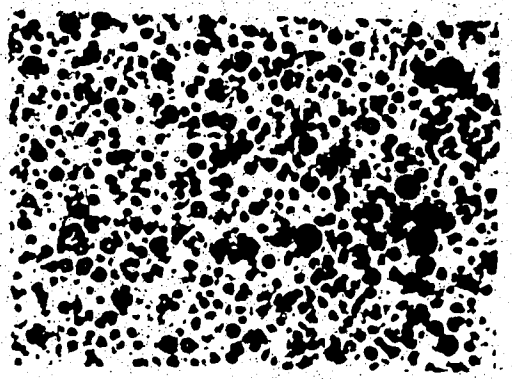

Plate C.39, 175°C

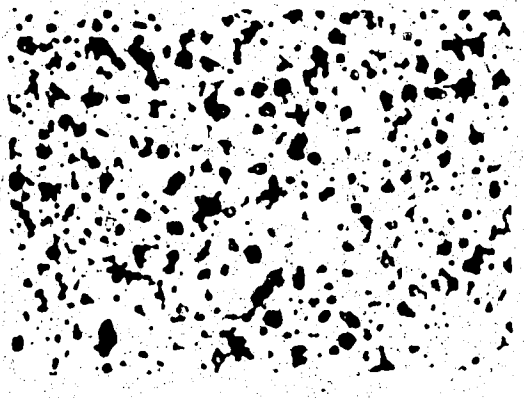

Plate C.37, 75°C

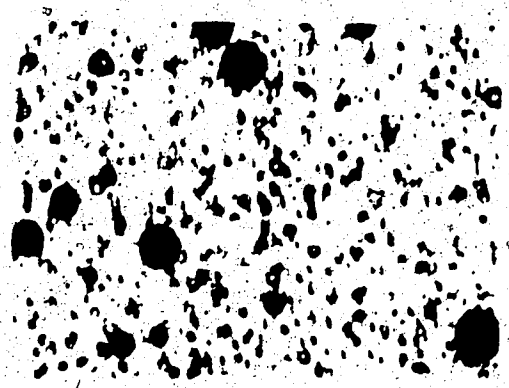

Plate C.40, 225°C

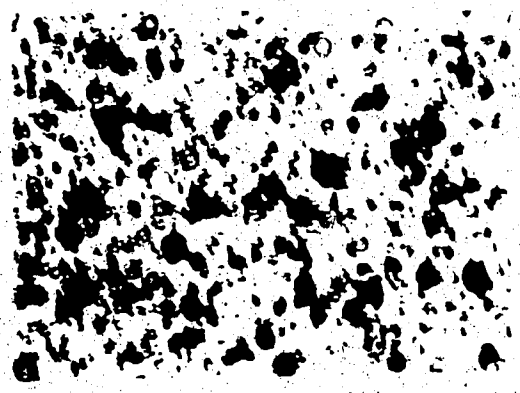

Plate C.38, 125°C

TABLE C.1 - Change in pH for 5% Primrose Oil Emulsions with Triton X-100 Surfactant @ Cure Temperature

SURFACTANT CONCENTRATION (ppm)	CURE TEMPERATURE °C 25	75	125	175	225
25	8.43/8.50*	8.68/8.51	9.23/9.10	9.01/8.93	9.13/6.59
50	8.65/8.54	8.91/9.03	9.25/9.35	9.27/8.75	8.89/7.71
100	9.03/8.98	8.82/8.75	9.49/9.20	9.45/8.83	9.22/7.88
300	8.92/8.80	8.61/8.69	9.12/9.12	9.22/8.51	9.11/8.07
700	8.92/8.85	8.90/8.85	9.15/8.97	8.75/7.77	8.57/6.02
1200	8.64/8.82	8.89/8.81	8.92/9.01	8.76/7.73	8.75/6.94
2000	8.90/8.82	8.75/8.70	8.79/8.75	8.47/8.31	8.80/7.20
5000	8.35/8.25	8.19/8.10	8.20/8.15	8.17/7.40	8.31/6.84

* - Data Values : (pH in/pH out)

Cure Time = 1 hour

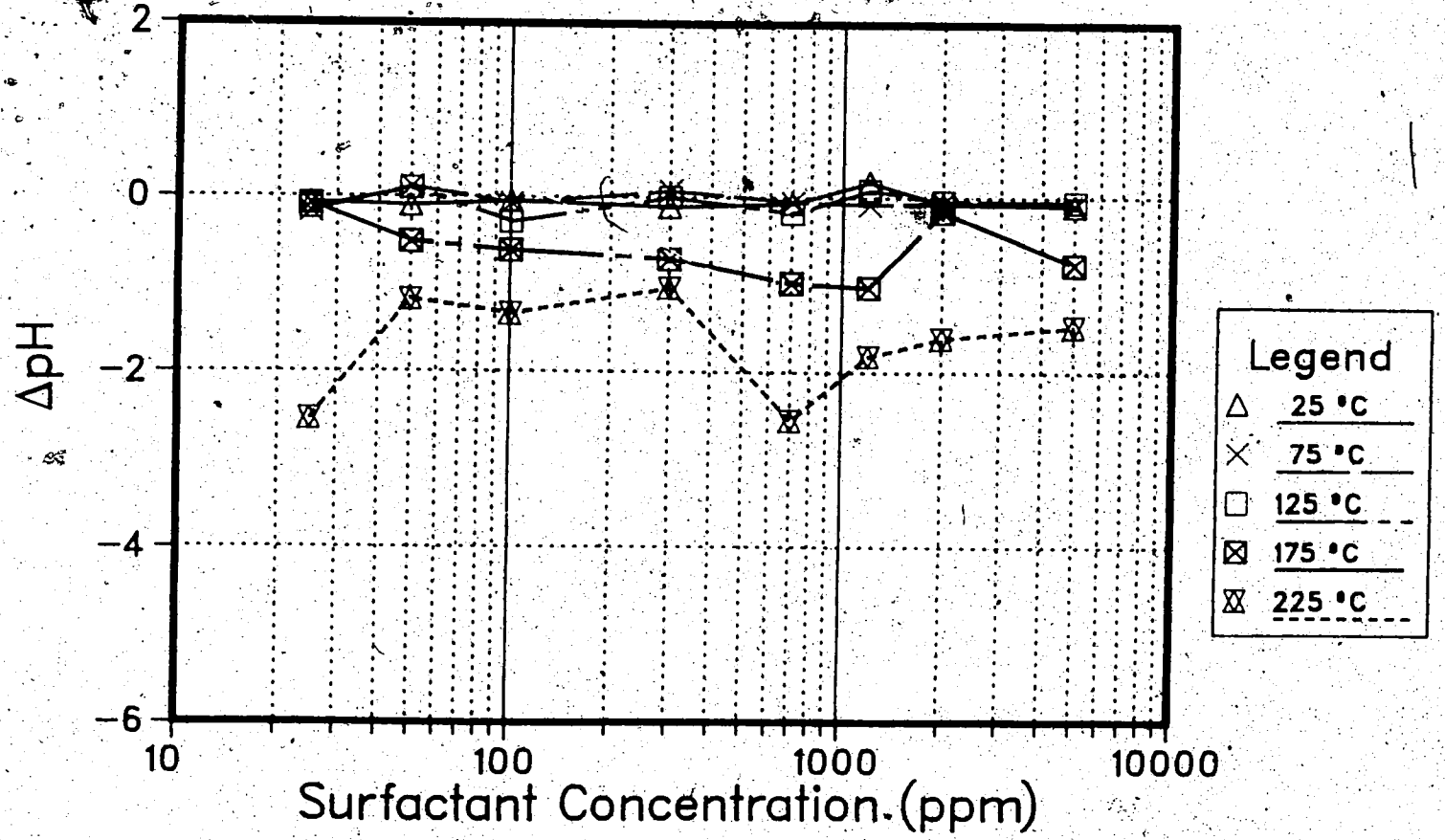

FIGURE C.1 – Primrose Oil / TX–100 Surfactant
ΔpH vs. Surfactant Concentration @ Cure Temperature

APPENDIX D

Microphotographs and pH Data for 5% Primrose Oil Emulsions Stabilized with Vista 250 Surfactant

PRIMROSE OIL/VISTA 250

Surfactant Concentration = 25 ppm @ Cure Temperature

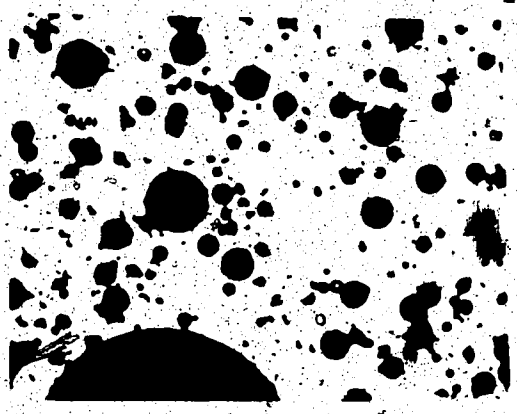

Plate D.1, 25°C

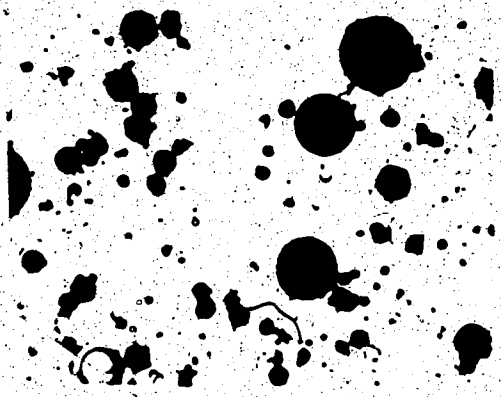

Plate D.4, 175°C

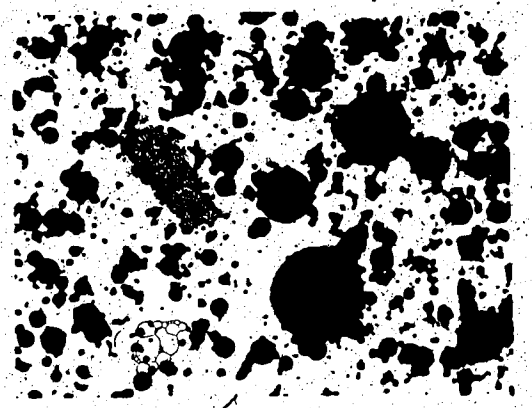

Plate D.2, 75°C

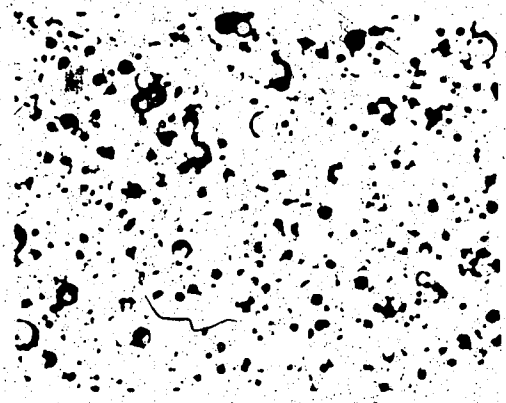

Plate D.5, 225°C

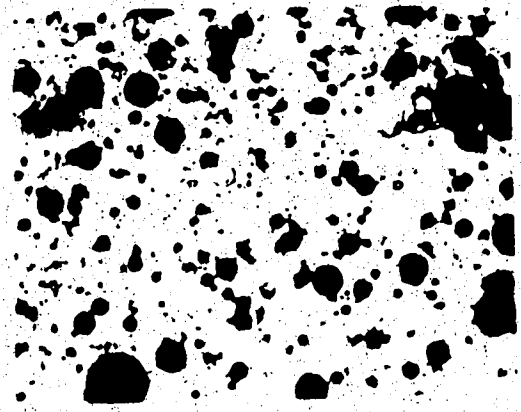

Plate D.3, 125°C

PRIMROSE OIL/VISTA 250

Surfactant Concentration = 50 ppm @ Cure Temperature

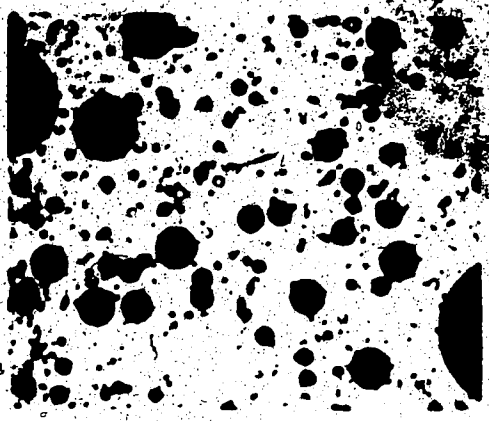

Plate D.6, 25°C

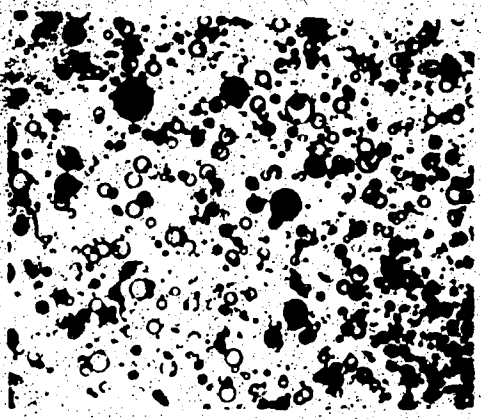

Plate D.9, 175°C

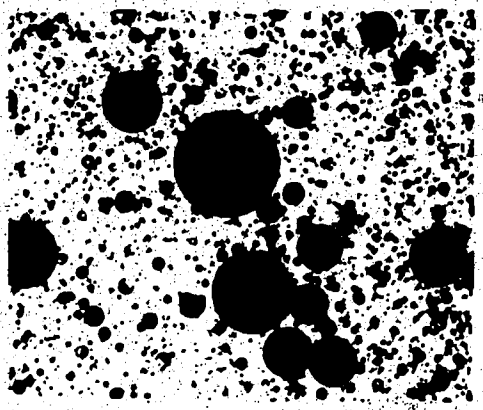

Plate D.7, 75°C

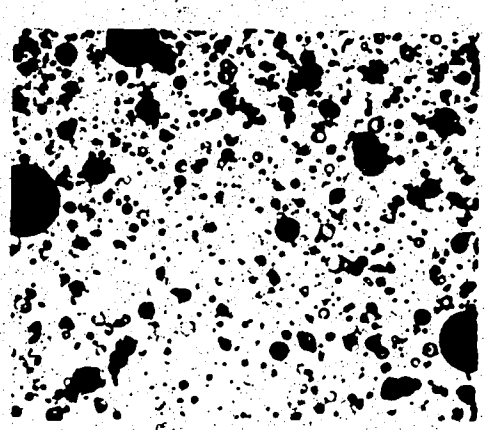

Plate D.10, 225°C

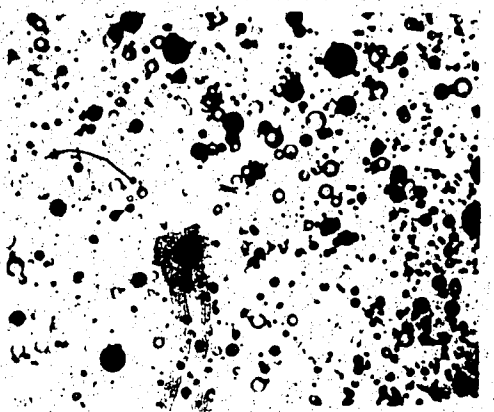

Plate D.8, 125°C

PRIMROSE OIL/VISTA 250

Surfactant Concentration = 100 ppm @ Cure Temperature

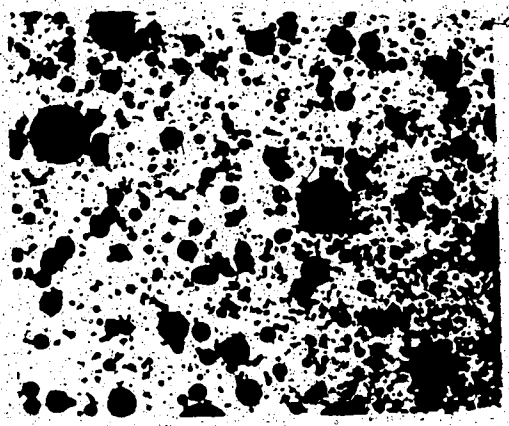

Plate D.11, 25°C

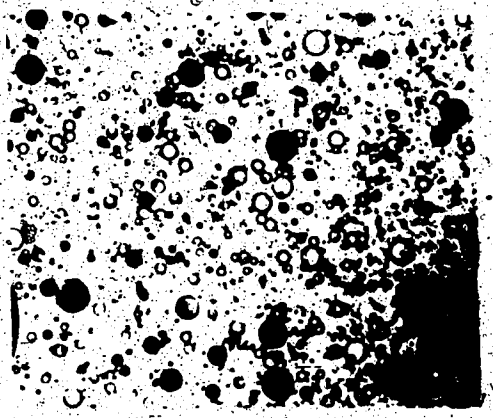

Plate D.14, 175°C

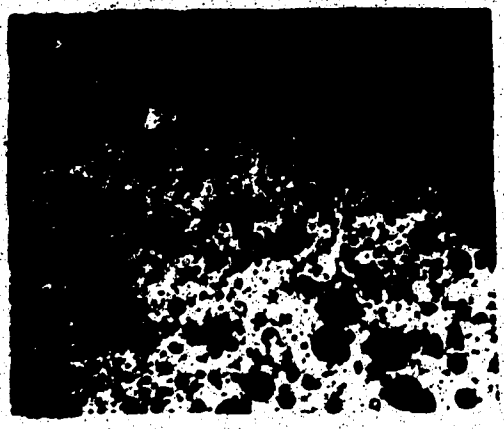

Plate D.12, 75°C

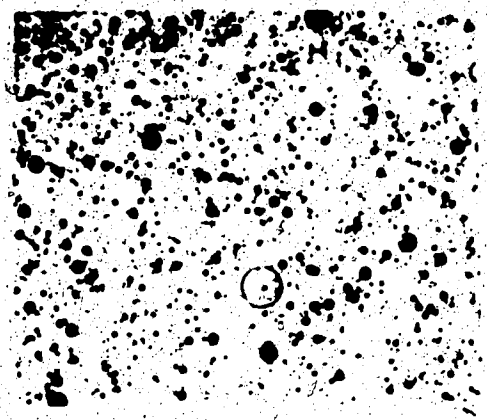

Plate D.15, 226°C

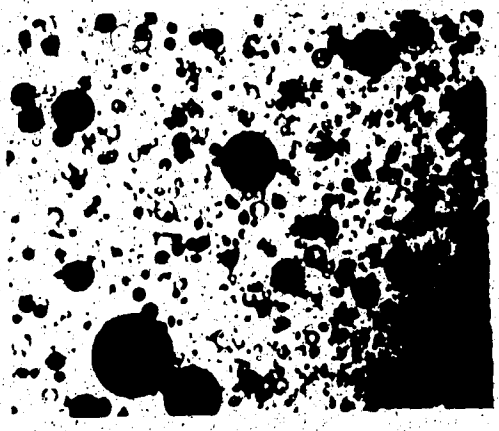

Plate D.13, 125°C

PRIMROSE OIL/VISTA 250

Surfactant Concentration = 300 ppm @ Cure Temperature

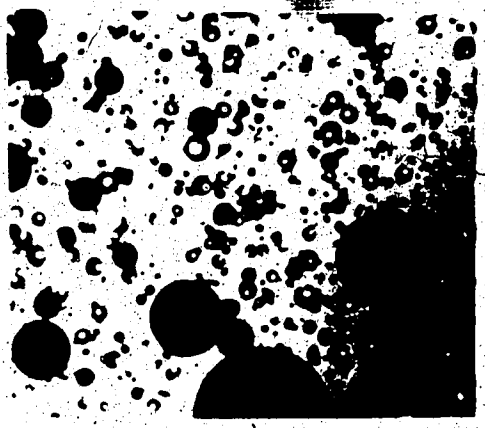

Plate D.16, 25°C

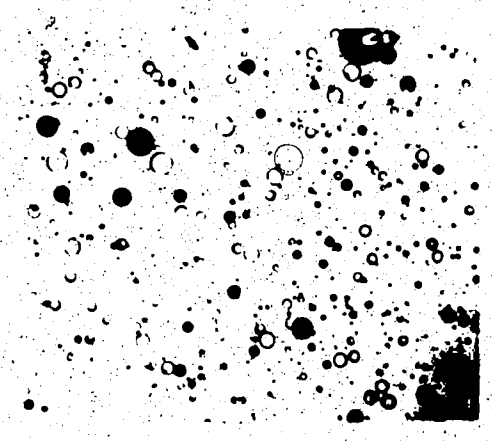

Plate D.19, 175°C

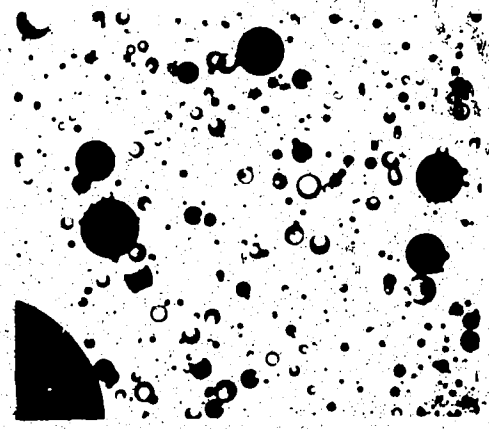

Plate D.17, 75°C

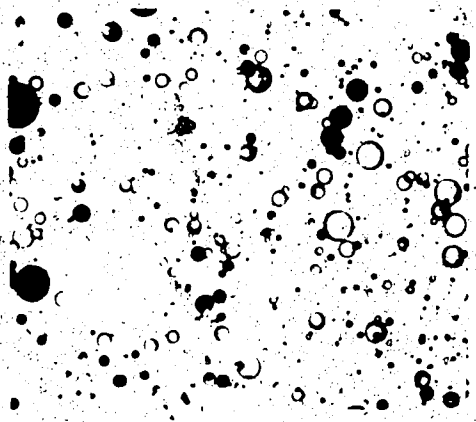

Plate D.20, 225°C

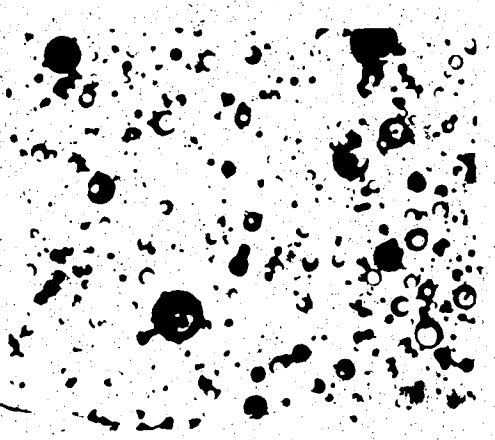

Plate D.18, 125°C

PRIMROSE OIL/VISTA 250

Surfactant Concentration = 700 ppm @ Cure Temperature

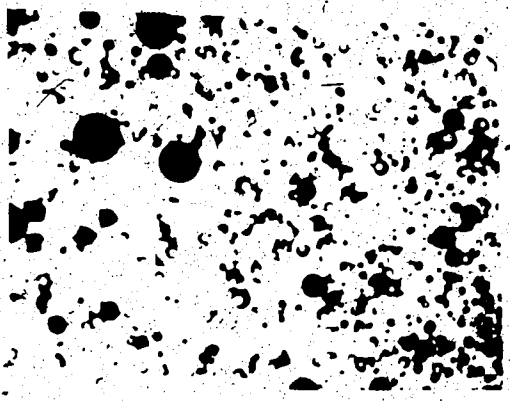

Plate D.21, 25°C

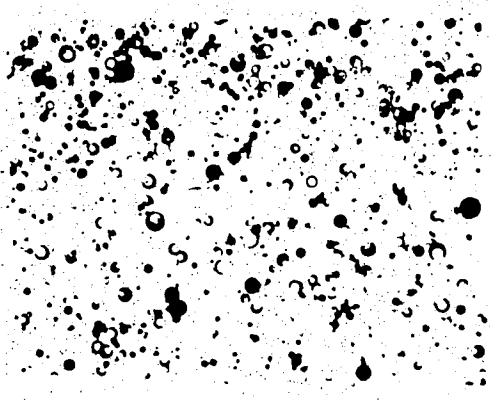

Plate D.24, 175°C

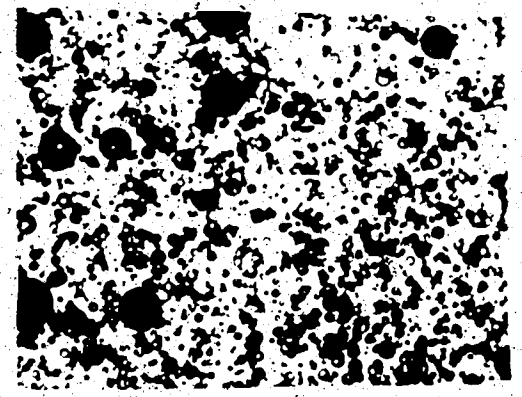

Plate D.22, 75°C

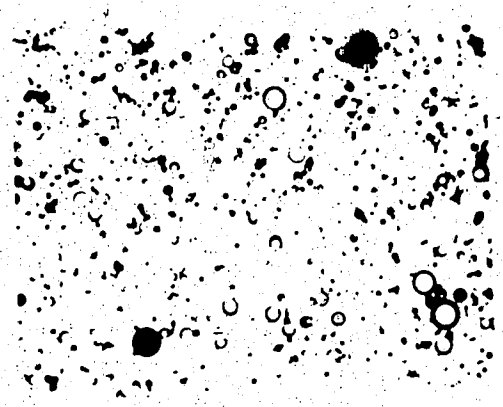

Plate D.25, 225°C

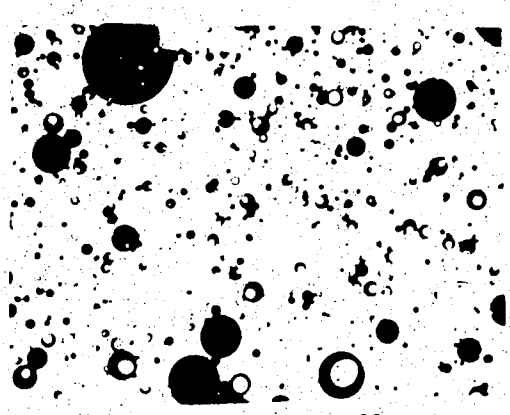

Plate D.23, 125°C

PRIMROSE OIL/VISTA 250

Surfactant Concentration = 1200 ppm @ Cure Tmperature

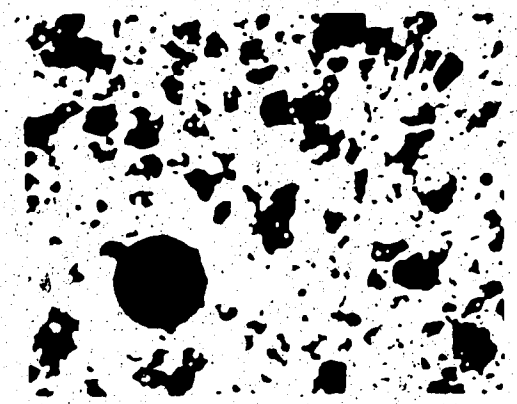

Plate D.26, 25°C

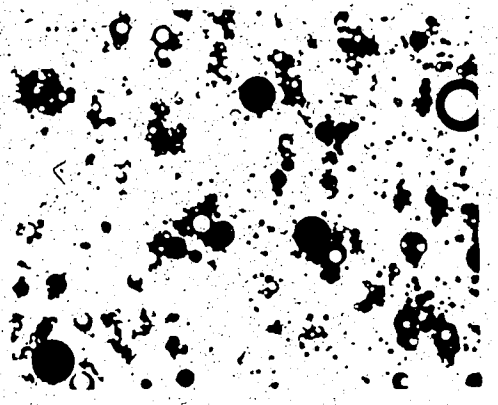

Plate D.29, 175°C

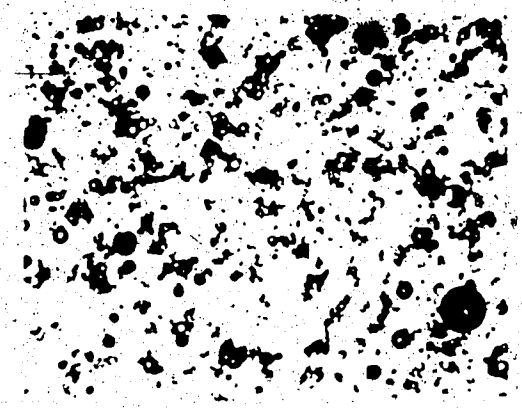

Plate D.27, 75°C

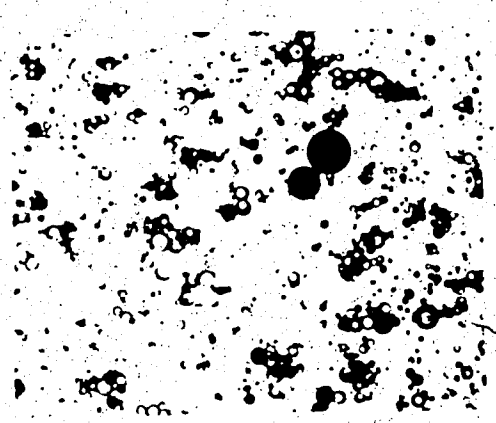

Plate D.30, 225°C

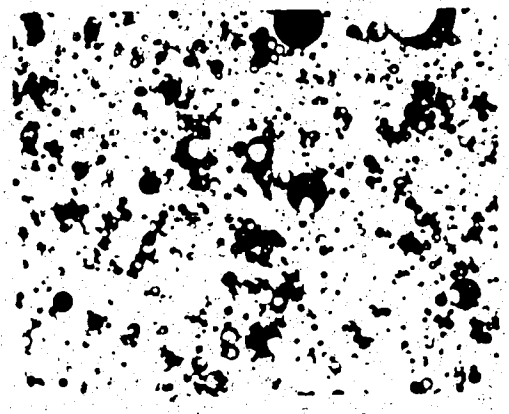

Plate D.28, 125°C

PRIMROSE OIL/VISTA 250

Surfactant Concentration = 2000 ppm @ Cure Temperature

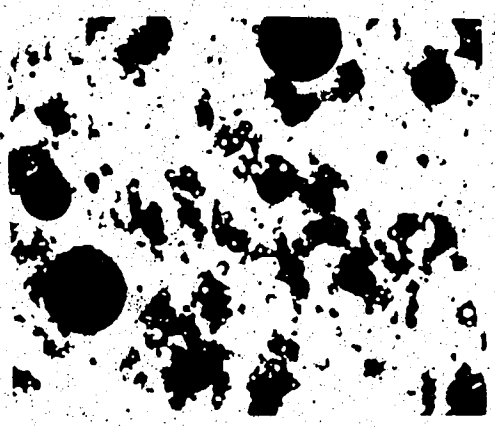

Plate D.31, 25°C

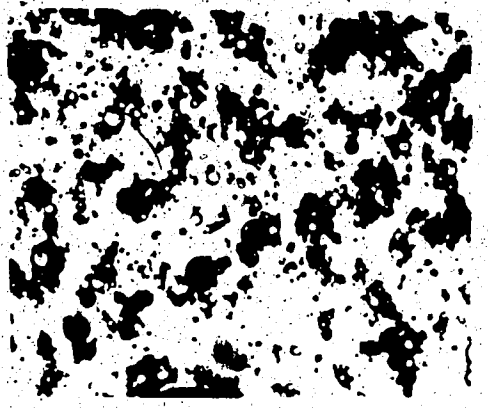

Plate D.34, 175°C

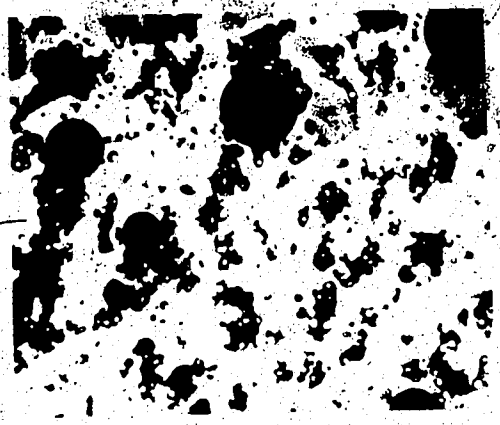

Plate D.32, 75°C

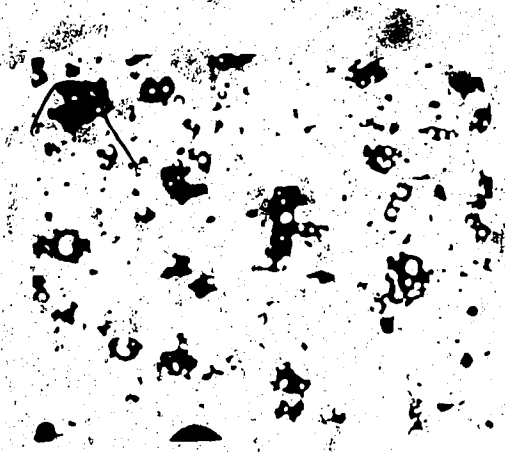

Plate D.35, 225°C

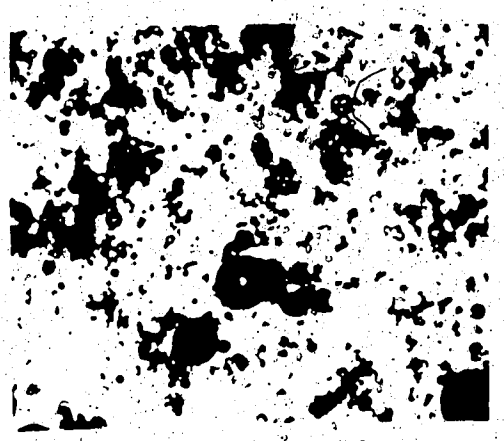

Plate D.33, 125°C

PRIMROSE OIL/VISTA 250

Surfactant Concentration = 5000 ppm @ Cure Temperature

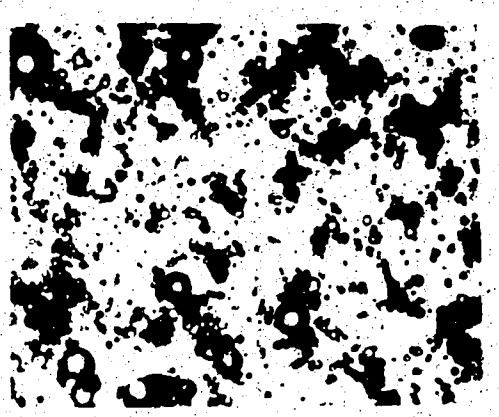

Plate D.36, 25°C

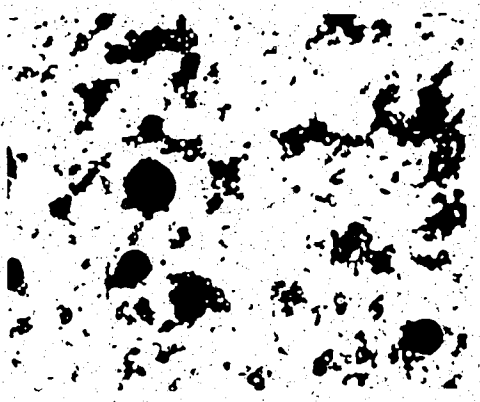

Plate D.39, 175°C

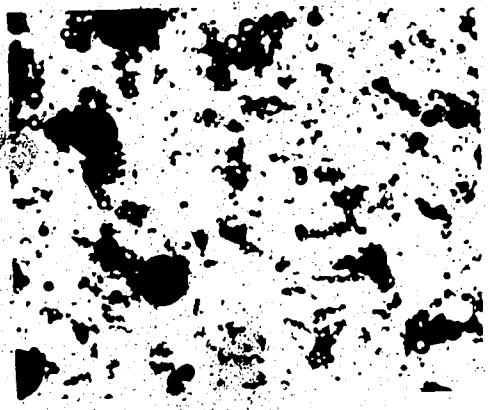

Plate D.37, 75°C

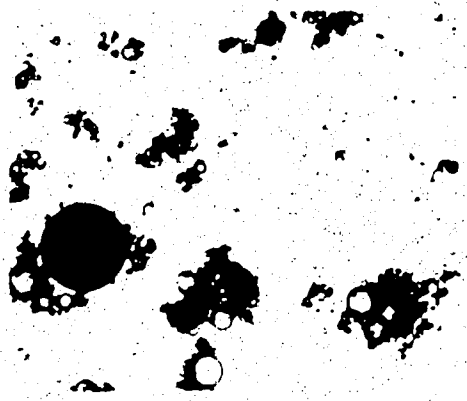

Plate D.40, 225°C

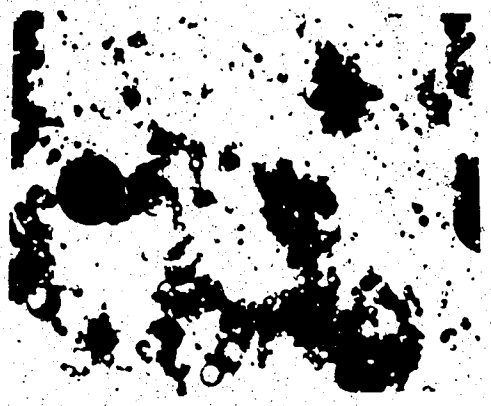

Plate D.38, 125°C

TABLE D.1 - Change in pH for 5% Primrose Oil Emulsions with Vista 250 Surfactant @ Cure Temperature

SURFACTANT CONCENTRATION (ppm)	CURE TEMPERATURE °C				
	25	75	125	175	225
25	9.25/9.19*	9.30/9.17	9.50/9.35	9.83/9.04	9.59/7.69
50	9.81/9.71	9.65/9.58	9.64/9.39	9.96/9.18	9.75/7.43
100	9.97/9.93	9.96/9.81	9.80/9.57	9.85/9.37	9.83/8.73
300	10.02/10.03	10.01/9.93	10.06/9.82	10.00/9.42	10.06/9.25
700	10.01/10.04	9.97/9.78	10.13/9.74	10.04/9.21	10.14/8.18
1200	9.97/9.93	9.96/9.65	9.99/9.56	9.72/9.26	9.95/8.30
2000	9.96/9.83	9.78/9.57	9.80/9.46	9.70/9.50	9.67/8.45
5000	9.35/9.29	9.40/9.32	9.37/9.30	9.29/9.20	9.40/8.56

* - Data Values : (pH in/pH out)

Cure Time = 1 hour

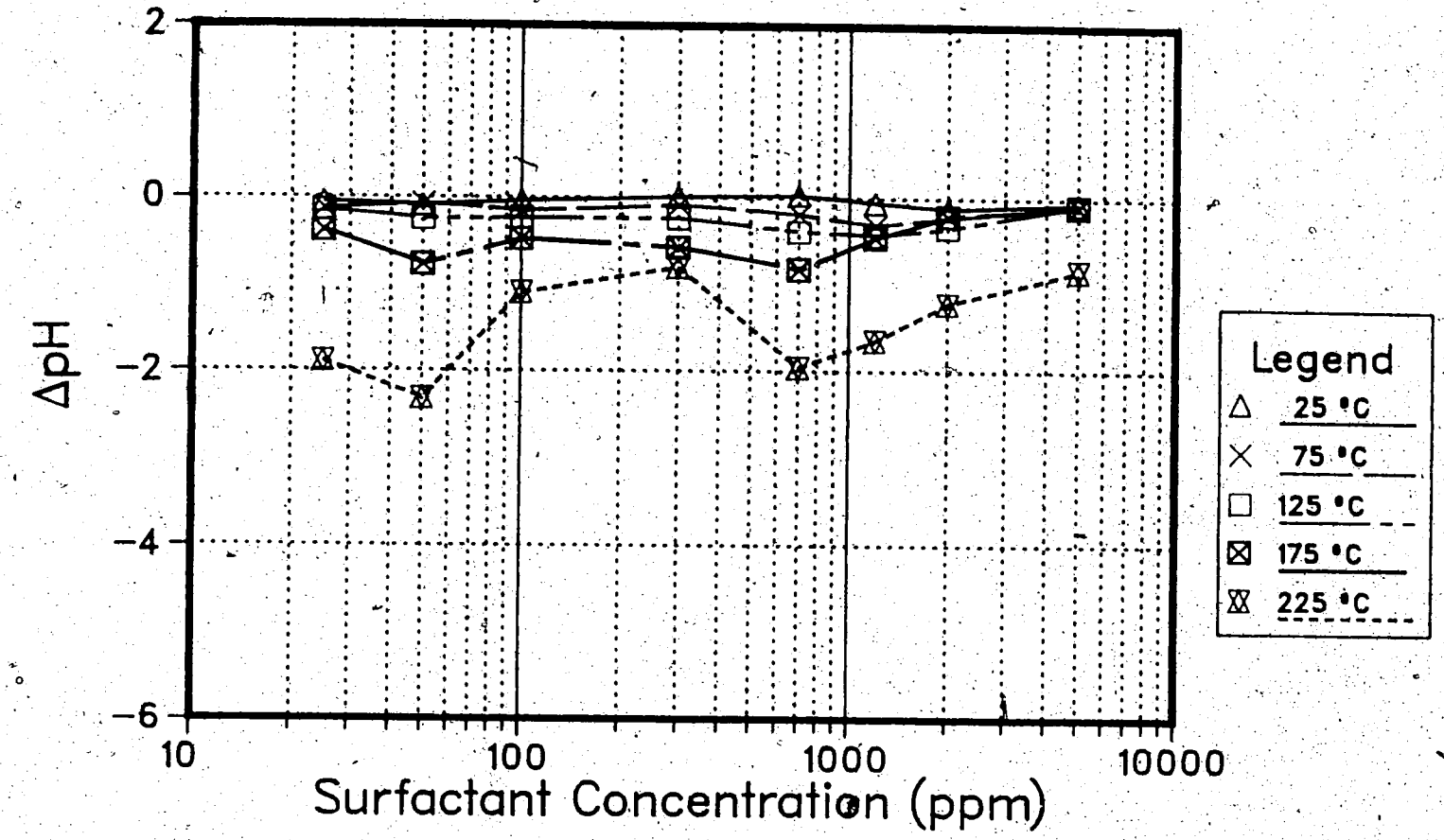

FIGURE D.1 – Primrose Oil / Vista 250 Surfactant
ΔpH vs. Surfactant Concentration @ Cure Temperature

APPENDIX E

Viscosity Determination of Lloydminster and Primrose Oil and 5% O/W Emulsions

Viscosity is an important rheological parameter for characterizing emulsions and their flow behaviour. A Brookfield Synchro-Lectric viscometer (Model LVTD) was used here to determine the viscosity of the oils and their emulsions.

Oil Viscosity Calculation: Cylindical Spindle

For measurement of fluid viscosity between 100 and 2,000,000 mPa·s a set of cylindrical spindles were used. The instrument rotates a spindle in the fluid at constant speed and measures the torque necessary to overcome the viscous drag. [1] The spindle is rotated by a calibrated spring and, for a given rotational speed and spindle, dial readings were produced which are proportional to the viscosity. The viscosity was then calculated by multiplying a conversion factor corresponding to the rotational speed to the dial reading. This was obtained from the company supplied "factor finder". Presuming the fluid is Newtonian i.e. viscosity was independent of shear rate, a correct apparent viscosity was determined by this procedure.

For non-Newtonian systems, the apparent viscosity is a function of shear rate and the viscosity determined from the dial reading differs from the true apparent viscosity with

---

[1] Brookfield Engineering Laboratories, Inc., Stoughton, Massachusetts, Brookfield Synchro-Lectric Viscometer Instruction Manual (Model LVTD).

the magnitude of error increasing with increasing deviation from Newtonian behaviour (Van Wazer et al., 1963). One method to determine true apparent viscosity is to report one value of apparent viscosity, at a well defined shear rate, and an index which describes the deviation from Newtonian behaviour. Fluids characterized by two such parameters follow an empirical rheological equation known as the power law.

A 'Template' method (Rosen, 1971) exists for characterizing the non-Newtonian nature of a power law fluid by a single parameter known as the shear thinning index (STI). Rosen details this technique where well-defined shear rates can be determined for corresponding r.p.m. settings of the Brookfield Synchro-Lectric viscometer. This allows simple determination of apparent viscosity for Newtonian and Non-Newtonian fluid behaviour. For Newtonian fluids STI is equal to one (1). For shear thinning (pseudoplastic) and shear thickening (dilatant) the STI is greater and less than one, respectively. Rosen demonstrates the theoretical developments and assumptions behind the method. Following the procedure the rheological data was obtained for the dried Primrose and Lloydminster oils at various temperatures and presented in Tables E.1 through E.8.

Emulsion Viscosity Calculation: UL Adaptor

The UL Adaptor to the Brookfield Synchro-Lectric viscometer

was useful for measuring fluids of low viscosity. The viscometer geometry in this instance was the coaxial cylinder, or couette type. The viscosity of emulsions were calculated here using the Shear Thinning Index (STI) and template developed for application with the coaxial cylinder (Rosen, 1972). Theoretical development, assumptions, and restrictions are fully detailed in this publication.

Emulsions created in this work had approximately a 5% oil content by volume in water. In general, emulsions tend to have a viscosity similar to the continuous phase (Becher) therefore, the viscosity value would be close to distilled water, but may exhibit non-Newtonian behaviour at higher disperse phase concentrations. It was found that emulsion behaviour of these oils was adequately characterized by the power law model in previous work (King). Emulsion viscosity measurements are recorded in Tables E.9 to E.14 for various temperatures.

TABLE E.1

LLOYDMINSTER OIL: Temperature = 22.5 °C, spindle = LV3

Shear Rate, (sec^{-1})	Apparent Viscosity, (mPa·s)
0.314	9,880
0.628	9,920
1.260	10,100

TABLE E.2

LLOYDMINSTER OIL: Temperature = 40 °C, spindle = LV3

Shear Rate, (sec^{-1})	Apparent Viscosity, (mPa·s)
0.64	3040
1.28	2880
2.56	2800
6.41	2740

TABLE E.3

LLOYDMINSTER OIL: Temperature = 62 °C, spindle = LV3

Shear Rate, (sec^{-1})	Apparent Viscosity, (mPa·s)
2.51	630
6.28	608
12.60	592

TABLE E.4

LLOYDMINSTER OIL: Temperature = 79 °C, spindle = LV3

Shear Rate, (sec^{-1})	Apparent Viscosity, (mPa·s)
2.64	260
6.60	236
13.20	204

TABLE E.5

PRIMROSE OIL: Temperature = 22.5 °C, spindle = LV4

Shear Rate, (sec^{-1})	Apparent Viscosity, (mPa·s)
0.314	47,000
0.628	46,000
1.260	45,700
2.520	45,700

TABLE E.6

PRIMROSE OIL: Temperature = 40 °C, spindle = LV3

Shear Rate, (sec^{-1})	Apparent Viscosity, (mPa·s)
0.128	12,000
0.319	11,600
0.638	11,280
1.280	10,960

TABLE E.7

PRIMROSE OIL: Temperature = 63.5 °C, spindle = LV3

Shear Rate, (sec^{-1})	Apparent Viscosity, (mPa·s)
1.31	2100
2.61	2030
6.54	1984
13.10	1964

TABLE E.8

PRIMROSE OIL: Temperature = 80.5 °C, spindle = LV3

Shear Rate, (sec^{-1})	Apparent Viscosity, (mPa·s)
2.61	770
6.54	728
13.10	708

TABLE E.9

LLOYDMINSTER 5% O/W EMULSION: Temperature = 25 °C, UL Adaptor

Shear Rate, (sec^{-1})	Apparent Viscosity, (mPa·s)
14.76	1.24
36.92	1.17
73.83	1.14

TABLE E.10

LLOYDMINSTER 5% O/W EMULSION: Temperature = 36 °C, UL Adaptor

Shear Rate, (sec^{-1})	Apparent Viscosity, (mPa·s)
14.71	1.12
36.78	1.10
73.56	1.08

TABLE E.11

LLOYDMINSTER 5% O/W EMULSION: Temperature = 60 °C, UL Adaptor

Shear Rate, (sec^{-1})	Apparent Viscosity, (mPa·s)
14.71	1.140
36.78	0.978
73.57	0.973

TABLE E.12

PRIMROSE 5% O/W EMULSION: Temperature = 31 °C, UL Adaptor

Shear Rate, (sec^{-1})	Apparent Viscosity, (mPa·s)
14.71	1.50
36.78	1.20
73.56	1.15

TABLE E.13

PRIMROSE 5% O/W EMULSION: Temperature = 41 °C, UL Adaptor

Shear Rate, (sec^{-1})	Apparent Viscosity, (mPa·s)
14.98	1.35
37.46	1.17
74.91	1.09

TABLE E.14

PRIMROSE 5% O/W EMULSION: Temperature = 62 °C, UL Adaptor

Shear Rate, (sec^{-1})	Apparent Viscosity, (mPa·s)
14.71	1.10
36.78	1.08
73.56	1.04

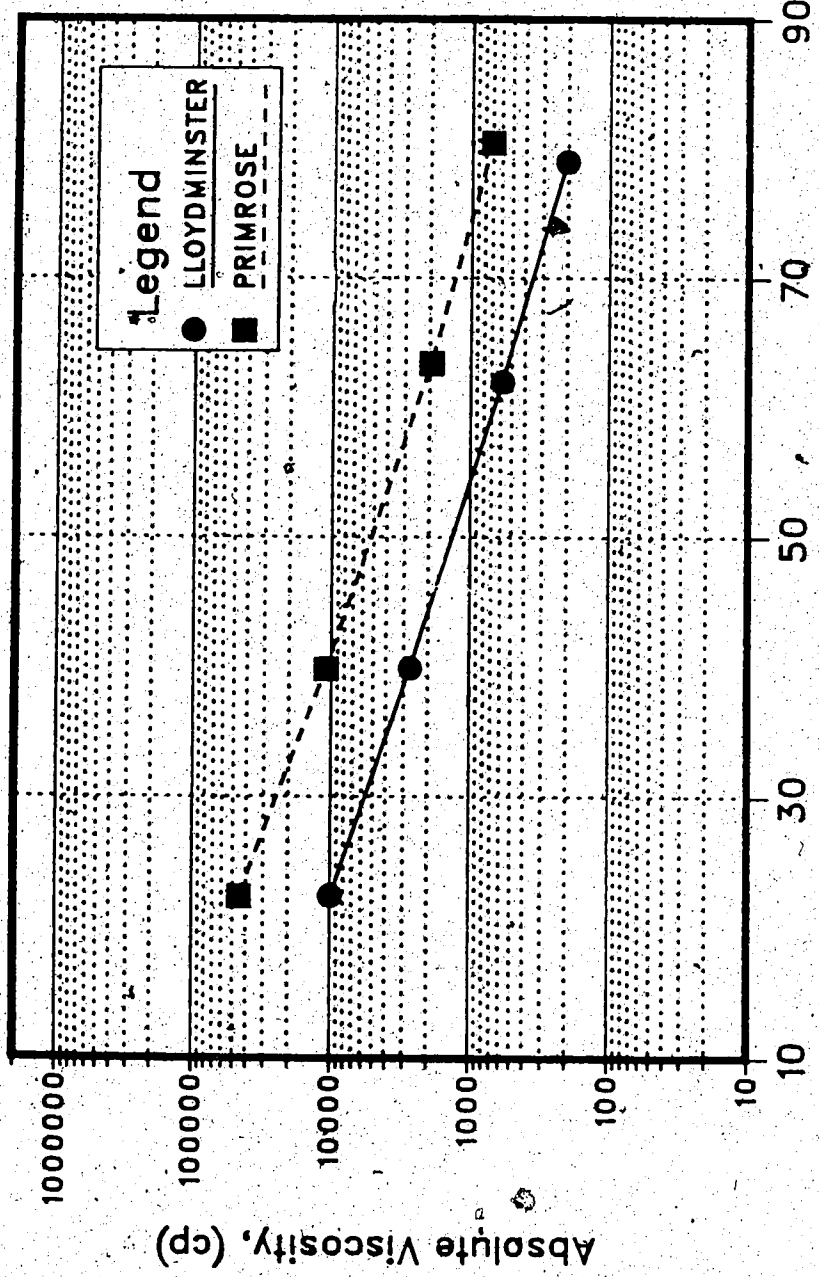

FIGURE E.1 – Oil Viscosity (Gas Free @ P = 1 atm)
Absolute Viscosity vs. Temperature

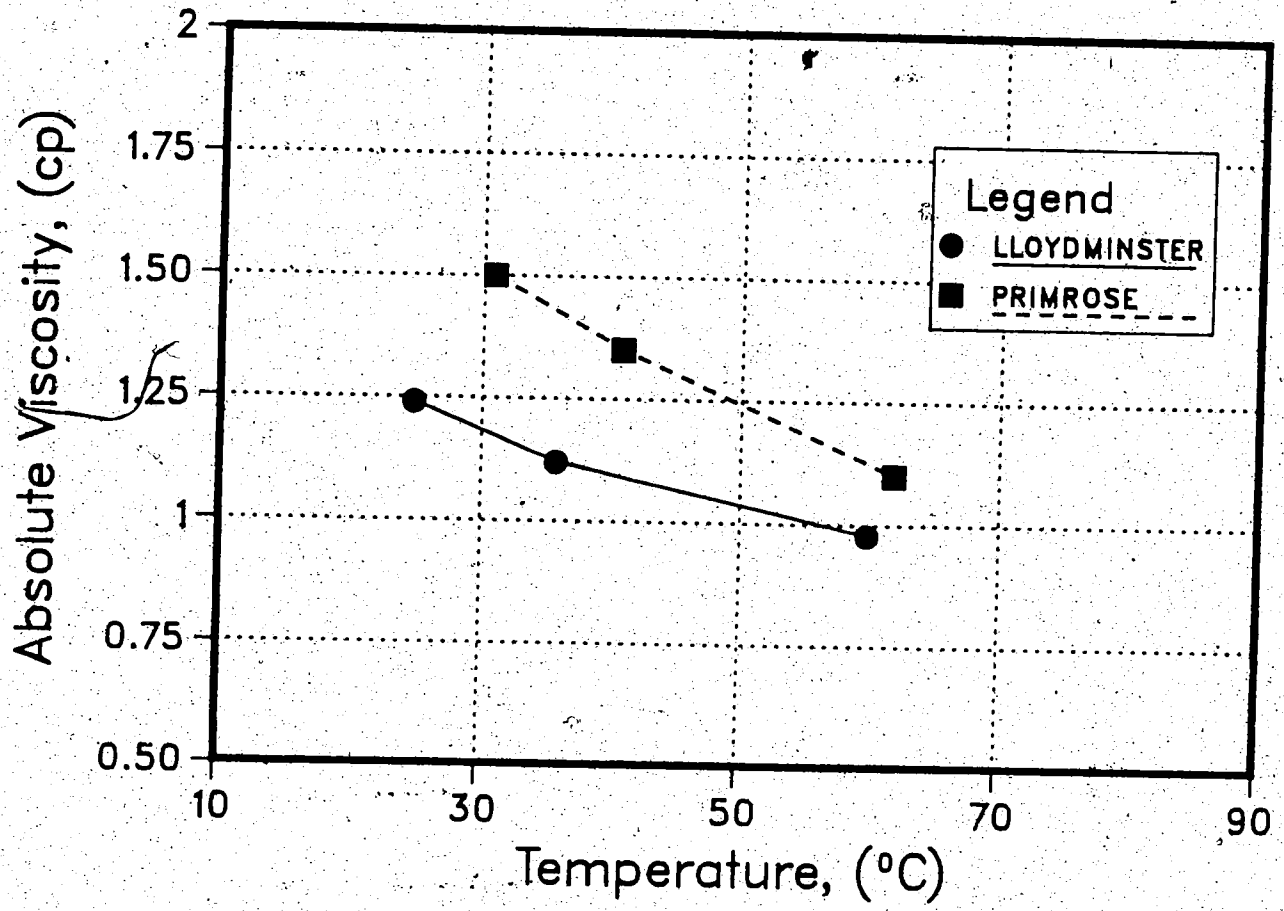

FIGURE E.2 – 5% Heavy Oil Emulsion Viscosity @ P = 1 atm

APPENDIX F

Experimental Data and Production Results for Steam/Emulsion Injection Floods

TABLE F.1 - LLOYDMINSTER OIL: RUN #1 - Experimental Data and Production Results -

- Base Steamflood (60-120 mesh sand)

Date of Run = 11/06/1985
Bulk Volume = 1870. cc
Sand Pack = Ottawa Silica 60-120 mesh
Sand Density = 1.88 g/cc
Pore Volume = 720.0 cc
Porosity = 38.5 %
Permeability = 12.9 d

Initial Oil In Place = 696.2 cc
Oil Saturation = 96.7 %
Oil Viscosity = 10100. mPa.s @ 0 MPag & 22 C

CYL #	TIME (hr)	FLUID PROD. (cc)	CRUDE PROD. (cc)	WATER IN CRUDE (%)	OIL IN WATER (%)	OIL PROD. (cc)	WATER PROD. (cc)	OIL PROD. RATE (cc/hr)	CUM. FLUID PROD. (PV)	CUM. OIL PROD. (cc)	CUM. OIL REC. (%IOIP)	WATER OIL RATIO (cc/cc)	pH
1	2.2[illegible]	[illegible]	200.0	23.4	0.0	153.20	96.80	69.64	0.35	153.20	22.0	0.63	8.74
2	2.8[illegible]	[illegible]	80.0	41.9	0.0	46.48	203.52	69.37	0.69	199.68	28.7	4.38	8.39
3	3.5[illegible]	[illegible]	120.0	41.1	0.0	70.68	179.32	108.74	1.04	270.36	38.8	2.54	8.38
4	4.03	250.	120.0	36.2	0.0	76.56	173.44	150.12	1.39	346.92	49.8	2.27	8.04
5	4.48	270.	140.0	39.0	0.0	85.40	184.60	189.78	1.76	432.32	62.1	2.16	7.93
6	4.65	256.	140.0	50.2	0.0	69.72	186.28	410.12	2.12	502.04	72.1	2.67	7.91
7	4.82	250.	140.0	53.0	0.0	65.80	184.20	387.06	2.47	567.84	81.6	2.80	7.25
8	4.98	250.	136.0	71.7	0.0	38.49	211.51	240.55	2.81	606.33	87.1	5.50	7.34
9	5.27	250.	16.0	95.1	0.0	0.78	249.22	2.70	3.16	607.11	87.2	317.88	7.68
10	5.58	250.	10.0	95.1	0.0	0.49	249.51	1.58	3.51	607.60	87.3	509.20	7.68
11	5.87	250.	10.0	95.1	0.0	0.49	249.51	1.69	3.86	608.09	87.3	509.20	7.75
12	6.20	250.	5.0	95.1	0.0	0.24	249.75	0.74	4.20	608.34	87.4	>999	7.81
13	6.57	250.	5.0	95.1	0.0	0.24	249.75	0.66	4.55	608.58	87.4	>999	8.01
14	6.80	250.	0.0	100.0	0.0	0.0	250.00	0.0	4.90	608.58	87.4	---	7.98
15	7.00	184.	0.0	100.0	0.0	0.0	184.00	0.0	5.15	608.58	87.4	---	8.10

TABLE F.2 - LLOYDMINSTER OIL: RUN #2 - Experimental Data and Production Results

- Base Steamflood (20-40 mesh sand)

Date of Run = 11/12/1985
Bulk Volume = 1870. cc
Sand Pack = Ottawa Silica 20-40 mesh
Sand Density = 1.91 g/cc
Pore Volume = 640.0 cc
Porosity = 34.2 %
Permeability = 38.7 d

Initial Oil In Place = 611.8 cc
Oil Saturation = 95.6 %
Oil Viscosity = 10100. mPa.s @ 0 MPag & 22 C

CN #	TIME (hr)	FLUID PROD. (cc)	CRUDE PROD. (cc)	WATER IN CRUDE (%)	OIL IN WATER (%)	OIL PROD. (cc)	WATER PROD. (cc)	OIL PROD. RATE (cc/hr)	CUM. FLUID PROD. (PV)	CUM. OIL PROD. (cc)	CUM. OIL REC. (%IOIP)	WATER OIL RATIO (cc/cc)	pH
1	0.80	250.	100.0	19.7	0.0	80.30	169.70	100.38	0.39	80.30	13.1	2.11	8.24
2	1.27	250.	50.0	24.2	0.0	37.90	212.10	80.64	0.78	118.20	19.3	5.60	8.29
3	1.82	262.	120.0	25.7	0.0	89.16	172.84	162.11	1.19	207.36	33.9	1.94	8.42
4	2.33	270.	110.0	22.8	0.0	84.92	185.08	166.51	1.61	292.28	47.8	2.18	8.04
5	2.75	290.	100.0	22.6	0.0	77.40	212.60	184.29	2.07	369.68	60.4	2.75	8.33
6	3.00	250.	125.0	31.1	0.0	86.12	163.88	344.50	2.46	455.80	74.5	1.90	8.23
7	3.15	270.	160.0	43.7	0.0	90.08	179.92	600.53	2.88	545.88	89.2	2.00	8.15
8	3.30	250.	30.0	60.2	0.0	11.94	238.06	79.60	3.27	557.82	91.2	19.94	8.24
9	3.47	250.	10.0	60.2	0.0	3.98	246.02	23.41	3.66	561.80	91.8	61.81	8.01
10	3.65	250.	10.0	60.2	0.0	3.98	246.02	22.11	4.05	565.78	92.5	61.81	8.25
11	3.83	250.	12.0	60.2	0.0	4.78	245.22	26.53	4.44	570.56	93.3	51.35	8.70
12	4.03	250.	10.0	70.8	0.0	2.92	247.08	14.60	4.83	573.48	93.7	84.62	8.40
13	4.23	250.	5.0	70.8	0.0	1.46	248.54	7.30	5.22	574.94	94.0	170.23	8.08
14	4.42	250.	5.0	70.8	0.0	1.46	248.54	7.68	5.61	576.40	94.2	170.23	8.18
15	4.62	250.	5.0	70.8	0.0	1.46	248.54	7.30	6.00	577.86	94.5	170.23	8.53
16	4.80	250.	5.0	70.8	0.0	1.46	248.54	8.11	6.39	579.32	94.7	170.23	8.42
17	5.02	250.	5.0	70.8	0.0	1.46	248.54	6.64	6.78	580.78	94.9	170.23	8.37
18	5.12	130.	5.0	70.8	0.0	1.46	128.54	14.60	6.99	582.24	95.2	88.04	8.26

TABLE F.3 - PRIMROSE OIL: RUN #3 - Experimental Data and Production Results

- Base Steamflood (60-120 mesh sand)

Date of Run = 11/18/1985
Bulk Volume = 1870. cc
Sand Pack = Ottawa Silica 60-120 mesh
Sand Density = 1.86 g/cc
Pore Volume = 720.0 cc
Porosity = 38.5 %
Permeability = 14.3 d

Initial Oil In Place = 703.0 cc
Oil Saturation = 97.6 %
Oil Viscosity = 45700. mPa.s @ 0 MPag & 22 C

CYL #	TIME (hr)	FLUID PROD. (cc)	CRUDE PROD. (cc)	WATER IN CRUDE (%)	OIL IN WATER (%)	OIL PROD. (cc)	WATER PROD. (cc)	OIL PROD. RATE (cc/hr)	CUM. FLUID PROD. (PV)	CUM. OIL PROD. (cc)	CUM. OIL REC. (%IOIP)	WATER OIL RATIO (cc/cc)	pH
1	7.27	250.	190.0	35.0	0.0	123.50	126.50	16.99	0.35	123.50	17.6	1.02	9.15
2	8.47	252.	70.0	30.8	0.0	48.44	203.56	40.37	0.70	171.94	24.5	4.20	9.10
3	9.18	250.	60.0	33.2	0.0	40.08	209.92	56.45	1.04	212.02	30.2	5.24	9.04
4	9.90	250.	90.0	32.3	0.0	60.93	189.07	84.63	1.39	272.95	38.8	3.10	8.99
5	10.60	250.	115.0	32.1	0.0	78.08	171.92	111.56	1.74	351.03	49.9	2.20	8.95
6	10.97	254.	120.0	35.5	0.0	77.40	176.60	209.19	2.09	428.43	60.9	2.28	9.05
7	11.03	250.	150.0	49.7	0.0	75.45	174.55	1257.50	2.44	503.88	71.7	2.31	8.82
8	11.18	290.	110.0	68.2	0.0	34.98	255.02	233.20	2.84	538.86	76.7	7.29	8.75
9	11.32	250.	10.0	70.0	1.8	7.32	242.68	52.29	3.19	546.18	77.7	33.15	8.35
10	11.42	250.	5.0	70.0	1.8	5.91	244.09	59.10	3.54	552.09	78.5	41.30	8.20
11	11.55	250.	5.0	70.0	1.8	5.91	244.09	45.46	3.88	558.00	79.4	41.30	8.32
12	11.70	250.	5.0	70.0	1.8	5.91	244.09	39.40	4.23	563.91	80.2	41.30	8.10
13	12.02	250.	25.0	75.3	0.0	6.17	243.82	19.30	4.58	570.09	81.1	39.49	9.40
14	12.18	250.	5.0	75.3	0.0	1.23	248.76	7.72	4.92	571.32	81.3	201.43	8.38
15	12.35	250	5.0	75.3	0.0	1.23	248.76	7.26	5.27	572.56	81.4	201.43	8.48
16	12.52	250.	5.0	75.3	0.0	1.23	248.76	7.26	5.62	573.79	81.6	201.43	8.37
17	12.68	250.	5.0	75.3	0.0	1.23	248.76	7.72	5.97	575.03	81.8	201.43	8.42
18	12.85	250.	5.0	75.3	0.0	1.23	248.76	7.26	6.31	576.26	82.0	201.43	8.56
19	13.42	125.	0.0	100.0	0.0	0.0	125.00	0.0	6.49	576.26	82.0	---	8.72

TABLE F.4 - PRIMROSE OIL: RUN #4 - Experimental Data and Production Results

- Base Steamflood (20-40 mesh sand)

Date of Run = 11/26/1985
Bulk Volume = 1870. cc
Sand Pack = Ottawa Silica 20-40 mesh
Sand Density = 1.91 g/cc
Pore Volume = 730.0 cc
Porosity = 39.0 %
Permeability = 33.9 d

Initial Oil In Place = 651.0 cc
Oil Saturation = 89.2 %
Oil Viscosity = 45700. mPa.s @ 0 MPag & 22 C

CYL. #	TIME (hr)	FLUID PROD. (cc)	CRUDE PROD. (cc)	WATER IN CRUDE (%)	OIL IN WATER (%)	OIL PROD. (cc)	WATER PROD. (cc)	OIL PROD. RATE (cc/hr)	CUM. FLUID PROD. (PV)	CUM. OIL PROD. (cc)	CUM. OIL REC. (%IOIP)	WATER OIL RATIO (cc/cc)	pH
1	2.18	250.	80.0	24.2	0.0	60.64	189.36	27.82	0.34	60.64	9.3	3.12	9.30
2	3.20	250.	80.0	25.3	0.0	59.76	190.24	58.59	0.68	120.40	18.5	3.18	9.00
3	3.95	250.	79.0	26.1	0.0	58.38	191.62	77.84	1.03	178.78	27.5	3.28	8.75
4	4.53	250.	92.0	27.3	0.0	66.88	183.12	115.32	1.37	245.66	37.7	2.74	8.74
5	4.97	250.	104.0	31.0	0.0	71.76	178.24	163.09	1.71	317.42	48.8	2.48	8.73
6	5.15	250.	116.0	33.1	0.0	77.60	172.40	431.13	2.05	395.03	60.7	2.22	8.70
7	5.25	250.	192.0	50.8	0.0	94.46	155.54	944.64	2.40	489.49	75.2	1.65	8.61
8	5.35	256.	81.0	56.9	3.6	41.21	214.79	412.11	2.75	530.70	81.5	5.21	8.71
9	5.48	250.	10.0	67.0	3.6	11.94	238.06	91.85	3.09	542.64	83.4	19.94	8.65
10	5.63	250.	4.0	67.0	1.3	4.52	245.48	30.12	3.43	547.16	84.0	54.33	8.29
11	5.80	250.	0.0	100.0	0.0	0.0	250.00	0.0	3.78	547.16	84.0	---	8.59
12	6.03	250.	31.0	72.8	0.0	8.43	241.57	36.66	4.12	555.59	85.3	28.65	9.15
13	6.20	250.	10.0	72.8	0.0	2.72	247.28	16.00	4.46	558.31	85.8	90.91	8.79
14	6.37	250.	5.0	72.8	0.0	1.36	248.64	8.00	4.80	559.67	86.0	182.82	8.85
15	6.50	54.	0.0	100.0	0.0	0.0	54.00	0.0	4.88	559.67	86.0	---	8.62

TABLE F.5 - LLOYDMINSTER OIL: RUN #5 - Experimental Data and Production Results

- Steam / Emulsion Slug Injection (2 Layer Sand)

Date of Run = 12/06/1985
Bulk Volume = 1870. cc
Sand Pack = Ottawa Silica 60-120, 20-40 mesh
Sand Density = 1.97 g/cc
Pore Volume = 760.0 cc
Porosity = 40.6 %
Permeability = 25.3 d

Initial Oil In Place = 635.3 cc
Initial Oil Saturation = 83.6 %
Oil Viscosity = 10100. mPa.s @ 0 MPag & 22 C
Emulsion Oil Injected = 162.9 cc

CYL #	TIME (hr)	FLUID PROD. (cc)	CRUDE PROD. (cc)	WATER IN CRUDE (%)	OIL IN WATER (%)	OIL PROD. (cc)	WATER PROD. (cc)	OIL PROD. RATE (cc/hr)	CUM. FLUID PROD. (PV)	CUM. OIL PROD. (cc)	CUM. OIL REC. (%IOIP)	WATER OIL RATIO (cc/cc)	pH
1	0.98	250.	80.0	30.6	0.0	55.52	194.48	56.65	0.33	55.52	8.7	3.50	7.73
2	1.55	260.	87.2	34.7	0.0	56.94	203.06	99.90	0.67	112.46	17.7	3.57	7.47
3	2.10	250.	102.7	35.8	0.0	65.93	184.07	119.88	1.00	178.39	28.1	2.79	7.45
4	2.55	270.	111.4	34.5	0.0	72.97	197.03	162.15	1.36	251.36	39.6	2.70	7.92
5	2.75	290.	140.7	38.6	0.0	86.39	203.61	431.95	1.74	337.75	53.2	2.36	7.37
6	2.93	300.	218.8	58.4	0.0	91.02	208.98	505.67	2.13	428.77	67.5	2.30	7.35
7	3.12	250.	87.3	56.2	0.0	38.24	211.76	201.25	2.46	467.01	73.5	5.54	7.02
8	3.20	250.	22.2	70.6	0.0	6.53	243.47	81.59	2.79	473.54	74.5	37.30	7.51
9	3.35	250.	16.1	70.6	0.0	4.73	245.27	31.56	3.12	478.27	75.3	51.82	7.85
10	3.52	250.	12.4	70.6	0.0	3.65	246.35	21.44	3.45	481.92	75.9	67.58	7.76
11	3.73	250.	30.1	70.6	0.0	8.85	241.15	42.14	3.78	490.77	77.3	27.25	7.16
12	3.80	60.	0.0	100.0	0.0	0.0	60.00	0.0	3.86	490.77	77.3	---	7.35
EMULSION INJECTION START													
13	3.81	254.	0.0	100.0	0.2	0.51	253.49	50.80	4.19	491.27	75.6	499.00	8.80
14	3.84	250.	0.0	100.0	0.3	0.75	249.25	25.00	4.52	492.02	74.0	332.33	8.84
15	3.88	250.	0.0	100.0	0.7	1.75	248.25	43.75	4.85	493.77	72.6	141.86	8.76
16	3.93	250.	0.0	100.0	0.0	0.0	250.00	0.0	5.18	493.77	71.1	---	8.44
17	4.65	250.	0.0	100.0	0.0	0.0	250.00	0.0	5.51	493.77	69.6	---	8.52
18	5.60	250.	0.0	100.0	0.6	1.50	248.50	1.58	5.83	495.27	68.4	165.67	8.58

* Net Cumulative Oil Recovery after Emulsion Injection

TABLE F.5 - LLOYDMINSTER OIL: RUN #5 - Experimental Data and Production Results [con'd]

CYL #	TIME (hr)	FLUID PROD. (cc)	CRUDE PROD. (cc)	WATER IN CRUDE (%)	OIL IN WATER (%)	OIL PROD. (cc)	WATER PROD. (cc)	OIL PROD. RATE (cc/hr)	CUM. FLUID PROD. (PV)	CUM. OIL PROD. (cc)	CUM. OIL REC. (%IOIP)	WATER OIL RATIO (cc/cc)	pH
19	6.38	250.	0.0	100.0	0.3	0.75	249.25	0.96	6.16	496.02	67.1	332.33	8.44
20	7.20	250.	0.0	100.0	0.2	0.50	249.50	0.61	6.49	496.52	65.9	499.00	8.66
21	8.07	250.	0.0	100.0	0.4	1.00	249.00	1.15	6.82	497.52	64.7	249.00	8.78
22	9.01	250.	0.0	100.0	0.4	1.00	249.00	1.06	7.15	498.52	63.6	249.00	8.68
23	9.98	250.	0.0	100.0	0.4	1.00	249.00	1.03	7.48	499.52	62.6	249.00	8.77
CHASE STEAM START													
24	10.52	250.	0.0	100.0	0.9	2.25	247.75	4.17	7.81	501.77	62.9	110.11	8.69
25	10.68	250.	0.0	100.0	3.6	9.00	241.00	56.25	8.14	510.77	64.0	26.78	8.98
26	10.85	260.	0.0	100.0	4.5	11.70	248.30	68.82	8.48	522.47	65.5	21.22	8.98
27	11.02	250.	0.0	100.0	8.4	21.00	229.00	123.53	8.81	543.47	68.1	10.90	9.12
28	11.15	250.	42.4	70.2	0.8	14.30	235.70	109.97	9.14	557.77	69.9	16.49	9.02
29	11.33	250.	42.4	69.2	1.6	16.38	233.62	91.00	9.47	574.15	71.9	14.26	8.33
30	11.53	250.	39.1	72.5	0.6	12.02	237.98	60.09	9.79	586.17	73.4	19.80	7.95
31	11.57	250.	20.0	61.2	2.2	12.82	237.18	320.50	10.12	598.99	75.0	18.50	8.40
32	11.68	250.	22.3	69.3	9.2	27.79	222.21	252.68	10.45	626.78	78.5	7.99	8.61
33	11.86	256.	51.4	61.3	12.8	46.08	209.92	256.00	10.79	672.86	84.3	4.56	8.56
34	12.01	256.	5.0	61.3	5.3	15.24	240.76	101.59	11.13	688.10	86.2	15.80	8.76
35	12.18	252.	0.0	100.0	3.4	8.57	243.43	50.40	11.46	696.67	87.3	28.41	8.64
36	12.33	250.	0.0	100.0	0.0	0.0	250.00	0.0	11.79	696.67	87.3	---	8.81
37	12.66	475.	35.0	75.8	1.7	15.95	459.05	48.33	12.41	712.62	89.3	28.78	8.76
38	12.93	420.	10.0	75.8	4.0	18.82	401.18	69.70	12.96	731.44	91.6	21.32	8.47

* Net Cumulative Oil Recovery after Emulsion Injection

TABLE F.6 -- LLOYDMINSTER OIL: RUN #6 - Experimental Data and Production Results

- Steam / Emulsion Co-Injection (2 Layer Sand)

Date of Run = 12/18/1985
Bulk Volume = 1870. cc
Sand Pack = Ottawa Silica 60-120, 20-40 mesh
Sand Density = 1.96 g/cc
Pore Volume = 720.0 cc
Porosity = 38.5 %
Permeability = 23.0 d

Initial Oil In Place = 597.7 cc
Initial Oil Saturation = 83.0 %
Oil Viscosity = 10100. mPa.s @ 0 MPag & 22 C
Emulsion Oil Injected = 188.4 cc

CYL. #	TIME (hr)	FLUID PROD. (cc)	CRUDE PROD. (cc)	WATER IN CRUDE (%)	OIL IN WATER (%)	OIL PROD. (cc)	WATER PROD. (cc)	OIL PROD. RATE (cc/hr)	CUM. FLUID PROD. (PV)	CUM. OIL PROD. (cc)	CUM. OIL REC. (%IOIP)	WATER OIL RATIO (cc/cc)	pH
1	1.02	300.	76.0	21.8	0.0	59.43	240.57	58.27	0.42	59.43	9.9	4.05	8.61
2	1.62	250.	61.9	25.5	0.0	45.93	204.07	76.55	0.76	105.36	17.6	4.44	8.04
3	2.27	260.	75.8	23.4	0.0	58.06	201.94	89.33	1.13	163.42	27.3	3.48	7.97
4	2.82	260.	81.2	22.8	0.0	62.69	197.31	113.98	1.49	226.11	37.8	3.15	7.96
5	3.28	260.	83.6	21.2	0.0	65.88	194.12	143.21	1.85	291.99	48.9	2.95	7.76
6	3.65	300.	143.0	31.0	0.0	98.67	201.33	266.68	2.26	390.66	65.4	2.04	7.80
7	3.78	300.	104.9	45.9	0.0	56.75	243.25	436.55	2.68	447.41	74.9	4.29	8.27
8	3.92	250.	26.7	61.0	0.0	10.41	239.59	74.38	3.03	457.82	76.6	23.01	8.60
9	4.08	250.	8.7	61.0	0.0	3.39	246.61	21.21	3.38	461.21	77.2	72.68	8.70
10	4.27	250.	12.9	61.0	0.0	5.03	244.97	26.48	3.72	466.25	78.0	48.69	8.21
11	4.43	250.	14.5	61.0	0.0	5.66	244.34	35.34	4.07	471.90	79.0	43.21	8.84
12	4.60	250.	11.3	70.8	0.0	3.30	246.70	19.41	4.42	475.20	79.5	74.77	8.87
13	4.61	150.	0.0	100.0	0.0	0.0	150.00	0.0	4.63	475.20	79.5	---	8.80
EMULSION / STEAM CO-INJECTION START													
14	4.80	250.	3.5	76.5	0.7	2.55	247.45	13.41	4.97	477.75	78.4	97.12	8.37
15	4.95	250.	4.7	76.5	0.6	2.58	247.42	17.18	5.32	480.32	77.3	96.04	8.83
16	5.05	250	11.3	76.5	0.6	4.09	245.91	40.88	5.67	484.41	76.5	60.16	8.70
17	5.20	250.	2.9	76.5	3.2	8.59	241.41	57.26	6.01	493.00	76.4	28.11	8.81
18	5.33	250	3.0	76.5	0.9	2.93	247.07	22.52	6.36	495.93	75.5	84.38	8.78

* Net Cumulative Oil Recovery after Emulsion Injection

TABLE F.6 - LLOYDMINSTER OIL; RUN #6 - Experimental Data and Production Results [con'd]

CYL. #	TIME (hr)	FLUID PROD. (cc)	CRUDE PROD. (cc)	WATER IN CRUDE (%)	OIL IN WATER (%)	OIL PROD. (cc)	WATER PROD. (cc)	OIL PROD. RATE (cc/hr)	CUM. FLUID PROD. (PV)	CUM. OIL PROD. (cc)	CUM. OIL REC. (%IOIP)	WATER OIL RATIO (cc/cc)	pH
19	5.47	250.	6.6	76.5	1.5	5.20	244.80	37.16	6.71	501.13	* 75.0	47.06	8.58
20	5.60	250.	5.6	76.5	0.6	2.78	247.22	21.40	7.06	503.91	74.1	88.85	8.61
21	5.72	250.	2.3	76.5	0.5	1.78	248.22	13.83	7.40	505.69	73.1	139.53	9.03
22	5.85	250.	2.3	76.5	0.4	1.53	248.47	11.78	7.75	507.22	72.1	162.26	8.82
23	5.98	260.	0.0	100.0	1.0	2.60	257.40	20.00	8.11	509.82	71.2	99.00	8.70
24	6.17	260.	29.6	62.1	4.9	22.51	237.49	118.46	8.47	532.33	73.2	10.55	9.02
25	6.30	250.	0.0	100.0	1.1	2.75	247.25	21.15	8.82	535.08	72.4	89.91	8.67
26	6.43	250.	0.0	100.0	0.0	0.0	250.00	0.0	9.17	535.08	71.3	---	8.80
27	6.70	510.	0.0	100.0	1.9	9.69	500.31	35.89	9.88	544.77	71.4	51.63	8.74
28	7.08	500.	0.0	100.0	1.1	5.50	494.50	14.47	10.57	550.27	71.1	89.91	8.70
29	7.47	500.	0.0	100.0	0.6	3.00	497.00	7.69	11.26	553.27	70.4	165.67	8.59
CHASE STEAM START													
30	7.89	560.	0.0	100.0	1.1	6.16	553.84	14.67	12.04	559.43	71.2	89.91	8.85
31	8.34	525.	24.3	55.7	1.3	17.27	507.73	38.39	12.77	576.71	73.4	29.39	9.05
32	8.74	540.	38.4	66.0	0.6	16.07	523.93	40.16	13.52	592.77	75.4	32.61	8.91
33	9.19	550.	64.8	52.8	1.1	35.92	514.08	79.83	14.28	628.69	80.0	14.31	8.80
34	9.59	525.	19.6	58.0	1.0	13.29	511.71	33.21	15.01	641.98	81.7	38.52	8.44
35	9.97	530.	9.4	58.0	0.9	8.63	521.37	22.72	15.75	650.61	82.8	60.39	8.45
36	10.36	500.	0.0	100.0	0.0	0.0	500.00	0.0	16.44	650.61	82.8	---	8.36

* Net Cumulative Oil Recovery after Emulsion Injection

TABLE F.7 - PRIMROSE OIL: RUN #7 - Experimental Data and Production Results

- Steam / Emulsion Slug Injection (2 Layer Sand)

Date of Run = 01/02/1986
Bulk Volume = 1870. cc
Sand Pack = Ottawa Silica 60-120, 20-40 mesh
Sand Density = 1.98 g/cc
Pore Volume = 690.0 cc
Porosity = 36.9 %
Permeability = 17.5 d

Initial Oil In Place = 614.0 cc
Initial Oil Saturation = 88.9 %
Oil Viscosity = 45700. mPa·s @ 0 MPag & 22 C
Emulsion Oil Injected = 157.5 cc

CYL #	TIME (hr)	FLUID PROD. (cc)	CRUDE PROD. (cc)	WATER IN CRUDE (%)	OIL IN WATER (%)	OIL PROD. (cc)	WATER PROD. (cc)	OIL PROD RATE (cc/hr)	CUM. FLUID PROD. (PV)	CUM. OIL PROD (cc)	CUM. OIL REC. (%IOIP)	WATER OIL RATIO (cc/cc)	pH
1	1.00	2[illegible]	66.0	35.0	0.0	42.90	207.10	42.90	0.36	42.90	7.0	4.83	9.03
2	3.33	[illegible]	50.5	36.8	0.0	31.92	218.08	13.70	0.72	74.82	12.2	6.83	9.15
3	4.42	[illegible]	57.4	33.2	0.0	38.34	211.66	35.18	1.09	113.16	18.4	5.52	9.12
4	5.43	250.	69.3	30.1	0.0	48.44	201.56	47.96	1.45	161.60	26.3	4.16	8.98
5	7.97	250.	73.6	34.0	0.0	48.58	201.42	19.12	1.81	210.18	34.2	4.15	8.93
6	9.85	250.	69.6	31.4	0.0	47.75	202.25	25.40	2.17	257.92	42.0	4.24	9.22
7	10.10	250.	25.3	35.0	1.5	19.82	230.18	79.26	2.54	277.74	45.2	11.62	9.20
8	10.23	300.	38.8	39.4	9.4	48.07	251.93	369.74	2.97	325.80	53.1	5.24	9.19
9	10.33	250.	80.3	55.7	8.2	49.49	200.51	494.88	3.33	375.29	61.1	4.05	9.22
10	10.43	250.	34.6	67.3	2.8	17.35	232.65	173.45	3.70	392.64	63.9	13.41	8.99
11	10.57	250.	41.5	75.0	0.0	10.38	239.63	74.11	4.06	403.01	65.6	23.10	9.16
12	10.83	250.	31.8	78.2	0.0	6.93	243.07	26.66	4.42	409.94	66.8	35.06	9.52
13	11.00	250.	0.0	100.0	3.6	9.00	241.00	52.94	4.78	418.94	68.2	26.78	9.33
14	11.08	75.	0.0	100.0	0.0	0.0	75.00	0.0	4.89	418.94	68.2	---	9.10
EMULSION INJECTION START													
15	11.16	280.	0.0	100.0	0.0	0.0	280.00	0.0	5.30	418.94	* 66.7	---	9.26
16	11.29	250.	0.0	100.0	0.0	0.0	250.00	0.0	5.66	418.94	65.2	---	9.35
17	11.50	250.	0.0	100.0	0.0	0.0	250.00	0.0	6.02	418.94	63.7	---	9.22
18	11.81	250.	0.0	100.0	0.0	0.0	250.00	0.0	6.38	418.94	62.4	---	9.28

* Net Cumulative Oil Recovery after Emulsion Injection

TABLE F.7 - PRIMROSE OIL: RUN #7 - Experimental Data and Production Results [con'd]

CYL. #	TIME (hr)	FLUID PROD. (cc)	CRUDE PROD. (cc)	WATER IN CRUDE (%)	OIL IN WATER (%)	OIL PROD. (cc)	WATER PROD. (cc)	OIL PROD. RATE (cc/hr)	CUM. FLUID PROD. (PV)	CUM. OIL PROD. (cc)	CUM. OIL REC. (%IOIP)	WATER OIL RATIO (cc/cc)	pH
19	12.38	250.	1.5	67.1	0.0	0.49	249.51	0.87	6.75	419.44	* 61.2	505.59	9.16
20	13.05	250.	2.5	67.1	0.0	0.82	249.18	1.23	7.11	420.26	60.0	302.95	9.30
21	13.80	250.	2.2	67.1	0.0	0.72	249.28	0.97	7.47	420.98	58.9	344.40	9.02
22	14.47	250.	1.2	67.1	0.0	0.39	249.61	0.59	7.83	421.38	57.8	632.23	9.07
23	15.30	250.	4.5	67.1	1.1	4.18	245.82	5.04	8.20	425.56	57.3	58.79	9.03
24	16.07	250.	1.8	67.1	0.0	0.59	249.41	0.77	8.56	426.15	56.3	421.15	9.55
25	16.90	250.	0.0	100.0	0.0	0.0	250.00	0.0	8.92	426.15	55.2	---	9.42
CHASE STEAM START													
26	17.09	250.	2.3	67.1	0.4	1.75	248.25	9.20	9.28	427.90	55.5	142.06	9.35
27	17.20	250.	1.1	67.1	0.0	0.36	249.64	3.29	9.64	428.26	55.5	689.80	9.01
28	17.28	250.	16.6	67.1	1.3	8.50	241.50	106.19	10.01	436.76	56.6	28.43	8.89
29	17.47	250.	46.0	60.9	0.1	18.19	231.81	95.74	10.37	454.95	59.0	12.74	9.12
30	17.80	280.	47.3	64.1	0.1	17.21	262.79	52.16	10.78	472.16	61.2	15.27	8.93
31	18.04	250.	30.4	70.1	0.2	9.53	240.47	39.70	11.14	481.69	62.4	25.24	8.67
32	18.36	250.	30.1	75.0	0.0	7.53	242.47	23.52	11.50	489.21	63.4	32.22	8.90
33	18.55	250.	11.6	77.0	0.0	2.67	247.33	14.04	11.86	491.88	63.8	92.70	9.07
34	18.79	250.	2.6	77.0	0.0	0.60	249.40	2.49	12.22	492.48	63.8	417.06	8.44
35	19.01	250.	17.8	82.5	0.0	3.11	246.88	14.16	12.59	495.59	64.2	79.26	8.70
36	19.20	250.	4.4	82.2	0.0	0.78	249.22	4.12	12.95	496.38	64.3	318.20	9.11
37	19.39	250.	15.0	82.2	0.0	2.67	247.33	14.05	13.31	499.05	64.7	92.63	9.05
38	19.78	500.	4.8	82.9	0.0	0.82	499.18	2.10	14.04	499.87	64.8	608.16	9.20
39	20.10	500	34.4	82.9	0.0	5.88	494.12	18.38	14.76	505.75	65.6	84.00	9.21
40	20.42	500.	9.9	82.9	0.0	1.69	498.31	5.29	15.49	507.44	65.8	294.35	8.80
41	20.72	500.	9.2	82.9	0.7	5.01	494.99	16.70	16.21	512.45	66.4	98.82	8.90
42	20.80	210.	0.0	100.0	0.0	0.0	210.00	0.0	16.51	512.45	66.4	---	8.71

* Net Cumulative Oil Recovery after Emulsion Injection

TABLE F.8 - PRIMROSE OIL: RUN #8 - Experimental Data and Production Results

Steam / Emulsion Co-Injection (2 Layer Sand)

Date of Run = 01/08/1986
Bulk Volume = 1870. cc
Sand Pack = Ottawa Silica 60-120, 20-40 mesh
Sand Density = 2.99 g/cc
Pore Volume = 650.0 cc
Porosity = 34.8 %
Permeability = 19.8 d

Initial Oil In Place = 570.9 cc
Initial Oil Saturation = 87.8 %
Oil Viscosity = 45700. mPa.s @ 0 MPag & 22 C
Emulsion Oil Injected = 142.8 cc

CYL. #	TIME (hr)	FLUID PROD. (cc)	CRUDE PROD. (cc)	WATER IN CRUDE (%)	OIL IN WATER (%)	OIL PROD. (cc)	WATER PROD. (cc)	OIL PROD RATE (cc/hr)	CUM. FLUID PROD. (PV)	CUM. OIL PROD. (cc)	CUM. OIL REC. (%IOIP)	WATER OIL RATIO (cc/cc)	pH
1	5.55	500.	140.6	31.0	0.0	97.01	402.99	17.48	0.77	97.01	17.0	4.15	9.34
2	6.27	250.	76.9	27.8	0.0	55.52	194.48	77.11	1.15	152.54	26.7	3.50	9.30
3	6.72	270.	89.0	30.5	0.0	61.86	208.14	137.46	1.57	214.39	37.6	3.37	9.20
4	6.92	250.	154.2	41.6	0.0	90.05	159.95	450.26	1.95	304.44	53.3	1.78	9.40
5	7.03	250.	177.5	62.5	0.0	66.56	183.44	605.11	2.34	371.01	65.0	2.76	9.07
6	7.20	250.	55.5	67.5	1.5	20.95	229.05	123.26	2.72	391.96	68.7	10.93	8.92
7	7.30	250.	38.5	75.7	0.0	9.36	240.64	93.55	3.11	401.32	70.3	25.72	8.99
8	7.45	250.	5.0	79.5	0.0	1.02	248.97	6.83	3.49	402.34	70.5	242.90	9.09
9	7.62	250.	8.4	79.5	0.0	1.72	248.28	10.13	3.88	404.06	70.8	144.18	9.29
10	7.75	250.	29.9	79.5	0.0	6.13	243.87	47.15	4.26	410.19	71.9	39.79	9.56
11	7.92	250.	2.2	72.0	1.1	3.34	246.66	19.66	4.65	413.53	72.4	73.81	9.32
12	8.00	55.	0.0	100.0	0.0	0.0	55.00	0.0	4.73	413.53	72.4	---	9.26
EMULSION / STEAM CO-INJECTION START													
13	8.17	250.	0.0	100.0	0.0	0.0	250.00	0.0	5.12	413.53	71.0	---	9.38
14	8.41	250.	0.0	100.0	0.0	0.0	250.00	0.0	5.50	413.53	69.5	---	9.14
15	8.62	250.	0.0	100.0	0.0	0.0	250.00	0.0	5.88	413.53	68.2	---	9.02
16	8.80	250.	0.0	100.0	0.0	0.0	250.00	0.0	6.27	413.53	66.9	---	8.99
17	9.05	250.	0.0	100.0	0.0	0.0	250.00	0.0	6.65	413.53	65.6	---	9.19
18	9.33	250.	0.0	100.0	0.0	0.0	250.00	0.0	7.04	413.53	64.4	---	9.05

* Net Cumulative Oil Recovery after Emulsion Injection

TABLE F.8 - PRIMROSE OIL: RUN #8 - Experimental Data and Production Results [con'd]

CYL #	TIME (hr)	FLUID PROD. (cc)	CRUDE PROD. (cc)	WATER IN CRUDE (%)	OIL IN WATER (%)	OIL PROD. (cc)	WATER PROD. (cc)	OIL PROD RATE (cc/hr)	CUM. FLUID PROD (PV)	CUM. OIL PROD. (cc)	CUM. OIL REC. (%IOIP)	WATER OIL RATIO (cc/cc)	pH
19	9.68	250.	0.0	100.0	0.0	0.0	250.00	0.0	7.42	413.53	63.2	---	9.24
20	10.00	250.	0.0	100.0	0.0	0.0	250.00	0.0	7.81	413.53	62.1	---	9.12
21	10.35	250.	0.0	100.0	0.0	0.0	250.00	0.0	8.19	413.53	61.0	---	9.11
22	10.66	250.	0.0	100.0	0.0	0.0	250.00	0.0	8.58	413.53	59.9	---	8.95
23	10.92	250.	0.0	100.0	0.0	0.0	250.00	0.0	8.96	413.53	58.9	---	8.96
24	11.18	250.	0.0	100.0	0.0	0.0	250.00	0.0	9.35	413.53	57.9	---	8.36
CHASE STEAM START													
25	11.42	250.	0.0	100.0	0.0	0.0	250.00	0.0	9.73	413.53	57.9	---	8.95
26	11.68	250.	0.0	100.0	0.0	0.0	250.00	0.0	10.12	413.53	57.9	---	9.03
27	12.68	500.	0.0	100.0	0.0	0.0	500.00	0.0	10.88	413.53	57.9	---	9.26
28	13.18	500.	0.0	100.0	0.0	0.0	500.00	0.0	11.65	413.53	57.9	---	9.09
29	13.70	500.	0.0	100.0	0.0	0.0	500.00	0.0	12.42	413.53	57.9	---	9.11
30	14.20	500.	0.0	100.0	0.0	0.0	500.00	0.0	13.19	413.53	57.9	---	9.12
31	14.72	500.	34.6	69.8	3.6	27.20	472.80	52.31	13.96	440.74	61.8	17.38	9.05
32	15.05	500.	11.2	69.8	1.4	10.23	489.77	30.99	14.73	450.96	63.2	47.90	8.88
33	15.12	500.	0.0	100.0	0.4	2.00	498.00	28.57	15.50	452.96	63.5	249.00	8.91

* Net Cumulative Oil Recovery after Emulsion Injection

TABLE F.9 - LLOYDMINSTER OIL: Run #9 - Experimental Data and Production Results

- Emulsion Slug Injection (2 Layer Sand)

Date of Run = 04/15/1986
Bulk Volume = 1870. cc
Sand Pack= Ottawa Silica 60-120, 20-40 mesh
Sand Density = 1.99 g/cc
Pore Volume = 660.0 cc
Porosity = 36.0 %
Permeability = 18.9 d

Initial Oil In Place = 612.8 cc
Initial Oil Saturation= 92.8 %
Oil Viscosity = 10100. mPa.s @ 0 MPag & 22 C
Emulsion Oil Injected = 16.5 cc

CYL. #	TIME (hr.)	FLUID PROD. (cc)	CRUDE PROD. (cc)	WATER IN CRUDE (%)	OIL IN WATER (%)	OIL PROD. (cc)	WATER PROD. (cc)	OIL PROD. RATE (cc/hr)	CUM. FLUI PROD. (PV)	CUM. OIL RROD. (cc)	CUM. OIL REC. (%IOIP)	WATER OIL RATIO (cc/cc)	pH
1	0.40	250.	61.7	27.3	0.0	44.86	205.14	112.14	0.38	44.86	7.3	4.57	6.79
2	0.70	250.	108.4	38.3	0.0	66.88	183.12	222.94	0.76	111.74	18.2	2.74	6.79
3	1.12	250.	121.3	35.6	0.0	78.12	171.88	185.99	1.14	189.86	31.0	2.20	7.00
4	1.48	250.	101.1	32.0	0.4	69.34	180.66	192.62	1.52	259.20	42.3	2.61	7.34
5	1.85	250.	119.1	26.6	2.0	90.04	159.96	243.34	1.89	349.24	57.0	1.78	7.92
6	2.27	250.	89.1	34.0	1.0	60.41	189.59	143.85	2.27	409.65	66.8	3.14	7.80
7	2.63	250.	66.6	34.0	1.0	45.79	204.21	127.19	2.65	455.44	74.3	4.46	7.90
8	2.98	250.	53.9	29.5	2.0	41.92	208.08	119.78	3.03	497.36	81.2	4.96	8.00
9	3.27	250	26.2	34.0	1.0	19.53	230.47	67.34	3.41	516.89	84.3	11.80	7.87
10	3.62	250	12.9	44.0	1.0	9.59	240.40	27.41	3.79	526.49	85.9	25.06	7.51
EMULSION SLUG INJECTION START													
11	4.58	250	6.2	25.7	1.0	7.04	242.96	7.34	4.17	533.53	* 84.8	34.49	7.32
12	4.88	250	1.7	38.0	0.0	1.05	248.95	3.51	4.55	534.59	84.9	236.19	8.94
CHASE STEAM START													
13	5.20	250.	0.8	38.0	0.0	0.50	249.50	1.55	4.92	535.08	* 85.0	503.03	9.11
14	5.55	250.	9.0	42.5	0.0	5.18	244.82	14.79	5.30	540.26	85.9	47.31	7.72

* Net Cumulative Oil Recovery after Emulsion Injection

TABLE F.9 - LLOYDMINSTER OIL, RUN #9 - Experimental Data and Production Results [con'd]

CYL. #	TIME (hr)	FLUID PROD (cc)	CRUDE PROD (cc)	WATER IN CRUDE (%)	OIL IN WATER (%)	OIL PROD (cc)	WATER PROD (cc)	OIL PROD RATE (cc/hr)	CUM FLUID PROD (PV)	CUM OIL PROD (cc)	CUM OIL REC. (%IOIP)	WATER OIL RATIO (cc/cc)	pH
15	5.90	250.	0.4	47.0	0.0	0.21	249.79	0.61	5.68	540.47	*85.9	>999.	7.39
16	6.20	250.	1.0	49.0	0.0	0.77	249.23	2.55	6.06	541.23	86.0	325.80	7.15
17	6.52	250.	5.6	53.3	0.0	2.62	247.38	8.17	6.44	543.85	86.4	94.59	6.90
18	6.78	250.	0.5	60.0	0.0	0.20	249.80	0.77	6.82	544.05	86.5	>999.	6.99
19	7.15	250.	13.0	42.5	0.0	7.48	242.52	20.20	7.20	551.53	87.6	32.44	6.91
20	7.37	250.	1.1	58.3	1.0	2.95	247.05	13.40	7.58	554.47	88.1	83.81	6.62
21	7.48	250.	12.9	58.3	1.0	7.75	242.25	70.46	7.95	562.22	89.3	31.26	6.75
22	7.57	250.	1.6	59.0	1.0	3.14	246.86	34.89	8.33	565.36	89.8	78.62	6.50
23	7.82	250.	2.9	59.0	1.0	3.66	246.34	14.64	8.71	569.02	90.4	67.31	6.20

* Net Cumulative Oil Recovery after Emulsion Injection

TABLE F.10 - LLOYDMINSTER OIL: Run #10 - Experimental Data and Production Results

- Emulsion Slug Injection (2 Layer Sand)

Date of Run = 04/24/1986
Bulk Volume = 1870. cc
Sand Pack= Ottawa Silica 60-120, 20-40 mesh
Sand Density = 1.97 g/cc
Pore Volume = 635.0 cc
Porosity = 34.6 %
Permeability = 17.6 d

Initial Oil In Place = 588.4 cc
Initial Oil Saturation= 92.7 %
Oil Viscosity = 10100. mPa.s @ 0 MPag & 22 C
Emulsion Oil Injected = 15.9 cc

CYL #	TIME (hr)	FLUID PROD. (cc)	CRUDE PROD. (cc)	WATER IN CRUDE (%)	OIL IN WATER (%)	OIL PROD. (cc)	WATER PROD. (cc)	OIL PROD. RATE (cc/hr)	CUM. FLUID PROD. (PV)	CUM. OIL PROD. (cc)	CUM. OIL REC. (%IOIP)	WATER OIL RATIO (cc/cc)	pH
1	0.45	250.	99.8	27.3	0.0	72.55	177.45	161.23	0.39	72.55	12.3	2.45	6.79
2	0.85	250.	108.4	42.2	0.0	62.66	187.34	156.64	0.79	135.21	23.0	2.99	6.79
3	1.17	250.	99.5	40.8	0.0	58.90	191.10	184.08	1.18	194.11	33.0	3.24	7.00
4	1.40	250.	112.2	39.0	0.0	68.44	181.56	297.57	1.57	262.56	44.6	2.65	7.34
EMULSION SLUG INJECTION START													
5	1.93	250.	165.8	38.6	0.0	101.80	148.20	192.08	1.97	364.36	60.3	1.46	7.92
6	2.12	250.	163.7	43.0	0.0	93.31	156.69	491.10	2.36	457.67	75.7	1.68	7.80
CHASE STEAM START													
7	2.22	250.	74.9	60.7	0.0	29.44	220.56	294.36	2.76	487.10	80.6	7.49	7.90
8	2.35	250.	17.5	66.3	0.0	5.90	244.10	45.37	3.15	493.00	81.6	41.39	8.00
9	2.52	250.	4.2	71.7	0.0	1.19	248.81	6.99	3.54	494.19	81.8	209.33	7.87
10	2.67	250.	7.1	71.7	0.0	2.07	247.93	13.77	3.94	496.25	82.1	120.01	7.51
11	2.83	250.	4.1	76.7	0.3	1.69	248.31	10.58	4.33	497.95	82.4	146.67	7.32

* Net Cumulative Oil Recovery after Emulsion Injection

TABLE F.10 - LLOYDMINSTER OIL: RUN #10 - Experimental Data and Production Results [con'd]

CYL #	TIME (hr)	FLUID PROD. (cc)	CRUDE PROD. (cc)	WATER IN CRUDE (%)	OIL IN WATER (%)	OIL PROD (cc)	WATER PROD. (cc)	OIL PROD RATE (cc/hr)	CUM FLUID PROD. (PV)	CUM OIL PROD. (cc)	CUM. OIL REC. (%IOIP)	WATER OIL RATIO (cc/cc)	pH
12	2.98	250.	0.6	80.0	0.2	0.62	249.38	4.13	4.72	498.57	* 82.5	403.01	8.94
13	3.15	250.	1.4	80.0	0.2	0.78	249.22	4.57	5.12	499.34	82.6	320.67	9.11
14	3.32	250.	4.3	79.9	0.2	1.36	248.64	7.97	5.51	500.70	82.9	183.41	7.72
15	3.47	250.	7.3	79.9	0.2	1.95	248.05	13.02	5.91	502.65	83.2	127.03	7.39
16	3.63	250.	1.4	80.0	0.0	0.28	249.72	1.75	6.30	502.93	83.2	891.86	7.15
17	3.78	250.	1.3	85.0	0.2	0.69	249.31	4.62	6.69	503.62	83.3	360.06	6.90
18	4.15	250.	4.6	85.0	0.0	0.69	249.31	1.86	7.09	504.31	83.5	361.32	6.99
19	4.40	250.	1.8	85.0	1.0	2.75	247.25	11.01	7.48	507.07	83.9	89.84	6.91
20	4.76	250.	0.0	85.0	1.8	4.50	245.50	12.50	7.87	511.57	84.7	54.56	6.62
21	5.12	250.	1.5	85.0	1.0	2.71	247.29	7.53	8.27	514.28	85.1	91.25	6.75

* Net Cumulative Oil Recovery after Emulsion Injection

TABLE F.11 - LLOYDMINSTER OIL: Run #11 - Experimental Data and Production Results

- Emulsion Slug Injection (2 Layer Sand)

Date of Run = 05/06/1986
Bulk Volume = 1870. cc
Sand Pack= Ottawa Silica 60-120, 20-40 mesh
Sand Density = 1.97 g/cc
Pore Volume = 690.0 cc
Porosity = 37.0 %
Permeability = 21.9 d

Initial Oil In Place = 642.3 cc
Initial Oil Saturation= 93.1 %
Oil Viscosity = 10100 mPa.s @ 0 MPag & 22 C
Emulsion Oil Injected = 17.3 cc

CYL. #	TIME (hr)	FLUID PROD. (cc)	CRUDE PROD. (cc)	WATER IN CRUDE (%)	OIL IN WATER (%)	OIL PROD. (cc)	WATER PROD. (cc)	OIL PROD. RATE (cc/hr)	CUM. FLUID PROD. (PV)	CUM. OIL PROD. (cc)	CUM. OIL REC. (%IOIP)	WATER OIL RATIO (cc/cc)	pH
1	0.47	250.	136.0	28.7	0.0	96.97	153.03	206.31	0.36	96.97	15.1	1.58	7.18
2	0.83	250.	127.3	42.3	0.0	73.45	176.55	204.03	0.72	170.42	26.5	2.40	7.50
3	1.10	250.	106.7	40.2	0.0	63.81	186.19	236.32	1.09	234.23	36.5	2.92	7.36
4	1.28	250.	124.7	38.7	0.0	76.44	173.56	424.67	1.45	310.67	48.4	2.27	6.93
5	1.38	250.	103.0	46.0	0.0	55.62	194.38	556.20	1.81	366.29	57.0	3.49	7.47
6	1.47	250.	206.6	59.0	0.0	84.71	165.29	941.18	2.17	450.99	70.2	1.95	8.60
7	1.58	250.	105.7	75.4	0.5	26.72	223.28	242.94	2.54	477.72	74.4	8.35	7.06
8	1.75	250.	23.4	74.0	0.2	6.54	243.46	38.45	2.90	484.25	75.4	37.24	6.71
9	1.90	250.	0.0	100.0	0.0	0.0	250.00	0.0	3.26	484.25	75.4	-	6.57
10	2.07	250.	5.0	79.2	0.0	1.04	248.96	6.12	3.62	485.29	75.6	239.38	6.80
11	2.23	250.	19.6	85.0	0.5	4.09	245.91	25.58	3.99	489.39	76.2	60.09	6.64
EMULSION SLUG INJECTION START													
12	2.38	250.	0.6	85.0	0.0	0.09	249.91	0.60	4.35	489.48	*74.2	>999	7.53
13	2.40	250.	0.4	85.0	0.5	1.31	248.69	65.40	4.71	490.78	*74.4	190.13	8.00
CHASE STEAM START													
14	2.43	250.	0.9	85.0	0.5	1.38	248.62	46.02	5.07	492.17	*74.6	180.09	7.88
15	2.58	250.	9.3	81.0	0.5	2.97	247.03	19.80	5.43	495.14	*75.1	83.16	6.96

* Net Cumulative Oil Recovery after Emulsion Injection

TABLE F.11 - LLOYDMINSTER OIL: RUN #11 - Experimental Data and Production Results [con'd]

CYL #	TIME (hr)	FLUID PROD. (cc)	CRUDE PROD. (cc)	WATER IN CRUDE (%)	OIL IN WATER (%)	OIL PROD. (cc)	WATER PROD. (cc)	OIL PROD. RATE (cc/hr)	CUM. FLUID PROD. (PV)	CUM. OIL PROD. (cc)	CUM. OIL REC. (%IOIP)	WATER OIL RATIO (cc/cc)	pH
16	2.73	250.	4.5	85.0	0.0	0.68	249.32	4.50	5.80	495.81	* 75.2	369.37	7.78
17	3.13	250.	24.2	73.0	0.5	7.66	242.34	19.16	6.16	503.47	76.3	31.62	7.38
18	3.40	250.	1.4	80.0	0.5	1.52	248.48	5.64	6.52	505.00	76.6	163.15	7.31
19	3.67	250.	1.9	80.0	0.6	1.87	248.13	6.92	6.88	506.87	76.9	132.79	7.09
20	3.92	250.	2.2	84.0	1.0	2.83	247.17	11.32	7.25	509.70	77.3	87.34	6.62

* Net Cumulative Oil Recovery after Emulsion Injection